Methods for Addressing Uncertainty and Variability to

Characterize Potential Health Risk from

Trichloroethylene-Contaminated Ground Water at

Beale Air Force Base in California: Integration of

Uncertainty and Variability in Pharmacokinetics and

Dose-Response

K.T. Bogen

September 30, 1999

U.S. Department of Energy

Lawrence
Livermore
National
Laboratory

DISCLAIMER

This report has been reproduced
directly from the best available copy.

Available to DOE and DOE contractors from the
Office of Scientific and Technical Information
P.O. Box 62, Oak Ridge, TN 37831
Prices available from (423) 576-8401
http://apollo.osti.gov/bridge/

Available to the public from the
National Technical Information Service
U.S. Department of Commerce
5285 Port Royal Rd.,
Springfield, VA 22161
http://www.ntis.gov/

OR

Lawrence Livermore National Laboratory
Technical Information Department's Digital Library
http://www.llnl.gov/tid/Library.html

Methods for Addressing Uncertainty and Variability to Characterize Potential Health Risk from Trichloroethylene-Contaminated Ground Water at Beale Air Force Base in California:

Integration of Uncertainty and Variability in Pharmacokinetics and Dose-Response

K.T. Bogen

Lawrence Livermore National Laboratory,
University of California, Livermore, CA*

September 30, 1999

*Address correspondence to: Dr. K.T. Bogen, Health and Ecological Assessment Div. (L-396), Lawrence Livermore National Laboratory, Livermore, CA 94550-9900, USA, Tel: (925) 422-0902, Fax: (925) 424-3255, NET: bogen@LLNL.gov.

DISCLAIMER

ACKNOWLEDGMENTS

TABLE OF CONTENTS

LIST OF TABLES AND FIGURES

Tables

Figures

ABBREVIATIONS and NOTATION

AM	arithmetic mean
$B_{MA,P}$	normalized MA-specific biologically effective (TCE or TCA) dose by pathway P
cdf	cumulative probability distribution function
C	cytotoxic
C_x	concentration of x
CH	chloral hydrate
CV	coefficient of variation = SD/AM
CVM	CV of the AM
der	dermal
df	degrees of freedom
D_C	chronic effective TCA dose
D_{Ca}	acute effective TCA dose
$D_{MA,P}$	MA-specific biologically effective (TCE or TCA) dose by pathway P
DCA	dichloroacetic acid
DCVC	S-(1,2-dichlorovinyl)-L-cysteine
EPA	U.S. Environmental Protection Agency
$f_x(y)$	probability density function pertaining to x, evaluated at y
$F_x(y)$	cdf pertaining to x, evaluated at y
G	genotoxic
GM	geometric mean
GSD	geometric standard deviation
ing	ingestion
inh	inhalation
JUV	joint uncertainty and (interindividual) variability
K_x	a constant pertaining to x
LN	lognormal
$LN(\mu,\sigma)$	lognormally distributed with GM = e^μ and GSD = e^σ
LTWA	lifetime time-weighted average
MA	mechanistic assumption, i.e., assumed mode/mechanism of action
$N(\mu,\sigma)$	normally distributed with AM = μ and SD = σ
NRC	National Research Council
NTP	National Toxicology Program

P	pathway or route of TCE exposure (intake)
PBPK	physiologically based pharmacokinetic
R	increased individual lifetime probability of incurring a toxic (cancer and/or noncancer) endpoint due to TCE exposure
SD	standard deviation
SDM	SD of the AM
TCA	trichloroacetic acid
TCE	trichloroethylene
U_x	an uncertain variate pertaining to x
V_x	a "heterogeneous" variate pertaining to x; i.e., different variate values pertain to different individuals at risk
$X_{MA,P}$	MA-specific TCE exposure (intake) by pathway P
$\Phi(z)$	cdf of a standard normal (Gaussian) variate Z, $= \text{Prob}(Z \le z)$
$\rho_r(x,y)$	rank correlation coefficient between variates x and y

ABSTRACT

Traditional estimates of health risk are typically inflated, particularly if cancer is the dominant endpoint and there is fundamental uncertainty as to mechanism(s) of action. Risk is more realistically characterized if it accounts for joint uncertainty and interindividual variability after applying a unified probabilistic approach to the distributed parameters of all (linear as well as nonlinear) risk-extrapolation models involved. Such an approach was applied to characterize risks to potential future residents posed by trichloroethylene (TCE) in ground water at an inactive landfill site on Beale Air Force Base in California. Variability and uncertainty were addressed in exposure-route-specific estimates of applied dose, in pharmacokinetically based estimates of route-specific metabolized fractions of absorbed TCE, and in corresponding biologically effective doses estimated under a genotoxic/linear (MA_G) vs. a cytotoxic/nonlinear (MA_C) mechanistic assumption for TCE-induced cancer. Increased risk conditional on effective dose was estimated under MA_G based on seven rodent-bioassay data sets, and under MA_C based on mouse hepatotoxicity data. Mean and upper-bound estimates of combined risk calculated by the unified approach were $<10^{-6}$ and $<10^{-4}$, respectively, while corresponding estimates based on traditional deterministic methods were $>10^{-5}$ and $>10^{-4}$, respectively. It was estimated that no TCE-related harm is likely occur due any plausible residential exposure scenario involving the site. The unified approach illustrated is particularly suited to characterizing risks that involve uncertain and/or diverse mechanisms of action.

1. INTRODUCTION

This report describes methods and results pertaining to Phase 2 of a study involving quantitative consideration of joint uncertainty and interindividual variability in risk to hypothetical future residents posed by trichloroethylene (TCE) in ground water at the inactive landfill Site LF-13 on Beale Air Force Base in California. The background of this study is discussed below, followed by summaries of the rationale for this study's focus on quantitative analysis of joint uncertainty and variability, of the technical hurdles posed by undertaking such an analysis in a way that explicitly addresses carcinogenic dose-response of TCE in view of fundamental uncertainty concerning its carcinogenic mode of action, and finally of the study goals of Phase 2 of the analysis undertaken of risk posed by TCE at Site LF-13. Specific methods used to address the latter goals are presented in Section 2 of this report. Results obtained by applying these methods are presented in Section 3, followed in Section 4 by a discussion of the results obtained. References cited in this report are listed in Section 5. Appendix 1 supplies mathematical details concerning the "method of moments" used throughout in this report to make assumptions about lognormal variates. Finally, Appendix 2 documents of all calculations performed for this study.

The general background of the present study and its Phase-1 counterpart is provided in Section 1.1 below, followed by: a summary of the rationale for the emphasis in this report placed on quantitative analysis of joint uncertainty and variability (Section 1.2), a discussion of the present fundamental uncertainty pertaining to mechanism(s) of action for TCE-induced cancer (Section 1.3), issues involving quantitative analysis of joint uncertainty and variability in dose-response for TCE-induced cancer (Section 1.4), and the specific goals of the present report (Section 1.5).

1.1. Background

Traditional point estimates of risk are calculated deterministically using worst-case assumptions for some or all input parameters, in a way that does not quantitatively account for uncertainty and interindividual variability pertaining to these parameters. Traditional point-estimates of risk are thus typically inflated and health-conservative, particularly if the cancer is the dominant endpoint and there is fundamental uncertainty as to mechanism(s) of action. Risk is more realistically characterized if it accounts for

joint uncertainty and interindividual variability after applying a unified probabilistic approach to the distributed parameters in all (linear as well as nonlinear) risk-extrapolation models for all (cancer as well as noncancer) endpoints involved. The present case study was designed to address the problem that no such unified probabilistic approach has never been developed or demonstrated. The case study addresses inactive Landfill Site LF-13 on Beale Air Force Base in California, where groundwater contaminated with trichloroethylene (TCE) has moved beyond the site boundary. Soil-vapor extraction and air-stripping treatment of groundwater have been undertaken to reduce concentrations of TCE and other volatile organic compounds in ground water beneath Site LF-13 (URSGWC, 1998). Site LF-13 is located in currently rural area of the Sacramento Valley of California, where groundwater wells are the principle source of domestic water supplies. The present analysis was undertaken to provide a realistic characterization of hypothetical TCE-related risks associated with potential future domestic/residential uses of groundwater from beneath Site LF-13, in view of the possibility that residential populations may eventually occupy lands adjacent to the site.

This study was conducted in two phases. Phase 1 focused on the impact of joint uncertainty and interindividual variability (JUV) on estimates of combined TCE exposure via different exposure pathways (Daniels et al., 1999). Uncertainty here refers to an absence of measurement data or incomplete knowledge; interindividual variability (or "variability") here refers to true differences or heterogeneity in an empirical, risk-related characteristic (e.g., physiological differences) among individuals in a population (Bogen and Spear, 1987; NRC, 1994). Although results of the Phase 1 analysis were presented as a characterization of risk rather than exposure, risk was estimated in that analysis simply as the product of estimated combined exposure (in mg kg^{-1} d^{-1}) and carcinogenic potency (in kg d mg^{-1}), where the latter potency factor was taken to be a constant. Thus, JUV in risk characterized in Phase 1 reflected only JUV in estimated exposure, and in no way addressed JUV associated with TCE pharmacokinetics, dose-response, alternative mechanisms of toxic action, or multiple toxic endpoints. TCE concentration in Phase 1 was estimated based on groundwater-monitoring data for a well on Site LF-13 near the possible location of a future groundwater extraction and distribution system (Purrier, 1997). After considering

5

concentration uncertainty and JUV in potential multi-route exposures to TCE from Site LF-13 ground water, corresponding JUV in risk was characterized and compared to corresponding risk estimators that were calculated using traditional deterministic methods (Daniels et al., 1999).

Phase 2 of the study described above is the subject of the present report. Phase 2 involved the development of new methods allowing additional information to be integrated into a Phase-1-type TCE risk assessment for Site LF-13. This additional information involves JUV in predicted risk *conditional on* route-specific TCE exposures. As further explained below, this was accomplished by combining exposure distributions and methods presented in the Phase-1 study with TCE-related pharmacokinetic and dose-response methods and information developed in the present study, to provide an improved characterization of TCE-related risk associated with Site LF-13 at Beale AFB.

1.2. Importance of Quantitative Analysis of Joint Uncertainty and Variability

This study focuses on integrating information on joint uncertainty and interindividual variability (JUV) to obtain more meaningful and more realistic estimates of exposure and risk. In the report, *Science and Judgment in Risk Assessment*, the National Research Council (NRC) emphasized the importance of distinguishing clearly between uncertainty (i.e., lack of knowledge) and interindividual "variability" (i.e., heterogeneity or differences pertaining to people at risk) in risk assessment (NRC, 1994). Uncertainty in characterized risk reflects the extent to which a risk estimate is likely to be erroneous, due to gaps in data and/or theory that imply statistical and/or model-specification error. Interindividual variability in characterized risk reflects the extent to which a risk is unequally imposed on members of the population at risk. While uncertainty reduces the confidence or reliability that can be placed in a risk estimate, variability can be viewed as a measure of perceived unfairness or inequity represented by the distribution of imposed risks. Because reliability and equity issues are clearly related to perceived and/or statutorily defined risk acceptability criteria, both these dimensions may be relevant to risk management policy decisions.

Quantitative characterization of joint uncertainty and variability (JUV) in risk is a way to address risk-related uncertainty and variability concisely and explicitly to

6

facilitate risk management decisions. When JUV is addressed quantitatively in the input distributions used to characterize the inputs (e.g., on ambient concentration, uptake, and dose-response) of a risk assessment, the distinction between uncertainty and variability ought to be maintained rigorously throughout the analytic process so that uncertainty and variability can be reflected distinctly in the calculated risk. This recommendation was expressed by the NRC (1994, p. 242) as follows:

> "A distinction between uncertainty (i.e., degree of potential error) and inter-individual variability (i.e., population heterogeneity) is generally required if the resulting quantitative risk characterization is to be optimally useful for regulatory purposes, particularly insofar as risk characterizations are treated quantitatively. The distinction between uncertainty and individual variability ought to be maintained rigorously at the level of separate risk-assessment components (e.g., ambient concentration, uptake, and potency) as well as at the level of an integrated risk characterization."

If no distinction is made between uncertainty-related and heterogeneity-related distributions associated with inputs to a given risk calculation, then the resulting distribution necessarily reflects risk to an individual selected at random from the exposed population (Bogen and Spear, 1987). By definition, this resulting distribution cannot be used for any regulatory decision intending to address equity issues by focusing on risk borne by relatively more sensitive and/or relatively more highly exposed members of the population at risk. Another advantage of distinguishing between uncertainty and variability is that it permits one to estimate the uncertainty in the risk to the individual who is "average" with respect to all characteristics that are heterogeneous among individuals at risk. Only the latter quantity can be used to estimate corresponding uncertainty in predicted population risk (i.e., uncertainty in the predicted number of cases), and thus, in particular, to estimate the likelihood of zero cases (i.e., the likelihood that remediation of the exposure scenario considered will have no positive impact whatsoever on public health) (Bogen and Spear, 1987).

1.3. Uncertainty in Mechanism(s) of Toxic Action

Liver is clearly a target tissue for TCE-induced cancer based on lifetime bioassay data on chronically exposed mice; relatively large acute, subchronic, or chronic TCE exposures are hepatotoxic in multiple species; and hepatocellular toxicity in mice about the most sensitive TCE-induced noncancer (but possibly cancer-related) endpoint

(Bogen and Gold, 1997; Bogen et al., 1988; EPA, 1985). DNA-binding and weak mutagenicity associated with TCE metabolites after TCE administration indicates that genotoxicity may be responsible for some or all TCE-induced cancer (Bogen and Gold, 1997; Fahrig et al., 1995). Two TCE metabolites in particular, trichloroacetic acid (TCA) and dichloroacetic acid (DCA), both induce and promote liver tumors in a mouse strain (B6C3F1) which is positive for TCE-induced liver cancer, whereas liver tumors did not appear in rats exposed to either TCE by gavage or to TCA via drinking water (Bogen and Gold, 1997; Bull et al., 1990; DeAngelo et al., 1997; DeAngelo et al., 1991; Herren-Freund et al., 1987; Pereira, 1996; Pereira and Phelps, 1996). DCA in particular was found recently to be weakly mutagenic in mouse lymphoma cells with a mutagenic potency similar to the classic mutagen ethyl methanesulfonate, whereas only very weak mutagenic activity was detected using either the major reactive TCE metabolite, chloral hydrate (CH), or its breakdown product TCA (Harrington-Brock et al., 1998). Initial studies found DCA to be more reactive and toxic than TCE, and thus more likely to account for observed TCE-induced cancer in bioassay mice (Larson and Bull, 1992a-b; Templin et al., 1993). However, more recent studies that controlled for *ex vivo* formation of DCA during sample preparation indicate that very little, if any, DCA was actually produced in TCE-exposed B6C3F1 mice, imply the same for humans as well, and conclude that DCA is unlikely to explain TCE-induced mouse tumors (Andersen et al., 1998; Merdink et al., 1998).

Correlations between hepatotoxic indicators induced by reactive TCE metabolites and precursors to TCE-induced liver tumorigenesis provide substantial, but not definitive, support a cytotoxic mechanism of TCE-induced carcinogenic action (Bogen and Gold, 1997). Hepatotoxic lipid peroxidation was found to be induced by TCA in mice and rats, but mice were found to be more sensitive than rats (Larson and Bull, 1992a). This differential sensitivity to a TCA-induced cytotoxic endpoint is consistent with a cytotoxicity-based explanation of TCE-induced liver tumors in mice but not rats. A more recent study of lipid peroxidation induced in B6C3F1 mouse liver concluded that the amount of such peroxidation induced by "TCA equaled that induced by CH, whereas that from [trichloroethanol, another major, but less toxic and reactive, TCE metabolite] was 3- to 4-fold lower, suggesting that metabolism of CH to TCA may be the predominant pathway leading to lipid peroxidation" (Ni et al., 1996).

Lipoperoxidation-induced oxidative stress may explain or correlate with the induction of hepatocellular replicative DNA synthesis and hepatocellular proliferation that has been observed in TCA-exposed B6C3F1 mice (Dees and Travis, 1994). Increased cell proliferation, in turn, either alone or in combination with genotoxic conditions, has long been considered sufficient to explain increased rates of cancer in view of biologically based mechanistic cell-kinetic multistage cancer theory, as well as based on experimental, epidemiological and clinical observations (Ames and Gold, 1990a; Ames and Gold, 1990b; Ames et al., 1993,1995; Armitage and Doll, 1957; Bogen, 1989; Cohen and Ellwein, 1990,1991; Moolgavkar, 1983; Moolgavkar and Knudson, 1981; Moolgavkar et al., 1988).

Statistical considerations support rejecting lung as a significant target site for TCE-induced cancer in rodents (Bogen and Gold, 1997). The remaining major site for cancer induced experimentally by chronic TCE exposure is the rat (but not mouse) kidney, based on National Toxicology Program (NTP) bioassays all judged to be "inadequate" after NTP review, with mild to severe renal toxicity observed at every non-control dose level in every species/sex combination in the bioassays (Bogen and Gold, 1997; NTP, 1988,1990). These NTP rats studies nevertheless provide the best available bioassay data on TCE-induced renal tumors plausibly relevant to humans (Bogen and Gold, 1997; Bogen et al., 1988; EPA, 1985). The rat tumor data are consistent with a cytotoxic mechanism of action for renal carcinogenesis, although mutagenicity of renal TCE-metabolites such as S-(1,2-dichlorovinyl)-L-cysteine (DCVC) indicates that genotoxicity may also play a role (Bogen and Gold, 1997; Fahrig et al., 1995). Interestingly, while subchronically administered TCA and acutely administered DCVC were both found to be nephrotoxic and to induce cell proliferation in rat kidney tubules, the DCVD-induced response in mice was much more pronounced in mice (for which species there is no evidence of TCE-induced kidney tumors) than in rats (for which species evidence exists indicating TCE-induced kidney tumors) (Acharya et al., 1997; Eyre et al., 1995). Consequently, the same issues regarding uncertainty in the mechanism of TCE-induced hepatocarcinogenicity apply also to the issue of mechanism underlying evidence, such as it is, for TCE-induced renal tumors.

EPA has not explicitly endorsed the quantitative combination of "model" uncertainty with other types of uncertainty in cancer risk assessments for compounds

like TCE (EPA, 1996), consistent with a recent NRC recommendation against this type of quantitative treatment as opposed to narrative/qualitative comparisons of model-specific analyses (NRC, 1994). However, the fact that environmental carcinogens like TCE pose risks that are relatively delayed and anonymous compared to, say, more immediate risks that demand accountable triage decisions, hardly justifies a suppression of analytic clarity. Moreover, there is no logical merit to the distinction between "model" and "parameter" uncertainty. As the NRC report itself points out, the former is logically equivalent to the latter when incorporated into a suitably general model that specifies, through values assigned to one or more uncertain parameters, any particular but uncertain model characteristics (i.e., substructures) of concern (NRC, 1994; p. 187).

1.4. Technical Issues Posed by Quantitative Analysis of Joint Uncertainty and Variability in Dose-Response for TCE-Induced Risk

In view of the issues discussed above, there were several technical issues that had to be addressed in this study due to its primary focus on quantitative analysis of JUV in dose-response for TCE-induced risk. These issues concern the lack of coordinated methods that consistently and simultaneously address:

(a) multiple toxic (in this case, cancer and noncancer) endpoints with potentially disparate dose-response relations,

(b) multiple plausible mechanisms of carcinogenic action,

(c) efficient treatment of pharmacokinetic relations, and

(d) integrated quantitative treatment of JUV in exposure, dose-response, and risk calculations.

General approaches to issues (a) and (d) have been reviewed (Bogen, 1995; NRC, 1994). Also pertaining to issues (a) and (d) are proposed methods to extend quantitative probabilistic methods now commonly applied in cancer risk assessment to noncancer endpoints, which involve replacing traditional uncertainty/safety factors by corresponding empirically based, or reasonable default, probability distributions (Baird et al., 1996; Carlson-Lynch et al., 1999; Dourson et al., 1996; Lewis, 1993; Renwick, 1993; Slob and Pieters, 1998; Weil, 1972). Issue (b) is a major focus of the proposed U.S. Environmental Protection Agency (EPA) guidelines for carcinogen risk assessment (EPA, 1996), but in this regard EPA recommends a non-quantitative, narrative approach

that cannot possibly address issue (d). Concerning issue (c), a number of physiologically based pharmacokinetic (PBPK) models have been developed for TCE (Abbas and Fisher, 1997; Allen and Fisher, 1993; Fisher and Allen, 1993; Fisher et al., 1998; Stenner et al., 1998), and corresponding methods for efficient PBPK analysis have been developed under different mechanistic assumptions concerning TCE-induced cancer (Bogen, 1988; Bogen and Gold, 1997). Concerning issues (b) and (c), PBPK methods for TCE have been applied under alternative mechanistic assumptions (Fisher and Allen, 1993), but this has never been done in a way that integrates JUV information or efficient analytic (as opposed to numerical) PBPK-calculation methods.

In recently proposed revised methods for deriving Ambient Water Quality Criteria, the EPA indicated that a goal of these methods should be to integrate cancer and noncancer assessments, and more specifically "to harmonize cancer and noncancer dose-response approaches and permit comparisons of cancer and noncancer risk estimates" (EPA, 1998; p. 59,97). To the extent this goal were achieved, these proposed methods would provide guidance on how to address issues (a)-(d) in a unified probabilistic approach for risk assessment. While the proposed methods do address multiple (cancer and noncancer) endpoints and alternative (linear vs. nonlinear) mechanisms of carcinogenic action, they do not specifically facilitate or even address their stated goal of integrating cancer and noncancer dose-response methods to yield comparable or aggregate measures of risk. Furthermore, this goal is unnecessarily impeded by some of the proposed methods, including those that: (1) address dose-response differently for noncarcinogens vs. "nonlinear" carcinogens; (2) address generic pharmacokinetic considerations differently for noncarcinogens vs. ("linear" or "nonlinear") carcinogens; (3) consider non-ingestive exposure as well as human interindividual variability in dose-response for noncarcinogens and "nonlinear" carcinogens but not for "linear" carcinogens; and (4) yield estimates of risk for "linear" carcinogens but do not for noncarcinogens and "nonlinear" carcinogens.

The impact of such inconsistencies on the problem of how to do unified risk assessment for cancer and noncancer endpoints is illustrated by the issue of whether or how to apply a toxicodynamic scaling factor to account for systematic interspecies differences in response as a function of biologically effective dose. For noncarcinogens, recently proposed EPA methods include a good explanation of why, in the absence of

relevant data, it is appropriate to apply two separate scaling factors (by default, each equal to a factor of 3) to account for interspecies toxicokinetic and toxicodynamic differences, respectively (EPA, 1998; p. 140):

> "The rationale for the use of PBPK models is that the pharmacokinetics and pharmacodynamics of a chemical each contribute to a chemical's observed toxicity, and specifically, to observed differences among species in sensitivity. Pharmacokinetics describes the absorption, distribution, metabolism, and elimination of chemicals in the body, while pharmacodynamics describes the toxic interaction of the agent with the target cell. In the absence of specific data on their relative contributions to the toxic effects observed in species, each is considered to account for approximately one half of the variability in observed effects, as is assumed in the development of RfCs and RfDs [i.e., of reference concentrations and doses, respectively]. The implication of this assumption is that an interspecies uncertainty factor of 3 rather than 10 could be used for deriving an RfD when valid pharmacokinetic data and models can be applied ... ."

For carcinogens, there is agreement that animal-to-human extrapolation of toxicokinetically equivalent effective dose may be accomplished by the use of an appropriate, validated PBPK model if one is available, and if not, by assuming that toxicokinetically equivalent doses scale proportional to body surface area or (body weight)$^{0.75}$ (EPA, 1992, 1996, 1998). However, federal policy concerning how/whether to apply an interspecies toxico*dynamic* scaling factor is not consistent. For example, the Health/Risk Assessment Committee of the Integrated Chlorinated Solvents Project (a committee comprised of representatives from four federal agencies) held that "it is strongly arguable that the surface area correction is not a correction on dose to allow for pharmacokinetics, but rather a correction on risk to allow for many factors, including pharmacodynamics" (EPA, 1987a; p. 125). For "linear" carcinogens, however, EPA has more recently proposed that no interspecies toxicodynamic scaling factor is required for carcinogens whenever a PBPK approach has been used to account for interspecies toxicokinetic differences (EPA, 1998).

Likewise, interindividual variability in sensitivity/susceptibility *per se* to environmentally induced cancer is not typically considered in risk extrapolations for carcinogens assumed to have a genotoxic/linear-no-threshold mechanism of action (EPA, 1996; EPA, 1998). In this respect, past practice has been to focus (implicitly) on risk to persons who have an average level of susceptibility, when there is no reason to

predict that the exposed population is one that may reflect an unusual degree of hypersusceptibility to environmentally induced cancer (NRC, 1994). For noncarcinogens, however, a so-called "uncertainty" factor of up to 10 has traditionally been applied "to account for the variation in sensitivity (intraspecies variation) among the members of the human population"; and a similar factor was proposed recently by EPA for use with all "nonlinear" carcinogens (EPA, 1998; p. 110,122). Confusion between uncertainty and interindividual variation also appears in proposed new approaches to model differences in human sensitivity by probabilistic methods rather than by the traditional use of "uncertainty" factors (Carlson-Lynch et al., 1999; Slob and Pieters, 1998). Because there is little doubt that substantial human variability exists in susceptibility to environmentally induced cancer (NRC, 1994), a truly unified probabilistic approach to assessing risks pertaining to cancer and noncancer endpoints clearly requires a consistent approach to intraspecies variability in dose-response.

Recent proposals for so-called "unified" or "comprehensive" approaches to risk assessment for cancer and noncancer endpoints (Butterworth and Bogdanffy, 1999; Gaylor et al., 1999) fail to address the complete set of issues (a)-(d). These proposals essentially recommend merely that a traditional safety-factor approach be used for cancer and noncancer endpoints alike; they focus on how to define exposure levels that protect against a single endpoint, rather than on how to calculate actual levels of aggregate risk for both cancer and noncancer endpoints. Therefore, no methods or studies exist that address the complete set of issues (a)-(d) for integrated risk characterization.

1.5. Study Objectives

This study (Phase 2 together with Phase 1) was designed to accomplish two overall objectives. The first overall objective was to provide to the U.S. Air Force and regulatory agencies new quantitative procedures that address JUV in exposure and dose-response assessment to better characterize potential health risk. Such methods could be used at sites where populations may now or in the future be faced with using groundwater contaminated with low concentrations of TCE. The second overall objective was to illustrate and explain the application of these procedures with respect to available data for TCE in ground water beneath an inactive landfill site that is

13

undergoing remediation at Beale Air Force Base in California. The results of this case study are intended to illustrate how the more realistic and more meaningful risk estimates obtained using methods we describe compare to corresponding conservative risk estimates calculated using a traditional deterministic screening-level approach. Application of the methods developed in this project can lead to more reasonable and equitable risk-acceptability criteria for potentially exposed populations at specific sites.

The specific objective of the present report is to describe consistent and coherent methods devised to address issues (a)-(d) discussed in the previous subsection, and to report and discuss an application of these methods, together with other methods and information developed in Phase 1 of this project, to the specific problem of characterizing risk posed by TCE in ground water at Site LF-13 at Beale Air Force Base.

2. METHODS

Methods used to address joint uncertainty and interindividual variability (JUV) in risk posed by TCE contamination at Site LF-13 was calculated and characterized as described below in subsections pertaining to: (1) the unified probabilistic approach adopted for this analysis, (2) TCE concentration and route-specific exposures, (3) corresponding biologically effective doses and related physiologically based pharmacokinetic (PBPK) considerations, (4) dose-response for cancer and noncancer endpoints, (5) characterization of joint uncertainty and interindividual variability (JUV) in risk as a function of JUV in input parameters relating to topics (2)-(4), and (6) data analysis and computation.

Consistent with established JUV notation, an overbar (i.e., $^{-}$) here denotes expectation with respect to heterogeneous parameters only, angle brackets (i.e., $\langle\ \rangle$) denote expectation with respect to uncertain parameters only, each subscripted U denotes a corresponding purely uncertain variate, and each subscripted V denotes a corresponding purely interindividually heterogeneous variate (Bogen and Spear, 1987; NRC, 1994; Bogen, 1995). Also, each subscripted V denotes a corresponding constant used below to estimate risk, $X_{MA,P}$ (in mg kg^{-1} d^{-1}) denotes a mechanistically relevant measure of TCE intake by the indicated exposure pathway (P) that pertains to the indicated mechanism/mode of action (MA) for TCE-induced toxicity, and $D_{MA,P}$ denotes a corresponding biologically effective dose, where, for both X and D, the subscript MA specifies either a genotoxic (G) or cytotoxic (C) assumed mode of action, and the subscript P indicates either an ingestion (ing), inhalation (inh), or dermal (der) exposure pathway. Quantities related to X and D are defined below using similar subscript notation.

Some variates defined in Daniels et al. (1999) are referred to below, denoted as they were in that report. All constants and variates defined in this report used as input to estimate risk are defined below and are summarized in Table 2, which appears at the end of Methods (after Section 2.6) prior to Results (Section 3).

15

2.1. Unified Probabilistic Approach

Health risk associated with residential exposure to TCE from ground water at Site LF-13 on Beale Air Force Base in California was analyzed using the unified probabilistic approach summarized in Figure 1. Total associated risk, R, was defined as the increased individual lifetime probability of incurring a toxic (cancer and/or noncancer) endpoint due to TCE exposure from three pathways: direct ingestion of TCE-contaminated groundwater, dermal absorption of TCE while showering or bathing, and inhalation of TCE volatilized from water to household air. For volatile organic compounds such as TCE, these three pathways typically are the most significant contributors to total daily residential intake. Each route-specific TCE intake was converted to a corresponding biologically effective dose for each MA and toxic endpoint considered, where this conversion was made using efficient MA-specific forms of a human PBPK model. Route-specific effective doses were summed for each MA to obtain (two) measures of MA-specific total effective dose (see Section 2.2). As detailed in Section 2.4, two MAs were considered for TCE: a genotoxic MA (MA_G) and a cytotoxic MA (MA_C), with both MAs considered potentially relevant to cancer risk posed by TCE exposure, but only MA_C considered relevant to noncancer risk posed by TCE exposure. Briefly, it was assumed that liver cytotoxicity is the most sensitive noncancer endpoint for TCE in humans based on the most sensitive experimental (mouse) data, that hepatotoxicity may (itself, or as the most sensitive available cytotoxic indicator) also explain and/or contribute to TCE-induced cancer observed in animal bioassays, and that genotoxicity may additionally explain and/or contribute to TCE-induced cancer observed in rodent bioassays. Increased likelihoods of cancer and of hepatotoxicity were each modeled as a MA-specific function of PBPK-based biologically effective dose in animals. Interspecies extrapolation of pharmacokinetic differences was obviated by consistent application of relevant PBPK models. Interspecies pharmacodynamic differences in dose-response were extrapolated using a single method applied to both cancer and noncancer endpoints. Intraspecies (interindividual) variability in human dose-response was modeled identically for both cancer and noncancer endpoints. Finally, increased risks of incurring either or both endpoints were estimated with respect to associated JUV, and these estimates were compared to corresponding traditional-type risk estimates obtained using deterministic methods.
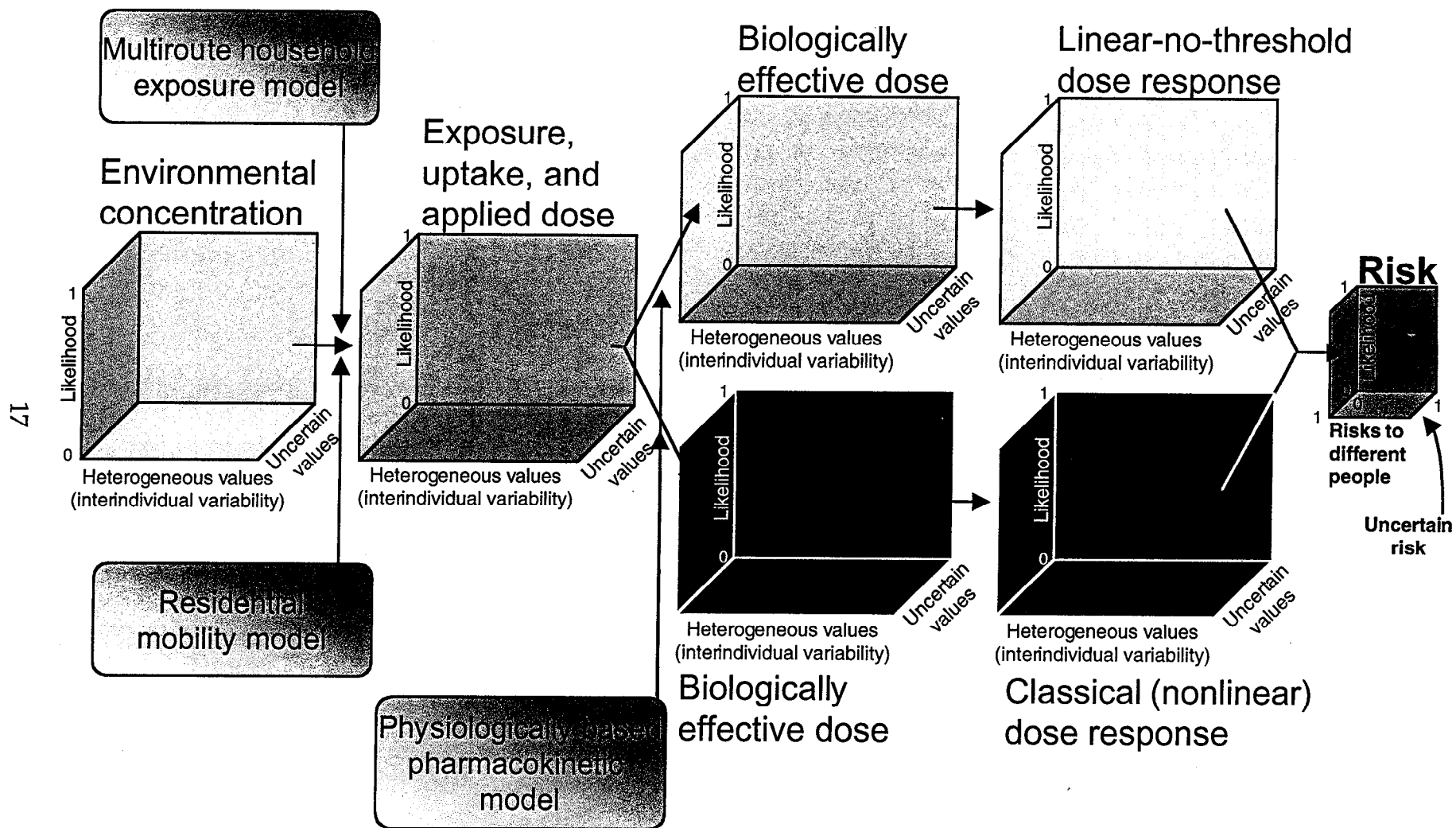
Figure 1. Unified probabilistic approach to risk assessment for TCE.

The following subsections describe the specific methods used to apply the general approach just summarized, with respect to route-specific TCE exposures (Section 2.2), corresponding biologically effective doses (Section 2.3), dose-response for TCE-induced toxicity (Section 2.4), and unified risk characterization (Section 2.5).

2.2. TCE Exposure

Predicted route-specific LTWA rates ($X_{G,ng}$, $X_{G,inh}$, and $X_{G,der}$; mg kg^{-1} d^{-1}) of exposure to TCE due to Site LF-13 groundwater contamination at Beale AFB were based directly on corresponding rates (E_{Ing}, E_{Inh}, and E_{Derm}) and associated JUV defined in Equations 1-3 of the Phase-1 report (Daniels et al., 1999). Specifically, it was assumed that,

$$X_{G,Ing} = E_{Ing} \quad , \tag{1a}$$

$$X_{G,der} = E_{Derm} \quad , \tag{1b}$$

$$X_{G,inh} = (V_{alvR}/Inh)\,E_{Inh} \quad , \text{ where} \tag{1c}$$

Inh = total respiratory ventilation rate used in Daniels et al. (1999) (m^3 kg^{-1} d^{-1}); and

$$V_{alvR} = \frac{V_{alvr}}{1000\ \text{L h}^{-1}}V_{alv} = \frac{12.9\ \text{L h}^{-1}}{1000\ \text{L m}^{-3}}(V_W/kg)^{0.74-1}V_{alv} \quad , \text{ in which:} \tag{2}$$

V_{alvR} = weight-normalized ventilation rate used in present study (m^3 h^{-1}),

V_{alvr} = non-normalized ventilation rate (L h^{-1}),

V_W = body weight (kg), and

V_{alv} = normalized interindividual variability in V_{alvR} that is independent of variability in V_W (unitless).

Equation 2 is an adaptation of the alveolar ventilation rate V_{alvr} defined in a validated PBPK model for TCE in humans (Allen and Fisher, 1993). Because, as explained in Section 2.3, this PBPK model was integrated into the UPA applied in the present study, $X_{G,inh}$ was defined in terms of V_{alvR} rather than the total ventilation rate Inh used by Daniels et al. (1999).

Variability in V_W for U.S. adults was modeled as approximately lognormal (LN) with an arithmetic mean (AM) of 71.0 kg, standard deviation (SD) of 15.9 kg, and corresponding coefficient of variation (CV = SD/AM) of 0.224 (CalEPA, 1996; Finley et al., 1994). Based on the method of moments (Aitchison and Brown, 1957) explained and

developed in Appendix 1, the assumed AM and SD of V_W imply that $V_W \sim LN(4.24, 0.221)$.

Weight-normalized rates of total respiratory ventilation for U.S. adults are approximately lognormally distributed with a CV of ~0.3 (CalEPA, 1996). As implied by Equation 1, the non-normalized alveolar ventilation rate V_{alvr} (L h^{-1}) is approximated as

$$V_{alvr} \approx (12.9 \text{ L h}^{-1}) (V_W \text{ kg}^{-1})^{-0.3} V_{alv} \ . \tag{3}$$

The alveolar proportion of total lung volume was assumed to be nearly constant, and consequently variability in V_{alv} was modeled as LN with an AM of 1. Based on the method of moments (Appendix 1), it follows that $V_{alv} \sim LN(-0.0409, 0.286)$. To facilitate PBPK analyses described in Section 2.3, it was assumed that V_{alv}, V_{alvr} and V_{alvR} pertain to children as well as to adults.

Predicted daily (non-LTWA) peak TCE exposures ($X_{C,P}$, in mg kg^{-1} d^{-1}) due to Site LF-13 groundwater contamination at Beale AFB were defined for ingestion and dermal exposure routes as follows, in terms of $X_{G,P}$ defined above (Equations 1a-b) and of the constants EF and AT and the variate ED defined in Equation 1 of the Phase-1 report (Daniels et al., 1999):

$$X_{C,ing} = [AT/(ED \times EF)]X_{G,ing} \ , \quad \text{and} \tag{4a}$$

$$X_{C,der} = [AT/(ED \times EF)]X_{G,der} \ , \quad \text{where} \tag{4b}$$

ED = household exposure/residence duration used in Daniels et al. (1999) (y);

EF = exposure frequency used in Daniels et al. (1999) (d y^{-1});

AT = averaging time used in Daniels et al. (1999) corresponding to a 70-y exposure (d).

Predicted daily peak respiratory TCE exposure, $X_{C,inh}$, was similarly related to $X_{G,inh}$, except that E_{Inh} (see Equation 1c) was defined by Daniels et al. (1999) to refer to total household LTWA exposure, whereas $X_{C,inh}$ pertains to peak respiratory TCE exposure, which is assumed to occur during showering (and without reference to non-shower respiratory TCE exposures). Therefore, $X_{C,inh}$ was modeled as follows based on the

method of Daniels et al. (1999) as adapted in Equation 1c, but solely with reference to shower-related TCE exposure:

$$X_{C,inh} \;=\; V_{alvr}\!\left(\frac{W_{sh}\;\phi_{TCE\text{-}sh}}{1000\ \text{L m}^{-3}\times AE_{sh}}\right)C_w\,\frac{V_{t,inh}}{1\,d}\ , \quad \text{where} \tag{4c}$$

W_{sh} = water-usage rate per person for shower (L h^{-1});

$\phi_{TCE\text{-}sh}$ = water-to-air transfer efficiency of TCE in the shower (unitless);

AE_{sh} = air-exchange rate in the shower or bath stall (m^3 h^{-1});

C_w = TCE concentration in ground water (mg L^{-1}); and

$V_{t,inh}$ = $(ET_{sh}\times 1\,d)$ = shower duration (h);

where variability in W_{sh}, $\phi_{TCE\text{-}sh}$, AE_{sh}, and ET_{sh}, and uncertainty in C_w, were all modeled as previously described (Daniels et al., 1999).

2.3. Biologically Effective Dose

For reasons discussed in Section 1.3, liver was assumed to model susceptible target tissue for TCE-induced cancer based on mouse bioassay data, and mouse hepatocellular toxicity to model the most sensitive TCE-induced noncancer (but possibly cancer-related) endpoint. Dose-response relations for TCE-induced endpoints were treated as functions of corresponding mechanism- and route-specific measures of biologically effective dose $D_{MA,P}$ (mg kg^{-1} d^{-1}) defined below. As indicated in Figure 1, PBPK and associated JUV models used to define $D_{MA,P}$ as functions of corresponding TCE exposures ($X_{MA,P}$) were treated differently in view of uncertainty as to the extent to which the MA for TCE involves genotoxic (G) processes with a plausibly linear dose-response vs. cytotoxic/mitogenic (C) processes with a likely nonlinear dose-response. To facilitate subsequent calculations, the following related quantities were also calculated:

$$D_{MA} \;=\; D_{MA,ing} + D_{MA,inh} + D_{MA,der}\ , \tag{5a}$$

$$f_{MA,P} \;=\; \langle\overline{D_{MA,P}}\rangle\big/\langle\overline{D_{MA}}\rangle\ , \tag{5b}$$

$$B_{MA,P} \;=\; D_{MA,P}\big/\langle\overline{D_{MA,P}}\rangle\ , \qquad\qquad \text{and} \tag{5c}$$

$$B_{MA} \;\sim\; \left(B_{MA,ing}\oplus B_{MA,inh}\oplus B_{MA,der}\right)\otimes 3^{-1}\ , \quad \text{where} \tag{5d}$$

D_{MA} = total of all pathway-specific biologically effective doses under mechanistic assumption MA (mg kg^{-1} d^{-1});

$B_{MA,P}$ = normalized biologically effective dose for pathway P under mechanistic assumption MA (unitless);

B_{MA} = functional (not stochastic) mean of all pathway-specific normalized biologically effective doses under mechanistic assumption MA (unitless); and

$f_{MA,P}$ = fraction of $\overline{D}_{MA}$ due to pathway P (unitless);

where in Definition 5d, "~" signifies "distributed as", and functional summation (denoted $\oplus$) signifies not ordinary (in this case, stochastic) summation, but rather the analytic sum of the probability (i.e., ordinate) values of each cumulative probability distribution function (cdf) of the indicated variates conditional on a common variate (i.e., abscissa) value, where this sum is obtained for all possible variate values. Likewise, functional multiplication (denoted $\otimes$) in Definition 5d signifies the analogous product operation. The order of (uncertainty- vs. variability) expectation operations in Equations 5a-b is arbitrary in this case study, because the order was not found to have a substantial effect on the value of $\langle \overline{D}_{MA} \rangle$ obtained—due principally to the linear structure and behavior of the models used for $D_{MA,P}$ previously described (Daniels et al., 1999).

The rationale for including both genotoxic and cytotoxic MAs into this analysis is discussed below, followed by subsections detailing PBPK models and methods used to calculate corresponding biologically effective genotoxic and cytotoxic doses to bioassay animals and to humans.

2.3.1. Uncertainty in mechanism of toxic action

As discussed in Section 1.3, there is fundamental "model" uncertainty regarding critical mechanism(s) explaining the observed ability of TCE to increase tumor incidence in rodent bioassays and its suspected ability to do the same in humans. This uncertainty can be represented by the following four alternative mechanistic assumptions (MAs):

Assumption 1 (MA$_G$) is the traditional approach to assessing TCE cancer risk, which presumes that TCE increases cancer risk only via one or more genotoxic mechanisms of action, involving DNA damage that is linearly proportional to the biologically effective concentration of one or more of TCE's reactive metabolites (Bogen, 1988; Bogen et al., 1988; Brown et al., 1990; EPA, 1985; EPA, 1987a).

21

Assumption 2 (MA_C) is that observed TCE-induced (e.g., liver) cancer is due entirely to increased net proliferation of spontaneous premalignant cells elicited primarily by TCA, by a cytotoxic and/or perhaps a directly mitogenic mechanism (Andersen et al., 1998; Bogen and Gold, 1997).

Assumption 3 ($MA_{G \cap C}$) is the composite assumption that both genotoxic and nongenotoxic mechanisms contribute to observed TCE carcinogenicity in bioassays, i.e., that both MA_G *and* MA_C are true. However, to the extent $MA_{G \cap C}$ is true, uncertainty remains as to the quantitative role played by each mechanism involved. This kind of uncertainty is often referred to as "parameter" uncertainty, because it is possible to reflect this as uncertainty pertaining to a single parameter (in a sufficiently general model) that governs the weight to be given to each of the two mechanisms considered to be operative under $MA_{G \cap C}$.

Assumption 4 ($MA_{G \cup C}$) is the "dichotomous" assumption that *either* MA_G *or* MA_C is true, but there is "model" uncertainty as to which one of these possibilities is true, in view of the fact that the "parameter" uncertainty discussed above in reference to $MA_{G \cap C}$ is quantitatively equivalent to "model" uncertainty.

In view of evidence discussed in Section 1.4 supporting the plausibility of both MA_G and MA_C, both of these mechanistic assumptions were used to define route-specific biologically effective dose and dose-response for TCE-induced cancer. Of course, MA_C was used exclusively as the basis for calculating biologically effective dose and dose-response for TCE-induced noncancer endpoints. Below, methods used to estimate biologically effective doses corresponding to mechanisms MA_G and MA_C are described, following an explanation of the PBPK modeling approach that was adopted in this study to accommodate both mechanisms.

2.3.2. PBPK modeling approach

A number of multi-compartment PBPK models have been developed that provide reasonably well-validated descriptions of the uptake, distribution, metabolism, and excretion of TCE administered by various routes to mice, rats and humans (Abbas and Fisher, 1997; Allen and Fisher, 1993; Bogen, 1988; Fisher and Allen, 1993; Fisher et al., 1991,1998; Stenner et al., 1998; EPA, 1985; EPA, 1987b). In contrast to earlier PBPK models describing TCE distribution, metabolism and excretion using four physiological compartments, the more recent "second generation" models include additional compartments to describe distribution, metabolism and excretion of TCA and of unbound and glucuronide-bound trichloroethanol in mice and humans (Abbas and

22

Fisher, 1997; Fisher et al., 1998), and to account for enterohepatic recirculation of TCA and of trichloroethanol-glucuronide (Stenner et al., 1998). Although the newer PBPK models are more realistic, they are less convenient to incorporate into the adopted UPA relative to earlier-type 4-compartment models. It is also not apparent that any improved ability to fit empirical data used to validate the newer vs. the earlier models implies any corresponding substantial improvement in the specific measures of biologically effective dose discussed below, namely, total metabolized TCE and peak plasma concentration of TCA. Indeed, an earlier-type 4-compartment model for TCE in humans appears to provide fairly accurate predictions of the peak value, $\text{Max}(C_{\text{TCA}})$, of TCA concentration in plasma measured in several different studies involving humans exposed by inhalation to various air concentrations of TCE (Allen and Fisher, 1993), whereas a corresponding "second generation" model appears to underpredict $\text{Max}(C_{\text{TCA}})$ by up to ~40% in human subjects exposed to 50 or 100 ppm TCE in air (Figure 8 of Stenner et al., 1998). Therefore, earlier-type 4-compartment models (Allen and Fisher, 1993; Bogen, 1988) were used for PBPK-based calculations of biologically effective dose in the present study, as described below. However, recently reported experimental data on human variability in key PBPK parameter values (Fisher et al., 1998; Lipscomb et al., 1998) was incorporated into the present analysis as discussed below.

2.3.3. Effective genotoxic dose

Under MA_{G} for TCE (i.e., assuming that TCE is a "linear"/genotoxic carcinogen), bioassay-based potency traditionally has been expressed as increased risk per unit of PBPK-estimated total LTWA metabolized TCE per kg body weight per day, without accounting for PBPK-related uncertainty and variability (Bogen, 1988; Brown et al., 1990; EPA, 1985; EPA, 1987b). There is an indication this policy will likely persist (EPA, 1996). Measures of biologically effective dose, as LTWA metabolized TCE (in mg kg^{-1} d^{-1}) to animals in bioassays positive for TCE-induced liver or kidney cancer were obtained from Table 4 of Bogen (1988). Similar measures of route-specific biologically effective dose $D_{\text{G,P}}$ to humans under MA_{G} were used for the present analysis, namely:

$$D_{\text{G,P}} = V_{\text{fm,P}} X_{\text{G,P}}, \quad \text{for P = ing, inh, or der, where} \tag{6}$$

$V_{\text{fm,P}}$ = limiting fraction of total TCE intake by pathway P that is metabolized conditional on intake sufficiently small to ensure that saturation of TCE metabolism remains negligible (unitless).

For multi-compartment PBPK models like that of Allen and Fischer (1993), these limiting metabolized fractions were shown previously to be

$$V_{\text{fm,ing}} = \left[1 + \frac{K_{\text{m}}}{V_{\text{max}}} \left(\frac{V_{\text{Pb}}}{V_{\text{alvr}}} + \frac{1}{V_{\text{liv}}} \right)^{-1} \right]^{-1} \text{, and} \tag{7a}$$

$$V_{\text{fm,inh}} = V_{\text{fm,der}} = \left[1 + \frac{V_{\text{alvr}}}{V_{\text{Pb}}} \left(\frac{K_{\text{m}}}{V_{\text{max}}} + \frac{1}{V_{\text{liv}}} \right) \right]^{-1} \text{, where} \tag{7b}$$

V_{alvr} = alveolar ventilation rate (defined in Equations 2 and 3) (L h^{-1});

V_{liv} = the rate of blood perfusion to liver (L h^{-1});

V_{Pb} = the blood:air partition coefficient for TCE (L$_{\text{air}}$ L$^{-1}_{\text{blood}}$);

V_{max} = maximum rate of TCE metabolism (mg h^{-1});

K_{m} = Michaelis-Menten affinity/saturation constant (mg L^{-1}); and

where V_{alvr} is alveolar ventilation rate defined above (Equation 3), and where, for Michaelis-Menten parameters K_{m} and V_{max} assumed to govern metabolic saturation kinetics for TCE, the mass unit (mg) refers to TCE and the volume (L) to venous blood exiting liver (Bogen, 1988; Bogen and Hall, 1989).

To derive human biologically effective doses under MA$_{\text{G}}$ (as well as under MA$_{\text{C}}$, as explained below), Equations 7a-b were applied assuming that: V_{alvr} is defined by Equation 2, $V_{\text{liv}} = 26\% \times (15.0/12.9) \times V_{\text{alv}}$ (Allen and Fisher, 1993), $K_{\text{m}} = 1.5$ mg L^{-1} (i.e., treated as a constant) (Allen and Fisher, 1993), and that $V_{\text{Pb}} \sim N(10.2, 1.6)$ for males and females combined (Fisher et al., 1998). Variability in the maximal rate of TCE metabolism, V_{max}, was modeled as LN with

$$V_{\text{max}} = (14.9 \text{ mg h}^{-1}) (V_{\text{W}}/\text{kg})^{-0.3} V_{\text{Vmax}} \text{,} \tag{8}$$

which adapts the definition used by Allen and Fisher (1993) to incorporate a multiplicative factor V_{Vmax} reflecting V_{max}-related variability, where V_{Vmax} was assumed to have an AM of 1. Under these assumptions, Equations 7a-b are simplified to:

$$V_{fm,ing} = \left\{1 + V_{alv}\left[V_{Vmax}(0.7700\,V_{Pb} + 2.547)\right]^{-1}\right\}^{-1} \quad \text{, and} \tag{9a}$$

$$V_{fm,inh} = V_{fm,der} = \left[1 + \frac{V_{alv}}{V_{Pb}}\left(\frac{1.299}{V_{Vmax}} + 3.307\right)\right]^{-1} \quad, \tag{9b}$$

in which no more than three significant figures are implied. From Equation 9b it is clear that $V_{fm,inh}$ is correlated with V_{alv}. From Equation 1c, it follows that this correlation is implied in Equation 6 defining $D_{G,inh}$, as well as in Equation 15b below (in Section 2.3.4) that defines the corresponding cytotoxic dose $D_{C,inh}$. Note, however, that the limiting metabolized fractions defined by Equations 9a-b are *independent* of body weight (V_W), and thus are independent of $D_{MA,P}$ for P = {ing, der} defined by Equation 6 (and by Equations 15a-b below).

Based on *in vitro* measures of V_{max} for TCE using human microsomes and hepatocytes sampled from 4 to 6 different donors (Lipscomb et al., 1998), the CV of V_{max} was estimated to be ~0.60, which, based on the method of moments (Appendix 1) conditional on assumed variability in V_W discussed above (after Equation 2), implies that $V_{max} \sim LN(-0.152, 0.551)$. Systematic uncertainties pertaining to $V_{fm,P}$ are likely to be small relative to the combined effect of interindividual pharmacokinetic variabilities, so uncertainty *per se* is not incorporated into Equations 9a-b used to define $V_{fm,P}$.

Note that, conditional on the adopted PBPK model, Equations 7a-b and 9a-b remain true *regardless* of any (dynamic or static) pattern of exposure(s) involved, provided that metabolism remains virtually unsaturated, which in turn ensures that the corresponding system of linked ordinary differential equations remains linear (Bogen, 1988; Bogen and Spear, 1987).

2.3.4. Effective cytotoxic dose

Under MA_C for TCE, hepatocellular oxidative damage is assumed to comprise or elicit premalignant liver-cell proliferation and consequent increased tumor risk in mice, and is further assumed to correlate best with the daily peak value $Max(C_{TCA})$, of TCA concentration in plasma, rather than with LTWA total metabolized TCE or related areas under concentration-times-time curves for blood or other tissues (Bogen and Gold, 1997). Similar reliance on peak rather than LTWA metabolic yield was used for MA_C-

based risk assessment for chlorinated methanes, based on empirical evidence supporting the former measure as the best predictor of oxidative damage (Bogen, 1990a). In the absence of dose-response data on TCA-induced rodent nephrotoxicity, and consistent with information discussed in Section 2.4, Max(C_{TCA}) was also taken to be the biologically effective cytotoxic dose for potential TCE-induced kidney cancer under MA_C. It was further assumed that Max(C_{TCA}) is the biologically effective cytotoxic dose for TCE-induced noncancer endpoints, so in general it was assumed that $D_{C,P}$ for any exposure pathway P is the value of Max(C_{TCA}) produced in response to a corresponding exposure $X_{C,P}$ defined in Equation 4a-c. Corresponding total effective dose (D_C) was (in Equation 5a) defined as the sum of $D_{C,P}$ from all exposure pathways, as discussed below following Equation 13b.

In the context of low-dose risk extrapolation based on the PBPK model used here for TCE humans, all saturable (Michaelis-Menten) PBPK relations linearize. Therefore, this PBPK model was evaluated using an entirely analytic approach previously described (Bogen and Gold, 1997), which is simpler yet equivalent to alternative, relatively cumbersome numerical methods more commonly applied. By this approach (see Equation 4 of Bogen and Gold, 1997),

$$\frac{dC_{TCA}(t)}{dt} = \frac{K_{fTCA} K_{MW}}{V_W V_{fd}} \left(\frac{C_{TCE}(t) V_{max}}{C_{TCE}(t) + K_m} \right) - V_{ke} C_{TCA}(t) \quad , \quad \text{where} \tag{10}$$

$C_{TCA}(t)=$ concentration at time t of TCA in plasma (mg L^{-1});

$C_{TCE}(t)=$ concentration at time t of TCE in venous blood exiting liver (mg L^{-1});

K_{fTCA} = net effective fraction of total TCE intake metabolized to TCA (unitless);

K_{MW} = TCA to TCE molecular-weight ratio (unitless); and

V_{fd} = fraction of body weight corresponding to apparent volume of distribution for TCA (L kg^{-1}); and

V_{ke} = first-order rate constant for elimination of TCA from plasma (h^{-1});

and where V_W, V_{max}, and K_m were defined above (after Equations 2, 7b, and 7b, respectively). It was assumed that $K_{fTCA} = 0.33$ (Allen and Fisher, 1993), and the ratio K_{MW} is 1.228 (see Bogen and Gold, 1997).

Conditional on any regular pattern of peak daily TCE exposures $X_{C,P}$ that—by any pathway P and corresponding duration $V_{t,P}$—are small enough to ensure that $C_{TCE}(t) \ll K_m$ for all t, Equation 10 implies that $C_{TCA}(t)$ attains a dynamic equilibrium in which

$$\text{Max}[C_{TCA}(t)] = D_{C,P} = \frac{K_{fTCA} K_{MW} V_{fm,P}}{V_{fd} V_{ke}} (X_{C,P} \times 1 \text{ d}) \left[\frac{f_{deq}}{V_{t,P}}\right] , \text{ where} \quad (11)$$

$$f_{deq} = \frac{1 - \exp(-V_{ke} V_{t,P})}{1 - \exp(-V_{ke} \times 24 \text{ h})} , \quad (12)$$

$V_{t,P}$ = duration (≤ 24 h) of peak daily exposure $X_{C,P}$ by pathway P (h); and

f_{deq} = fraction of $\text{Max}[C_{TCA}(t)]$ conditional on a hypothetical infinite exposure duration that is attained at dynamic equilibrium conditional on $V_{t,P}$;

in which $X_{C,P}$ and $V_{t,inh}$ were defined via Equations 4a-c, $V_{fm,P}$ was defined in Equations 9a-b, and all other variates in Equations 11-12 (i.e., besides f_{deq}, $V_{t,P}$, and $X_{C,P}$) were defined following Equation 10. Equation 11 is a multi-route generalization of Equations 6 and 7 of Bogen and Gold (1997). Figure 2 shows how the bracketed term in Equation 11 is well approximated by

$$\left[f_{deq}/V_{t,P}\right] \approx (24 \text{ h})^{-1} + 0.5053 V_{ke} + (1.661 \text{ h}) V_{ke}^2$$
$$\text{for } V_{t,P} \leq 0.5 \text{ h and } V_{ke} \leq 0.1 \text{ h}^{-1} \quad (13a)$$

$$\approx (24 \text{ h})^{-1} + 0.5053 V_{ke} \qquad \text{for } V_{t,P} \leq 0.5 \text{ h and } V_{ke} \leq 0.04 \text{ h}^{-1} , \quad (13b)$$

in which no more than three significant figures are implied.

As indicated following Equation 4c, variability in $V_{t,inh}$ was modeled as LN with $V_{t,inh} \sim LN(\ln 0.120, \ln 1.47)$ as previously described (Daniels et al., 1999), implying shower (or, more generally, bathing-related water-flow) durations that virtually never ($p < 10^{-11}$) exceed 0.5 h. It was further assumed that $V_{t,der} = V_{t,inh}$ as previously described (Daniels et al., 1999), that $V_{t,ing} < 0.5$ h, and that $V_{t,ing}$, $V_{t,inh}$, and $V_{t,der}$ are timed such that the total effective cytotoxic exposure, D_C (defined by Equation 5a), is maximized, so as to reflect the peak value of $\text{Max}[C_{TCA}(t)]$ predicted during a lifetime of different pathway-specific effective-exposure scenarios.
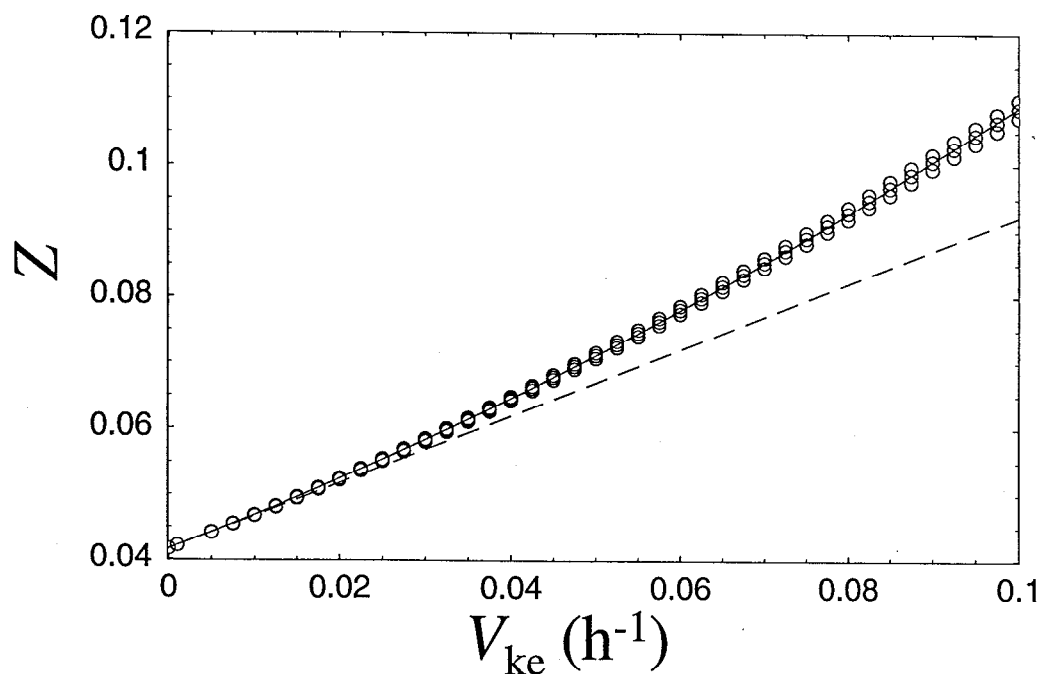
Figure 2. Approximation of the ratio $Z = (f_{deq}/V_{t,P})$, i.e., the fraction of steady-state that is attained under dynamic-equilibrium exposure conditions, divided by the duration $V_{t,P}$ of daily exposure pulses. Z (unitless) is plotted (using open points) as a function of 40 values of the (heterogeneous) TCA-elimination rate, V_{ke}, evenly spaced between 0 and 0.1 h^{-1}. The relatively small amount of vertical variation in the plotted points corresponds to three different values of $V_{t,P}$ used (0.01, 0.25, and 0.5 h) conditional on each value of V_{ke} used. To these points was fitted the linear quadratic curve shown: $Z = (0.05053 \text{ h})V_{ke} + (1.6608 \text{ h}^2)V_{ke}^2$. For $V_{ke} < 0.04 \text{ h}^{-1}$, the relative error of this fit using only the linear term (0.05053 h) is <5%.

Based on methods used and data reported by Allen and Fisher (1993), variability in V_{fd} was modeled as uniformly distributed between 5.2 and 15.2%, and as being negatively correlated with V_W with a rank correlation coefficient of $\rho_r(V_{fd}, V_W) = -0.50$; and it was assumed that

$$V_{ke} = 0.028 V_W^{-0.3} V_e \quad , \quad \text{where} \tag{14}$$

V_e = normalized variability in V_{ke} that is independent of variability in V_W (unitless),

and where V_W was previously defined (after Equation 2). It was further assumed that variability in V_{ke} is lognormally distributed. Experimental data reported for 17 male and female human subjects indicates that V_{ke} has a CV of ~0.60 (Fisher et al., 1998). Based on the method of moments (Appendix 1; see discussion concerning V_{max} following Equation 8), it follows that V_e has an AM of 1 and that $V_e \sim LN(-0.152, 0.551)$. Consequently, Equation 14 implies that $V_{ke} < 0.030$ h^{-1} for virtually (>99% of) all modeled individuals at risk. Because $V_{t,ing} < 0.5$ h is assumed as described above, Approximation 13b is accurate (to within <2.5%), and was thus used to evaluate Equation 11. These two equations, together with assumptions stated above, yield:

$$D_{C,P} = \left(X_{C,P} \times 1\,\mathrm{d}\right)\frac{V_{fm,P}}{V_{fd}}\left(\frac{0.6107 V_W^{0.3}}{V_e} + 0.2074\right) \quad , \quad \text{for } P = \{ing, der\}, \quad \text{and} \tag{15a}$$

$$D_{C,inh} = \left(X_{C,inh} \times 1\,\mathrm{d}\right)\frac{V_{fm,inh}}{V_{fd}}\left(\frac{7.878}{V_e} + \frac{2.674}{V_W^{0.3}}\right) \quad , \tag{15b}$$

in which no more than three significant digits are implied, and where: $X_{C,P}$ for pathways P = {ing, inh, or der} were defined by Equations 1a-c, V_W was defined after Equation 2, $V_{fm,P}$ for pathways P were defined in Equations 9a-b, V_{fd} was defined after Equation 10, and V_e was defined after Equation 14. Note that V_{fd} and V_W are assumed to be correlated (as discussed prior to Equation 14), as are V_{alv} and V_{inh} as discussed above (in Section 2.3.3, after Equation 9b).

2.4. TCE Dose-Response

The following subsections discuss methods used to model dose-response for TCE-induced cancer and noncancer endpoints, and associated JUV. Sections 2.4.1 and 2.4.2

describe methods used for dose-response modeling under MA_G and MA_C, respectively. Section 2.4.3 then describes the method used to incorporate uncertainty concerning the mechanism of action for TCE-induced cancer into estimates of cancer risk as well as of corresponding aggregate (cancer and noncancer) risk.

2.4.1. Dose-response assuming genotoxic mechanism(s)

Under MA_G, linear-no-threshold extrapolation of TCE cancer risk is based on the assumption that TCE can increase cancer risk via one or more genotoxic mechanisms of action. These mechanisms involve DNA damage that is presumed to be linearly proportional to the biologically effective concentration of one or more of TCE's reactive metabolites, where potency is estimated for each bioassay in terms of a pharmacologically based equivalent effective dose—namely, the total amount of TCE metabolized per kg body weight per day (Bogen, 1988; EPA, 1985; EPA, 1987b). Effective bioassay doses $D_{C,P}$ and corresponding positive, malignant (plus, where applicable, benign) tumor responses in mouse liver and rat kidney were obtained from information listed in Table 4 of Bogen (1998) concerning seven rodent bioassay data sets (Bell et al., 1978; Maltoni et al., 1986; NCI, 1976; NTP, 1990). The studies involved are summarized below in Table 1. For each data set, a cdf reflecting uncertainty (estimation-error) in estimated cancer potency (i.e., "slope factor", or risk per unit dose), here denoted U_{pot} (kg d mg^{-1}), was calculated as described below (Section 2.6).

A subjective weighting scheme was then used to address uncertainty associated with lack of knowledge concerning which of the multiple positive animal bioassay results for TCE in rodent liver and kidney best predicts TCE cancer risk in humans, similar to an approach previously applied to characterize JUV in cancer risk posed by environmental exposure to chloroform (Bogen, 1995). To each species/sex-specific potency distribution obtained as described above, the corresponding relative weight indicated in Table 1 was applied to obtain a single weighted-average distribution reflecting uncertainty in tumor likelihood conditional on effective dose. (This weighted average was obtained analytically, via calculations analogous to those indicated in Equation 5d.) The weights used assign equal likelihood (of reflecting true carcinogenic potency in humans) to bioassay data sets that differ: by sex within a given strain, by strain within a given species, and by species.

30

Table 1. Bioassay data sets used to estimate potency of TCE as a genotoxic/linear liver or kidney carcinogen

No.	Study[a]	Species	Strain	Sex	Route[b]	Tumor type[b]	No. dose grps.	Relative study weight[c]
1	NCI (1976)	mouse	B6C3F1	M	gav	HCC	3	1
2	NCI (1976)	mouse	B6C3F1	F	gav	HCC	3	1.5
3	NTP (1990)	mouse	B6C3F1	M	gav	HCA	2	1
4	NTP (1990)	mouse	B6C3F1	F	gav	HCA	2	1.5
5	NTP (1990)	rat	F344	M	gav	RTCA	3	12
6	Bell et al. (1978)	mouse	B6C3F1	M	inh	HCA	3	1
7	Maltoni et al. (1986)	mouse	Swiss	M	inh	MH	3	6

[a]More detailed study-specific information appears in Table 4 of Bogen (1988).

[b]Lifetime bioassay exposure scenarios: gav = gavage 5×/wk in oil vehicle; inh = inhalation 6 h/d 5×/wk. Tumor types: HCC = hepatocellular carcinomas; HCA = HCC or hepatocellular adenomas; RTCA = renal tubule-cell carcinomas or adenomas; MH = malignant hepatomas.

[c]Assigned *a priori* relative study weight (see text).

Animal-to-human extrapolation of toxicokinetically equivalent effective dose was done by using an appropriate PBPK model as described above, so no additional factor was employed in this regard in accordance with currently proposed policy (see Section 1.4). An uncertain factor U_{tdyn} was used to account for interspecies toxicodynamic dynamic differences between rodents and humans (i.e., in increased likelihood of cancer per unit effective genotoxic dose). Analogous to toxicodynamic factors recommended recently by EPA for noncarcinogens and "nonlinear" carcinogens (EPA, 1998), but using a probabilistic approach as previously proposed for noncancer endpoints (Carlson-Lynch et al., 1999; Slob and Pieters, 1998), it was assumed U_{tdyn} is lognormally distributed, has a GM of 1 (i.e., is as likely as not to exceed 1), and is unlikely (p < 0.01) to exceed a value of 3. A similar factor V_{tdyn} used to reflect intraspecies toxicodynamic variation was assumed to have an AM of 1 and to be unlikely (p < 0.01) to exceed 10. By the method of moments (Appendix 1), it thus was assumed that $U_{tdyn} \sim LN(0, 1.60)$ and $V_{tdyn} \sim LN(0.700, 2.33)$.

Combining the dose-response factors discussed above, increased risk R_G under MA_G was defined using a low-dose-linear multistage risk-extrapolation model as

$$R_{\mathrm{G}} = 1 - \exp\left\{-\left[U_{\mathrm{pot}}U_{\mathrm{tdyn}}V_{\mathrm{tdyn}}\langle D_{\mathrm{G}}\rangle \sum_{\mathrm{P}=\{\mathrm{ing,inh,der}\}} f_{\mathrm{G,P}}B_{\mathrm{G,P}}\right]\right\}, \qquad \text{with} \qquad (16a)$$

$$\overline{R_{\mathrm{G}}} \approx 1 - \exp\left(-U_{\mathrm{pot}}U_{\mathrm{tdyn}}\langle \overline{D_{\mathrm{G}}}\rangle \overline{B_{\mathrm{G}}}\right), \qquad \text{and} \qquad (16b)$$

$$\langle R_{\mathrm{G}}\rangle \approx 1 - \exp\left\{-\left[\langle U_{\mathrm{pot}}\rangle\langle U_{\mathrm{tdyn}}\rangle V_{\mathrm{tdyn}}\langle \overline{D_{\mathrm{G}}}\rangle \sum_{\mathrm{P}=\{\mathrm{ing,inh,der}\}} f_{\mathrm{G,P}}\langle B_{\mathrm{G,P}}\rangle\right]\right\}, \qquad (16c)$$

in which U_{pot}, U_{tdyn}, and V_{tdyn} were defined above in this subsection, and the remaining variates were defined in/after Equations 5a-b with reference to Equation 6. In Equation 16b, $\overline{B_{\mathrm{G}}} = \overline{B_{\mathrm{G,P}}}$ because (conditional on Equations 1a-c, on Equation 6, and on all heterogeneous variates involved in $B_{\mathrm{C,P}}$), uncertainty in $B_{\mathrm{C,P}}$ is due entirely to uncertainty in the variates ED and C_w (defined after Equations 4b and 4c, respectively) that are both independent of pathway P. Note that the $\langle B_{\mathrm{G,P}}\rangle$ variates in Equation 16c are correlated (see Section 2.6). Equations 16b-c are first-order approximations (see Bogen and Spear, 1987). However, for extrapolation of risks $< 10^{-3}$ the functions involved are effectively linear, so the approximations entail only negligible loss of accuracy.

2.4.2. Dose-response assuming cytotoxic mechanism(s)

The ability of TCE to induce cancer under MA_C was assumed to arise from TCA-induced cytotoxicity/mitogenicity indicated by increased formation of thiobarbituric-acid-reactive substances (TBARS), as previously suggested (Bogen and Gold, 1997). Absent better data, increased TBARS elevation above background was modeled using data on male B6C3F1 mice administered a single gavage dose of 0, 100, 300, 1000, or 2000 mg TCA per kg body weight in buffered water, and corresponding measured peak TCA concentrations in plasma, $Max(C_{TCA})$ (Larson and Bull, 1992a). Multiple independent interactions are likely to be involved in TCA-induced oxidative-stress. Consequently (Aitchison and Brown, 1957), dose-response under MA_C was modeled by fitting the two-parameter LN function

$$Y(A_{\mathrm{TCA}}) = Y_0 + 100\,\Phi\left(\frac{\log_{10}(A_{\mathrm{C}}) - \mu}{\sigma}\right), \qquad \text{where} \qquad (17)$$

A_C = administered acute TCA dose (mg TCA per kg body weight);

$Y(A_C)$= TBARS level induced by A_C (nmol malondialdehyde equiv. per g liver);

Y_0 = $Y(0)$ = background TBARS level (nmol malondialdehyde equiv. per g liver);

$\Phi(z)$ = cumulative probability distribution function (cdf) of a standard normal (Gaussian) random variate Z, equal to Prob($Z \leq z$);

μ = location parameter (unitless); and

σ = shape parameter (unitless);

to the mouse TBARS vs. A_C data (see Section 2.6), where the unit of $Y(A_C)$ is henceforth suppressed for convenience. The arbitrary constant (100) in the two-parameter model (Equation 16) was used because a three-parameter LN model fit to these data did not yield plausibly unique parameter estimates.

Raw $Y(A_C)$ data (4 measures × 4 noncontrol dose levels) summarized by Larson and Bull (1992) were assumed to be approximately normally distributed. Error in the reported Y_0 mean (equal to 40.0) was modeled as T-distributed with 3 degrees of freedom, using the reported value of 4 for the SD of that AM. TBARS elevations above the corresponding 2-tail upper 95% confidence limit on Y_0 were assumed to be biologically significant in the sense of being plausibly related to TCA-induced cytotoxicity. This upper bound on Y_0 shall be denoted Y_{sig}, and the mouse data indicate that $Y_{sig} = 49.4$.

A bootstrap approach was then used to derive the likelihood that any particular dose is associated with a significant, potentially cytotoxic response (Slob and Pieters, 1998). Specifically, 2000 sets of $\{\mu, \sigma\}$ parameter-value pairs were simulated using pairs of rank-correlated T-distributed variates $\{U_{t1}, U_{t2}\}$ each with $[(4 \times 4) - 2] = 14$ degrees of freedom, together with the estimated parameters $\{\hat{\mu}, \hat{\sigma}\}$ and corresponding SDs $\{s_{\hat{\mu}}, s_{\hat{\sigma}}\}$ and product-moment correlation (r) obtained from the LN-model fit to the mouse data. Parameter-value pairs were thus simulated as $\{\mu = \hat{\mu} + s_{\hat{\mu}}U_{t1}, \sigma = \hat{\sigma} + s_{\hat{\sigma}}U_{t2}\}$, using r as the approximate target rank correlation between U_{t1} and U_{t2}. Each of the simulated sets of parameter values corresponds to a critical A_C level at which a significant TBARS response is assumed as discussed above. At the lowest A_C level used (100 mg kg^{-1}) in B6C3F1 mice, it was found that Max(C_{TCA}) = 130 mg L^{-1} (Larson and Bull, 1992a). For convenience, and absent data at lower A_C levels, it was assumed that

$[\text{Max}(C_{TCA})/A_{TCA}] = [(130 \text{ mg L}^{-1})/(100 \text{ mg kg}^{-1})]$ independent of A_{TCA}. Critical effective doses corresponding to the 2000 simulated $\{\mu, \sigma\}$ parameter-value pairs were therefore modeled as

$$D_{Ca} = (1.3 \text{ mg L}^{-1})10^{\mu + \sigma\Phi^{-1}[(Y_{sig}-Y_0)/100]}$$

$$= (1.3 \text{ mg L}^{-1})10^{(\hat{\mu}+s_{\hat{\mu}}U_{t1}) + (\hat{\sigma}+s_{\hat{\sigma}}U_{t2})\Phi^{-1}[(Y_{sig}-Y_0)/100]} \sim F_C(D_{Ca}) \text{ , where} \qquad (18)$$

D_{Ca} = acute effective TCA dose (mg TCA per L plasma);

Y_{sig} = significantly elevated value of $Y(A_{TCA})$ above Y_0 (unit suppressed);

U_{ti} = (for i=1,2) correlated errors distributed as Student's T cdfs with df = 14; and

$F_C(D_{Ca})$ = cdf of D_{Ca} specifying the modeled likelihood of significant TBARS elevation conditional on D_{Ca};

where Y_0 was defined after Equation 17, and the parameter estimates $\hat{\mu}$, $s_{\hat{\mu}}$, $\hat{\sigma}$, and $s_{\hat{\sigma}}$, as well as the T-distributed variates U_{t1} and U_{t2}, were all defined just prior to Equation 18. The 2000 simulated (equally likely) D_{Ca} values obtained using Equation 18 were then sorted to provide a preliminary estimate of $F_C(D_{Ca})$. Because only 2000 simulated D_{Ca} values were used for the preliminary estimate of $F_C(D_{Ca})$, D_{Ca} values corresponding to risk values < 2001^{-1} were extrapolated from the preliminary cdf estimate (see Section 2.6). The resulting combined (preliminary + extrapolated) estimate of $F_C(D_{Ca})$ was used to represent the risk of significant TBARS response in mouse liver conditional on D_{Ca}. Absent dose-response data on TCA-induced lipoperoxidation or cytotoxicity in rat kidney, it was assumed that $F_C(D_{Ca})$ also applies to rat kidney. This assumption is probably conservative, because relation between A_C and $\text{Max}(C_{TCA})$ was observed to be similar in rats vs. mice, whereas TCA is less effective at inducing TBARS elevation in rats vs. mice (Larson and Bull, 1992a).

Detailed dose-response information relating chronically or subchronically administered TCA and induced TBARS or cytotoxicity are still unavailable. Therefore, extrapolation of D_{Ca} to equivalent subchronic effective TCA dose, and extrapolation of subchronic to chronic effective TCA dose (where the latter is denoted D_C, and is defined by Equations 5a, 11, and 15a-b), was accomplished using the two uncertainty factors, U_{acute} and $U_{subchron}$, respectively. As previously suggested (Slob and Pieters, 1998), these factors were assumed to be lognormally distributed. Based on the observation that ratio

of lowest observed effect levels for TCE-induced lethality in B6C3F1 mice is between 2 and 3 (NCI, 1976), it was assumed that U_{acute} has a GM of $GM_{acute} = 3$ and is unlikely ($p < 0.01$) to be greater than 6. The factor $U_{subchron}$ was assumed by default (see Slob and Pieters, 1998) to have a GM of $GM_{subchron} = \sim 2$ and to be unlikely ($p < 0.01$) to exceed 10. Because many repeated daily exposures to TCE and/or its metabolite TCA are expected to be always more (never less) toxic than fewer exposures, it was assumed that a combined uncertainty factor (U_{chron}) extrapolates effective dose from acute to chronic exposure conditions as follows:

$$D_C = (1 + U_{chron})D_{Ca} \, , \quad \text{where} \tag{19a}$$

$$U_{chron} = U_{acute} \times U_{subchron}\left(1 - (GM_{acute}GM_{subchron})^{-1}\right) . \tag{19b}$$

That is, the combined LN factor U_{chron} was assumed to have a GSD equal to that of $U_{acute} \times U_{subchron}$ and a GM equal to one less than that of $U_{acute} \times U_{subchron}$. By the method of moments (Appendix 1), it was thus assumed that $U_{chron} \sim LN(\ln 5, \ln 2.12)$.

Animal-to-human extrapolation of toxicokinetically equivalent effective dose was done by using an appropriate PBPK model as described above, so no additional factor was employed in this regard in accordance with currently proposed policy (see Section 1.4). An uncertain factor U_{tdyn} was used to account for interspecies toxicodynamic dynamic differences between rodents and humans, and a similar factor V_{tdyn} to reflect intraspecies toxicodynamic variation, where U_{tdyn} and V_{tdyn} were defined above (in Section 2.4.1, prior to Equation 16).

Combining the dose-response factors discussed above, increased risk R_C under MA_C was modeled as

$$R_C = F_C\left(U_{tdyn}V_{tdyn}(1 + U_{chron})\langle \overline{D_C} \rangle \sum_{P=\{ing,inh,der\}} f_{C,P}B_{C,P}\right) , \quad \text{with} \tag{20a}$$

$$\overline{R_{Cl}} \approx F_C\left(U_{tdyn}(1 + U_{chron})\langle \overline{D_C} \rangle \overline{B_C}\right) , \quad \text{and} \tag{20b}$$

$$\langle R_{Cl} \rangle \approx F_C\left(\langle U_{tdyn} \rangle V_{tdyn}(1 + \langle U_{chron} \rangle)\langle \overline{D_C} \rangle \sum_{P=\{ing,inh,der\}} f_{C,P}\langle B_{C,P} \rangle\right) , \tag{20c}$$

35

in which U_{chron}, U_{tdyn}, and V_{tdyn} were defined above in this subsection; the remaining variates were defined in/after Equations 5a-c with reference to Equations 11 and 15a-b; and the subscript "1" in R_{C1} denotes first-order approximation. In Equation 20b, $\overline{B_C} = \overline{B_{C,P}}$ because (conditional on Equations 1a-c and 15a-b, and on all heterogeneous variates involved in $B_{C,P}$) uncertainty in $B_{C,P}$ is due entirely to uncertainty in the variate C_w (defined after Equation 4c), which in turn is independent of pathway P. Note that the $\langle B_{C,P} \rangle$ variates in Equation 20c are correlated (see Section 2.6).

As indicated, Equations 20b-c are again first-order approximations (see text following Equations 16b-c). In this case, however, the approximations are expected to underestimate risk, because—in contrast to the exponentiated polynomial in Equations 16b-c—F_C is a rather nonlinear increasing function of effective dose (see Bogen and Spear, 1987). At low levels of risk ($< 10^{-3}$), $\log(F_C(D_{Ca}))$ turns out to be well modeled by a linear function of effective dose D_{Ca}, as explained below (Sections 2.6 and 3.2). Therefore, the approach of Bogen and Spear (1987) may be applied (as shown in Appendix 2.I, pp. H-8 to H-10) to provide corresponding, more accurate second-order approximations that were used to calculate the corresponding conditional risks under MA_C:

$$\overline{R_C} \approx \overline{R_{C1}} + \frac{1}{2}10^{\hat{a}}\left(U_{tdyn}(1+U_{chron})\times 0.0269\right)^{\hat{b}}(\hat{b}-1)(1.05+2.58) \quad , \text{ and} \qquad (20d)$$

$$\langle R_C \rangle \approx \langle R_{C1} \rangle + \frac{1}{2}10^{\hat{a}}\left(V_{tdyn}\times 0.0269\times 8.50\right)^{\hat{b}}(\hat{b}-1)\left(\frac{65.6}{8.50^2}+1.02\right) , \qquad (20e)$$

in which the log-linear regression parameters a and b are defined below in the context of Equation 23 (Section 2.6).

2.4.3. Model Uncertainty

In view of the plausibility of both MA_G and MA_C (see Section 1.3), uncertainty in the mechanism(s) of carcinogenic action for TCE was treated quantitatively, based on the "dichotomous" mechanistic assumption ($MA_{G \cup C}$) involving both MA_G and MA_C discussed above (Section 2.3). The alternative corresponding "composite" assumption ($MA_{G \cap C}$), which also involves both MA_G and MA_C (as discussed in Section 2.3), is more difficult to implement quantitatively than $MA_{G \cup C}$. $MA_{G \cap C}$ is more difficult to implement

because it requires a complete model structure accounting for possible but unknown interactions between the different mechanisms considered. In contrast, $MA_{G \cup C}$ may be implemented simply by assigning the component assumptions (MA_G and MA_C) corresponding, complementary *a priori* probabilities, and using the combination of these probabilities to reflect the (quantitatively equivalent) possibility that both MA_G and MA_C are true but to unknown degrees. $MA_{G \cup C}$ was therefore adopted using subjective probabilities U_G and $U_C = (1-U_G)$ to reflect the corresponding likelihoods that MA_G and MA_C, respectively, reflect the "true" mechanism of TCE-induced carcinogenic action. Consistent with our considered opinion that MA_C is *at least* as likely as not to explain observed TCE-induced cancer in rodent bioassays (see also Bogen and Gold, 1997), U_G was modeled as uniformly distributed between 0 and 0.5. Therefore, using de Morgan's rule (see NRC, 1994; Appendix I), increased *aggregate* risk R of incurring *either* a cancer *or* a noncancer endpoint was modeled as

$$R \quad = \quad 1 - (1 - U_G R_G)(1 - R_C) \ , \tag{21}$$

in which U_G was just defined; R_G and R_C were defined by Equations 16a and 20a, respectively; and correlations between R_G and R_C were incorporated (see Section 2.6).

2.5. Risk Characterization

Increased health risk and related JUV associated with residential exposure to TCE from ground water at Site LF-13 on Beale Air Force Base in California was characterized quantitatively using notation similar to those used in the Phase-1 report (Daniels et al., 1999). Specifically, increased individual risk R defined by Equation 21 was evaluated using established methods (Bogen, 1995; Bogen and Spear, 1987; NRC, 1994) to obtain mean and upper-bound values of the conditional expectations $\overline{R}$ and $\langle R \rangle$, where the cdf for $\overline{R}$ represents uncertainty in risk to a (hypothetical) person at a population-average level of risk relative to others, and the cdf of $\langle R \rangle$ represents interindividual variability in the expected values of risk predicted for different people. A subscript p $(0 \le p \le 1)$ on either of these conditional expectations is used to denote a $100p$th percentile at which the corresponding cdf is evaluated, while $R_{u,v}$ $(0 \le u \le 1,$ $0 \le v \le 1)$ is used to denote joint $100u$th-uncertainty and $100v$th-variability percentiles with respect to JUV in R. Estimates of $R_{u,v}$ were obtained jointly conditional on one of three upper bounds u (0.50, 0.95 or 0.99) with respect to aggregate uncertainty, and on

one upper bound ($v = 0.99$) with respect to aggregate variability. These $R_{u,v}$ estimators characterize median and upper uncertainty bounds on risk to a person who is relatively highly at risk compared to others at risk.

The JUV-explicit estimators of individual risk obtained (involving $\overline{R}$, $\langle R \rangle$, and $R_{u,v}$) were compared to traditional point-estimates of risk $\hat{R}_{RME}$ and $\hat{R}_{High}$ taken from Daniels et al. (1999). The $\hat{R}_{RME}$ estimate was calculated entirely analytically, using regulatory default values for all input variates where available; where default values were not available, expected values were used for all uncertain variates, and upper/unlikely bounds (e.g., 95th percentile values) were used for all heterogeneous variates. The $\hat{R}_{High}$ estimate was similarly calculated using only upper/unlikely bounds for all input variates.

Also of potential interest to stakeholders and decision makers are corresponding estimates of population risk, that is, of the uncertain total number N of additional cases of TCE-induced cancer or noncancer associated with population exposure to risk R. For an exposed population of total size n, N has an expected value of $\langle N \rangle = n \langle \overline{R} \rangle$, and the probability p_0 that there will be zero additional cases (and consequently zero health benefit from efforts to reduce R) is well approximated by the integral of the conditional Poisson likelihood function

$$p_0 \approx \int_0^1 e^{-n\overline{R}} f_{\overline{R}}(r)\, dr \ , \tag{22}$$

in which $f_{\overline{R}}(r)$ is probability density function of the uncertain conditional expectation $\overline{R}$ referred to above (in reference to R defined by Equation 21), and the compound-Poisson rate ($n\overline{R}$) incorporates this same conditional expectation (see Bogen and Spear, 1987; NRC, 1994; Bogen, 1995).

2.6. Data Analysis and Computation

Uncertain cancer potency U_{pot} for each animal-bioassay data set was calculated using a computationally efficient, non-asymptotic, analytic-bootstrap method previously described (Bogen, 1994). Briefly, potency was estimated for each bioassay data set using least-squares polynomial-regression fits of a polynomial in LTWA

effective bioassay dose $D_{C,P}$ to 500 simulated values of $-\ln[1 \pm P(D_{C,P})]$, based on observed tumor-occurrence rates $P(D_{C,P})$ at each level of $D_{C,P}$ used, and under the constraint that all fitted polynomial terms are ≥ 0. The polynomial degree was specified in the usual way, as previously described (Anderson et al., 1983). Uncertainty in U_{pot} reflected by each data set was then modeled as the empirical distribution corresponding to the 500 resulting fitted values of the linear polynomial term in dose.

Estimated parameter and asymptotic SD values were obtained for a lognormal model (Equation 17) fit to mouse TBARS-vs.-A_C data by Levenberg-Marquardt minimization of X^2, the sum of weighted squared deviations of observed from predicted values; corresponding goodness-of-fit was assessed as $\text{Prob}(X^2 > x)$ for x distributed as chi-square with (# data points) – (# parameters estimated) degrees of freedom (df) (Press et al., 1992). The weight used for each A_C level was the corresponding value s^{-2}, where s = the SD of raw TBARS measures calculated from the SD of the corresponding mean TBARS value reported by (Larson and Bull, 1992a).

Low-risk extrapolation of the 2000-point preliminary estimate of $F_C(D_{Ca})$ was done by obtaining the unweighted least-squares linear regression fit of the function

$$\log_{10} F_C(D_{Ca}) \;=\; a + b \log_{10} D_{Ca} \qquad\qquad (23)$$

to log-log transformed subset of the preliminary cdf, namely, to the first 50 $\{\log_{10} D_{Ca}, \log_{10} F_C(D_{Ca})\}$ points of the preliminary cdf. New points defined in terms of the estimated parameters $\{\hat{a}, \hat{b}\}$ were then added to the preliminary cdf. The added points were the 26 points $\{10^{(y-\hat{a})/\hat{b}}, 10^{y}\}$ defined for y ranging from -9 to -3.5 by intervals of 0.25.

Monte-Carlo methods were used to generate sample values for each of (say, k) distributed variates involved in a given calculation. Specifically, systematic Latin-hypercube sampling was used to simulate n_{sam} samples of each required set of k variates, where k was determined by the equation(s) being evaluated, and a method (Iman and Conover, 1982) was used to obtain rank-correlated sample vectors, each with a rank-correlation matrix M_i ($i = 1,...,k$) not significantly different ($p_{adj} > 0.05$) from a specified target matrix T, which by default was a $k \times k$ identity matrix modified to reflect correlations specified below. A value of $n_{sam} = 2000$ was used unless otherwise

39

specified. The k differences between M_i and T were each assessed using an asymptotic chi-square test (Jennrich, 1970), and the p-value from each test was adjusted (to p_{adj}, to account for k independent tests) using Hommel's Bonferroni-type procedure (Wright, 1992). Typically, $\text{Min}(p_{adj}) > 0.95$; occasional sample vectors not satisfying $p_{adj} > 0.01$ were rejected. Each simulation was repeated n_{sim} times, a grand AM and its CV (denoted CVM, where $\text{CVM} = \text{CV}[n_{sim}]^{-0.5}$) from the n_{sim} cdf-specific AMs, and the AM and CVM were calculated for each ith set of n_{sim} cdf-specific order statistics (i.e., cdf-abscissa values), where $i = 1,...,n_{sam}$. The calculated CVM values reflect simulation quality by indicating the relative size of Monte-Carlo sampling error produced for estimators of interest conditional on the values of n_{sam} and n_{sim} used.

Target rank-correlation values or matrices were estimated for all sets of correlated variates noted or implied above, namely, the sets: $\{V_{fm,inh}, V_{alv}\}$, $\{V_{fd}, V_W\}$, $\left\{ \langle B_{G,ing} \rangle, \langle B_{C,ing} \rangle, \langle B_{G,inh} \rangle, \langle B_{C,inh} \rangle, \langle B_{G,der} \rangle, \langle B_{G,der} \rangle \right\}$, $\left\{ \overline{B_G}, \overline{B_C} \right\}$, and $\{U_{t1}, U_{t2}\}$ (see Results, Sections 3.1 and 3.2). These correlations were used, respectively, to evaluate: $D_{G,inh}$ and $D_{C,inh}$ in Equations 6 and 15b; $D_{C,P}$ in Equations 15a-b; $\langle B_{MA,P} \rangle$ in Equations 16c and 20c; $\overline{B_{MA}}$ in Equations 16b and 20b, and $F_C(D_{Ca})$ in Equation 18. In calculations to estimate correlations involving $\langle B_{MA,P} \rangle$, values of $n_{sim} = 500$ and $n_{sam} = 50$ were used.

Correlations involving all the variate sets listed above were used in nested (i.e., two-dimensional) Monte-Carlo evaluations of Equation 21 (which, in this case, refers to Equations 16a and 20a) that were performed to estimate $R_{u,v}$. For these nested calculations, values of $n_{sim} = 100$ and $n_{sam} = 999$ were used, with n_{sam} used to simulate all uncertain variates, and then used again to simulate all heterogeneous variates conditional on each of the n_{sam} simulated sets of uncertain variates. Because $\langle B_{MA} \rangle \approx \langle B_{MA,P} \rangle$ and $\overline{B_{MA}} \approx \overline{B_{MA,P}}$ for all pathways P (see Results, Section 3.1), $\langle B_{MA} \rangle$ and $\overline{B_{MA}}$ were used to evaluate Equations 16b and 20d, rather than $\langle B_{MA,P} \rangle$ and $\overline{B_{MA,P}}$. However, to evaluate Equations 16a, 16c, 20a, and 20e, pathway-specific dose correlations noted above were applied to $\langle B_{MA} \rangle$ and $\overline{B_{MA}}$ to regenerate the pathway-specific variates involved in these equations.

All calculations were performed on a 400-MHz PowerMac G3 using the programs *Mathematica*® 3.0 (Wolfram, 1996) and *RiskQ* (Bogen, 1992). Documentation of these

calculations appears in Appendices 2.A through 2.I, in which calculations and related comments are organized by topic. Appendices 2.A (Concentration), 2.B (Intakes), and 2.C (Fraction of Lifetime at One Local Residence) all document the derivation or re-derivation of exposure-related input variates explained in Daniels et al. (1999), which were used to calculate TCE exposures as explained above (Section 2.2). Appendices 2.D (Effective Genotoxic Dose) and 2.E (Effective Cytotoxic Dose) document the calculation of corresponding biologically effective (TCE or TCA) doses. Note that calculations pertaining to the definition or characterization of variates V_W, V_{Vmax}, $V_{fm,ing}$, V_{fd}, $(f_{deq}/V_{t,P})$ and V_e all appear in Appendix 2.E. Appendix 2.F (Effective Dose Correlations) documents calculations made to estimate rank correlations among MA- and pathway-specific normalized biologically effective doses. Appendix 2.G (Potency) documents all calculations made pertaining to modeled dose-response under both mechanisms of carcinogenic action considered (MA_G and MA_C). Appendix 2.H (TCE Risk) documents all calculations made pertaining to corresponding predicted risk. Note that calculations pertaining to the definition of variates U_{chron}, U_{tdyn}, and V_{tdyn} appear in Appendix 2.H. Finally, Appendix 2.I (Functions Used) briefly describes all *Mathematica*® and *RiskQ* functions used to carry out calculations documented in Appendices 2.A-2.H. More detailed explanation of *Mathematica*®, *RiskQ*, and JUV analysis is beyond the scope of this report, and is provided in references cited.

All constants and variates defined in this report that were used as input to estimate risk, as described above in Sections 2.1 - 2.6, are summarized in the following table (Table 2).

41

Table 2. Constants and variates used as input for unified TCE risk assessment[a]

Input type[b]	ID[b]	Description	Unit	1st used in or near Equation(s) #	Distribution type, parameter value(s)[c]			Reference(s)[d]
					Dist	μ	σ	
K	fTCA	Fraction of total TCE intake metabolized to TCA	unitless	10		0.33		Allen & Fisher (1993)
K	MW	TCA to TCE molecular-weight ratio	unitless	10		1.228		Bogen & Gold (1997)
P	Y_0	Background relative TBARS level in mouse liver	unitless	17, 18		40		Larson & Bull (1992)
P	Y_{sig}	Significantly elevated relative TBARS level	unitless	18		49.4		Larson & Bull (1992)*
P	$\hat{\mu}, s_{\hat{\mu}}$	Estimated location parameter of lognormal cytotoxicity dose-response model, and its SD	unitless	18		3.05	0.0920	Calculated from data of Larson & Bull (1992)
P	$\hat{\sigma}, s_{\hat{\sigma}}$	Estimated shape parameter of lognormal cytotoxicity dose-response model, and its SD	unitless	18		0.732	0.176	Calculated from data of Larson & Bull (1992)
P	$\hat{a}$	Estimated log-linear-regression intercept parameter used to extrapolate cytotoxicity dose-response	unitless	23		-7.60		Calculated (see text)
P	$\hat{b}$	Estimated log-linear-regression slope parameter used to extrapolate cytotoxicity dose-response	unitless	23		3.68		Calculated (see text)
U	pot	Carcinogenic potency of TCE assuming a genotoxic mechanism of action	kg d mg⁻¹	16	Emp	3.7×10^{-4}		Calculated from data on 7 studies (see text)
U	tdyn	Uncertainty factor for interspecies extrapolation of toxicodynamically equivalent effective dose	unitless	16, 20	LN	0	1.6	EPA (1998)* Slob & Pieters (1999)*
U	chron	Uncertainty factor for extrapolation of acute to chronic cytotoxic dose	unitless	19	LN	ln 5	ln 2.12	NCI (1976)* Slob & Pieters (1999)*

Table 2. Constants and variates used as input for unified TCE risk assessment[a] (continued)

Input type[b]	ID[b]	Description	Unit	1st used in or near Equation(s) #	Distribution type, parameter value(s)[c]			Reference(s)[d]
					Dist	μ	σ	
U	t1	Normalized estimation error in $\hat{\mu}$	unitless	18	T[f]	14		Assumed
U	t2	Normalized estimation error in $\hat{\sigma}$	unitless	18	T[f]	14		Assumed
V	W	U.S. adult male and female body weight	kg	2	LN[e]	4.24	0.221	Finley (1994) CalEPA (1996, p. 10-7)
V	alv	Normalized variability in alveolar ventilation rate, independent of variability in V_W	unitless	2, 3	LN	-0.0409	0.286	CalEPA (1996, p. 3-31)*
V	Pb	Human blood:air partition coefficient for TCE	L_{air}/L_{blood}	7	N	10.2	1.6	Fisher (1998)*
V	liv	Human blood flow to liver = 26%×(15.0/12.9)×V_{alv}	mL h^{-1}	8	(see V_{alv})			Allen & Fisher (1993)
V	V_{max}	Normalized variability in the maximum rate of TCE metabolism, independent of variability in V_W	unitless	8	LN	-0.152	0.551	Lipscombe et al. (1998)*
V	fd	Fraction of V_W corresponding to apparent volume of distribution for TCA	L kg^{-1}	10	U[e]	0.052	0.152	Allen & Fisher (1993)*
V	e	Normalized variability in TCA elimination rate V_{ke}, independent of variability in V_W	unitless	10		-0.152	0.551	
V	tdyn	Variability factor modeling intraspecies differences in sensitivity (i.e., in toxicodynamically equiv. dose)	unitless	16, 20	LN	0.700	2.33	EPA (1998)* Slob & Pieters (1998)*

[a]Constants and variates listed are those defined in this report and used or implied in Equations 1 - 21 as inputs to risk estimation. Variates defined by Equations 1 - 21 are not repeated in this table. All other variates that were used to estimate risk are either defined in Daniels et al. (1999), or are defined in Equations 1 - 21 in terms of constants and variates listed in this table.

[b]Input types: K = constant, P = estimated (hence, constant) parameter value, U = uncertain variate, V = heterogeneous variate (i.e., values pertain to different individuals at risk). ID = the subscript that appears in the text on a K-, U- or V-type input; ID = the symbol used in the text to denote a P-type input.

Table 2. Constants and variates used as input for unified TCE risk assessment[a] (footnotes continued)

[c]Dist specifies distribution type: LN = lognormal, N = standard normal, T = Student's T, U = uniform, Emp = calculated empirical, Blank = not applicable. The values $\{\mu, \sigma\}$ = {the estimated/assigned value, (if applicable) the SD} of for K- or P-type inputs; otherwise $\{\mu, \sigma\}$ denote (for the specified Dist): {ln GM, ln GSD} (LN), {AM, SD} (N), {df, –} (T), and {min, max} (U).

[d]An asterisk signifies that the value or approach cited was modified slightly or generalized for use in this report.

[e,f]These variates assumed to have a rank correlation equal to: -0.50[e], 0.294[f].

3. RESULTS

Resulting estimates of biologically effective dose TCE contamination at Site LF-13 are presented below in Section 3.1, followed (in Section 3.2) by estimated dose-response relations obtained. Finally, Section 3.3 provides a characterization of corresponding risks and associated JUV estimated using the unified probabilistic approach applied in this study, as well as a comparison of these estimates with point-estimates of risk for Site LF-13 obtained using traditional methods.

3.1 Biologically Effective Dose

The cdfs obtained to characterize variability in the limiting fraction $V_{fm,ing}$ of low-level ingested TCE that is metabolized, and in the corresponding limiting fraction $V_{fm,inh}$ (= $V_{fm,der}$) of low-level respired or dermally absorbed TCE that is metabolized, are shown in Figure 3. The variates $\{V_{fm,inh}, V_{alv}\}$ were found to have an approximate rank correlation of -0.75 (CVM = 0.33%). Although not used in calculations performed in this study, the rank correlation between variates $\{V_{fm,ing}, V_{fm,inh}\}$ was found to be ~0.83 (CVM = 0.30%).

The JUV-expectation of genotoxic effective dose, $\langle \overline{D_G} \rangle$, was found to be 5.93×10^{-5} mg kg^{-1} d^{-1} (CVM < 1%), with corresponding pathway-specific dose fractions: $f_{G,ing} = 0.843$, $f_{G,ing} = 0.039$, and $f_{G,ing} = 0.118$. The JUV-expectation of cytotoxic effective dose, $\langle \overline{D_C} \rangle$, was found to be 0.0269 mg L^{-1} (CVM < 1%), with corresponding pathway-specific dose fractions: $f_{G,ing} = 0.604$, $f_{G,ing} = 0.312$, and $f_{G,ing} = 0.084$.

The cdfs obtained for the three pathway-specific expectations with respect to uncertainty in normalized effective genotoxic dose ($\langle B_{G,P} \rangle$ for P ={ing, inh, der}, shown as three bold curves), and for the corresponding three pathway-specific expectations with respect to variability in normalized effective genotoxic dose ($\overline{B_{G,P}}$, three light curves), are plotted in Figure 4a. The figure shows that the three pathway-specific curves that comprise each set of (bold or light) curves are virtually indistinguishable. The cdfs obtained for the three pathway-specific expectations with respect to uncertainty in normalized effective cytotoxic dose ($\langle B_{C,P} \rangle$, three bold curves), and for the corresponding three pathway-specific expectations with respect to variability in

normalized effective cytotoxic dose ($\overline{B_{C,P}}$, three light curves), are plotted in Figure 4b. The figure shows that the three pathway-specific curves that comprise $\overline{B_{C,P}}$ (light curves) are virtually indistinguishable, while those comprising $\langle B_{C,P} \rangle$ (bold curves) are nearly so. Thus $\langle B_{MA} \rangle \approx \langle B_{MA,P} \rangle$ and $\overline{B_{MA}} \approx \overline{B_{MA,P}}$ for all pathways P, which justifies the exclusive reliance on $\langle B_{MA} \rangle$ and $\overline{B_{MA}}$ for calculations described in Methods. The variates $\left\{ \overline{B_G}, \overline{B_C} \right\}$ were found to have an approximate rank correlation of -0.49 (CVM = 0.67%), and rank-correlation and corresponding CVM matrices obtained for the six $\langle B_{MA,P} \rangle$ variates are listed below in Table 3.

3.2 Dose-Response

The cdfs characterizing estimation error (uncertainty) in cancer potency U_{pot} estimated for each of seven animal-bioassay data sets considered are shown in Figure 5a; the corresponding weighted-average cdf based on weights indicated in Table 1 is shown in Figure 5b.

The fit of the lognormal model specified by Equation 17 to mouse TBARS-vs.-A_C data is shown in Figure 6a. The model fit the experimental data reasonably well ($X^2 = 13.6$, df = 14, p = 0.48). The two corresponding parameter estimates (±SD) $\{ \hat{\mu} = 3.05 \pm 0.0920, \hat{\sigma} = 0.732 \pm 0.176 \}$ obtained from the fit, as well as their approximate rank correlation ($r = 0.294$), were used to obtain a preliminary estimate of $F_C(D_{Ca})$ (see Methods, Section 2.6). The fit of the function, $a + b \log_{10} D_{Ca}$, obtained to the first 50 $\{ \log_{10} D_{Ca}, \log_{10} F_C(D_{Ca}) \}$ points of the preliminary $F_C(D_{Ca})$ estimate is shown in Figure 6b; the two corresponding parameter estimates (±SD) obtained were $\{ \hat{a} = -7.60 \pm 0.0794,$ $\hat{b} = 3.68 \pm 0.521 \}$. The risk-extrapolation model fit the empirical (simulation-generated) data points of the preliminary cdf very well ($F_{1,48} = 4974.2$, $R^2 = 0.99$, df = 48, 2-tail p $\approx$ 0), indicating stable (hence, reliably modeled) lower-tail behavior. The resulting cdf (i.e., combined set of extrapolated + preliminary points) estimating $F_C(D_{Ca})$ is shown in Figure 7.
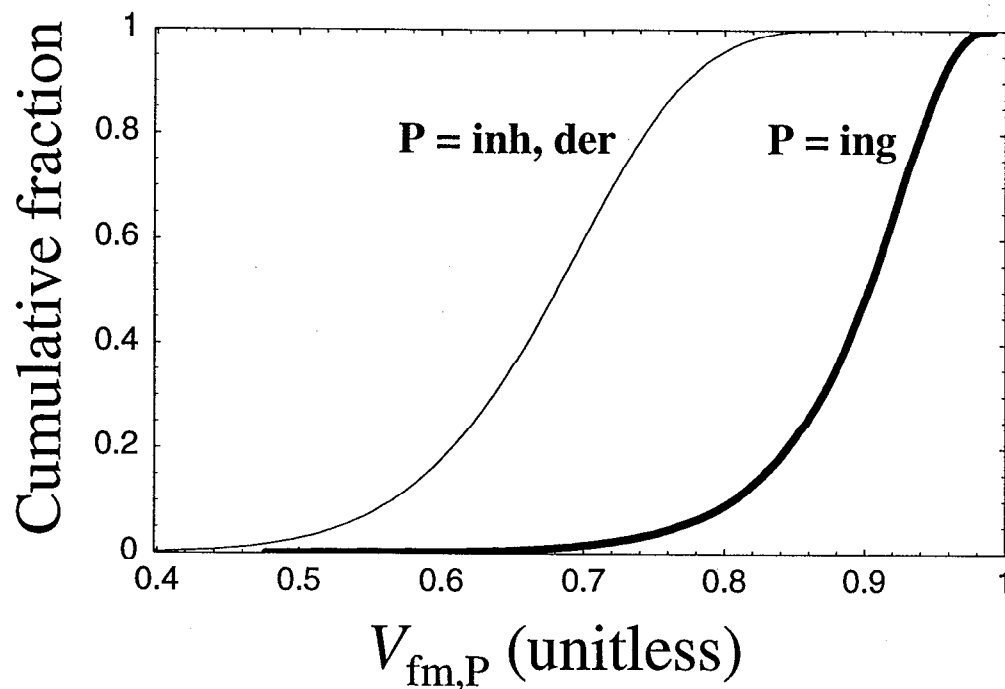
Figure 3. Cumulative distribution functions characterizing interindividual variability in limiting metabolized fractions $V_{fm,P}$ of low-level TCE absorbed via different exposure pathways P, where P = {ing, inh, and der} for {ingestion, ihalation, and dermal} pathways, respectively.
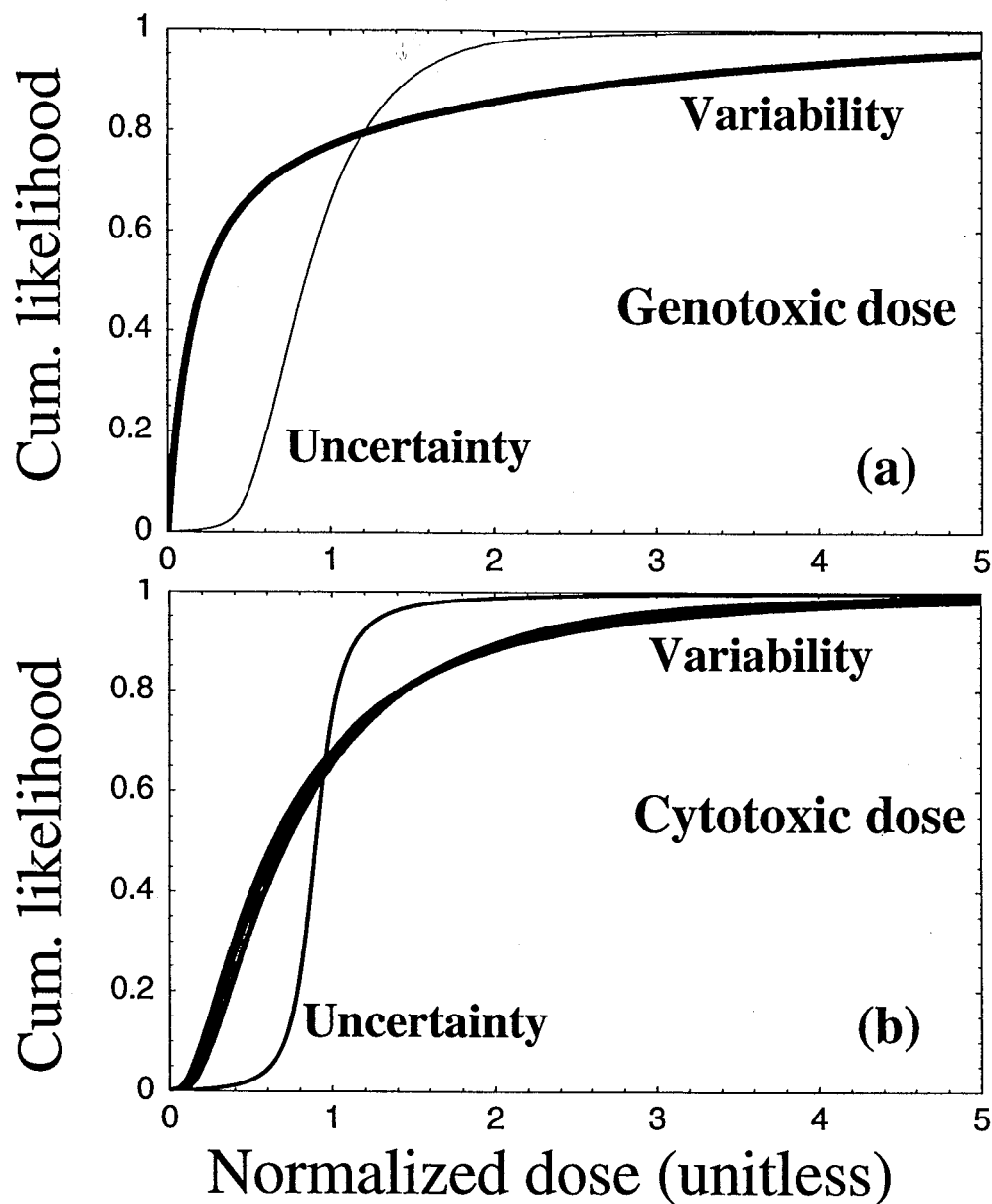
Figure 4. Expectations with respect to uncertainty vs. variability in normalized effective (a) genotoxic and (b) cytotoxic dose. Cumulative distribution functions (cdfs) shown characterize normalized interindividual variability in values of expected dose (bold curves), and normalized uncertainty in the population-average value of dose (light curves) predicted for hypothetical residents exposed to TCE from ground water at Site LF-13. Three bold and three light exposure-pathway-specific curves appear in each plot; however, all these curve sets very nearly coincide, except for slight divergence in the case of the bold curves in (b). All the cdfs have an arithmetic mean value of one by definition.

Table 3. Rank correlations among uncertainty-expectations of normalized biologically effective doses[a]

$\langle B_{\mathrm{MA,P}}\rangle$ variate		$\langle B_{\mathrm{MA,P}}\rangle$ variate										
		MA P		MA P		MA P		MA P		MA P		MA P
		G ing		C ing		G inh		C inh		G der		C der
MA P	G ing	1		0.23		0.88		0		0.89		0
MA P	C ing	0.23		1		0		0.42		0		0.51
MA P	G inh	0.88		0		1		0.19		0.92		0.035
MA P	C inh	0		0.42		0.19		1		0.077		0.65
MA P	G der	0.89		0		0.92		0.077		1		0.18
MA P	C der	0		0.51		0.035		0.65		0.18		1

[a]Estimated values of the Spearman rank correlation coefficient (r, shown with two significant digits) based on Monte-Carlo evaluation of the uncertainty-expectation of Equation 5c based on Equations 6 and 15a-b, where $n_{\mathrm{sam}} = 500$ and $n_{\mathrm{sim}} = 50$. For all r-values listed, SDM < 0.0025 where SDM $= (n_{\mathrm{sim}})^{-1/2}\mathrm{SD}(r)$ and SD(r) denotes the SD of the n_{sim} estimates of r obtained.

3.3 Predicted Risk

The individual risks predicted in this study correspond to the assumption that the assumed TCE concentration in ground water beneath Site LF-13 (~22 ppb, as of 1997) remains unchanged (see Daniels et al., 1999). The cdfs obtained that characterize uncertainty in the predicted population-average value of individual risk, $\overline{R}$, and interindividual variability in expected values (i.e., "best" estimates) of individual risk, $\langle R\rangle$, are shown in Figures 8a and 8b, respectively, plotted together with corresponding CVM values. The cdfs $\overline{R}$ and $\langle R\rangle$ are contrasted over different ranges of risk in Figures 9a-c. Figures 10a-b compare cdfs with respect to variability (v) in JUV estimators $R_{u,v}$

49

Bioassay-specific potency distributions

Weighted average potency distribution
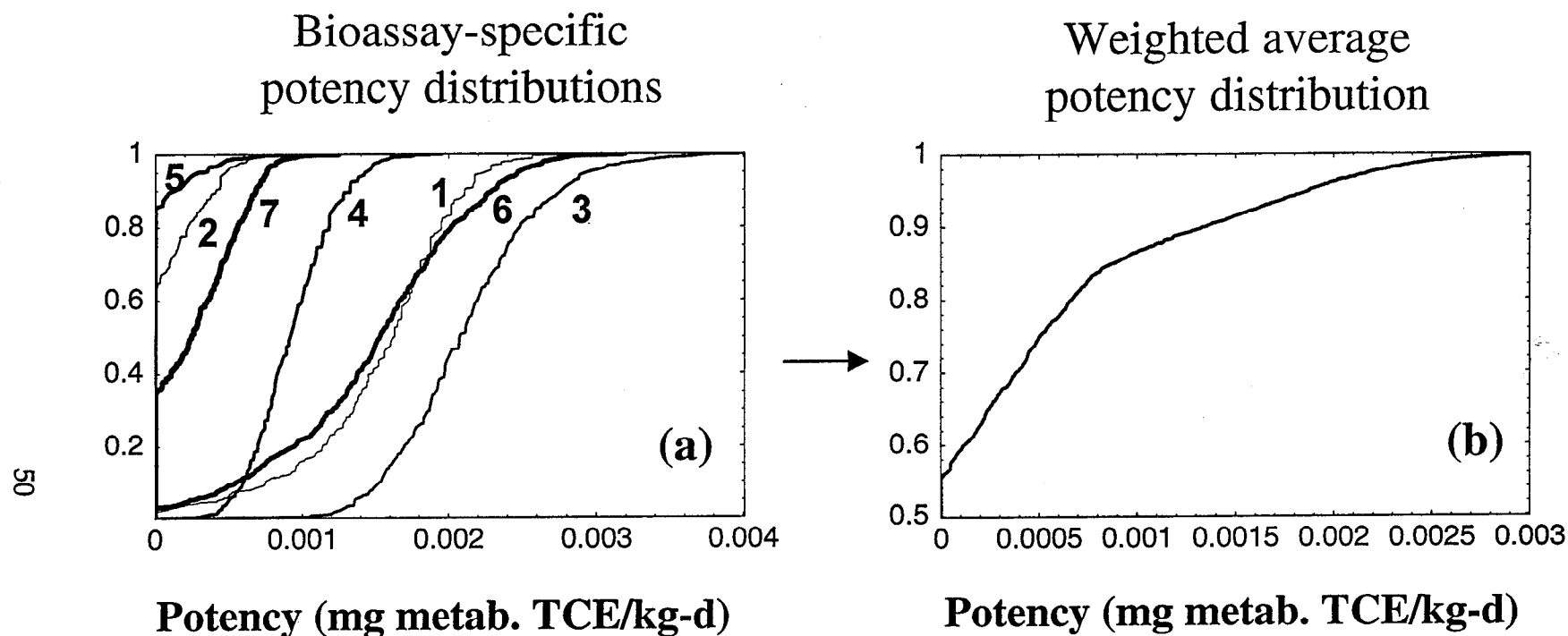
Figure 5. Estimation error (uncertainty) in cancer potency based on rodent-bioassay data. Cumulative distribution functions (cdfs) shown characterize uncertainty in potency estimates based on (a) individual data sets, and (b) a corresponding weighted average of the species/strain/sex-specific cdfs. The numbers labeling individual cdfs in (a) correspond to the study numbers listed in the first column of Table 1. The vertical axis represents cumulative probability.
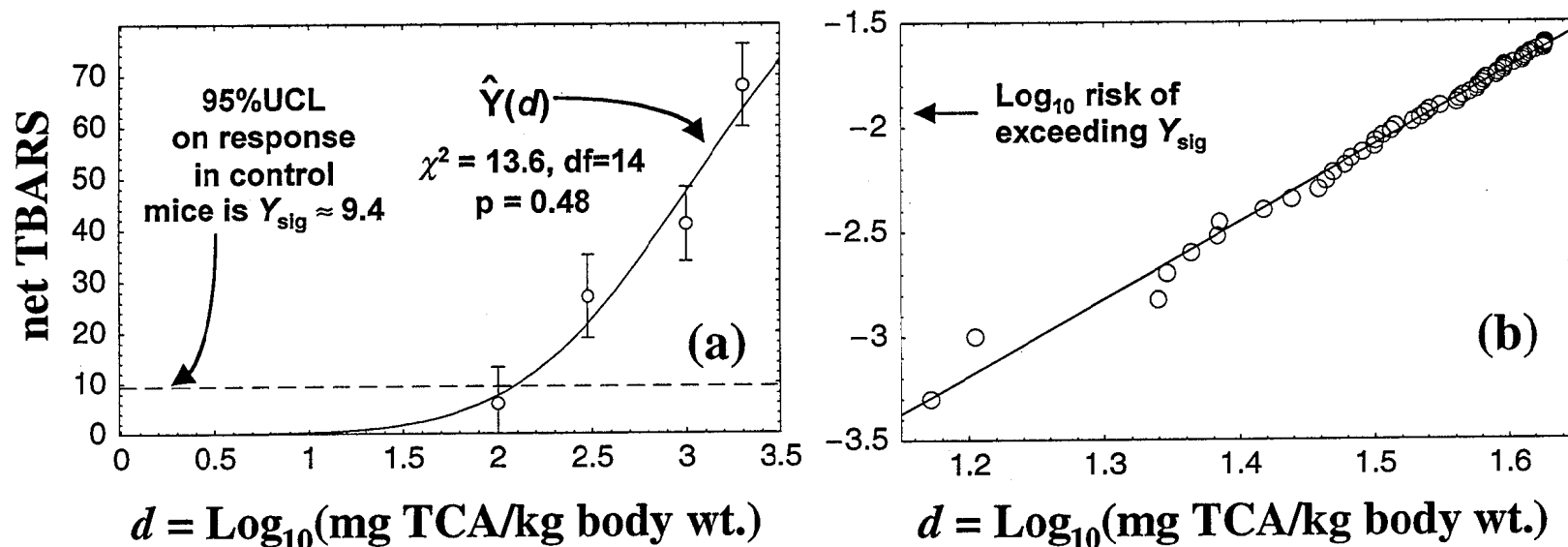
Figure 6. Fit and extrapolation of lognormal model to mouse cytotoxicity data from Larson and Bull (1992a). **(a)** Experimental mean (±1 SD) data are shown (open points) for TCA-induced net increases in an h epatocellular lipoperoxidative index (TBARS) associated with toxicity, compared to the upper bound on the normal TBARS range minus the mean background level. Fit to these data is the lognormal model specified by Equation 17 (curve). Simulated parameter values based on the latter fit were used to construct a bootstraped cdf (bdf) for significant TBARS response conditional on dose. The bdf required low-risk extrapolation, however, and plot **(b)** shows how this was done using 50 points from the left tail of the bdf.
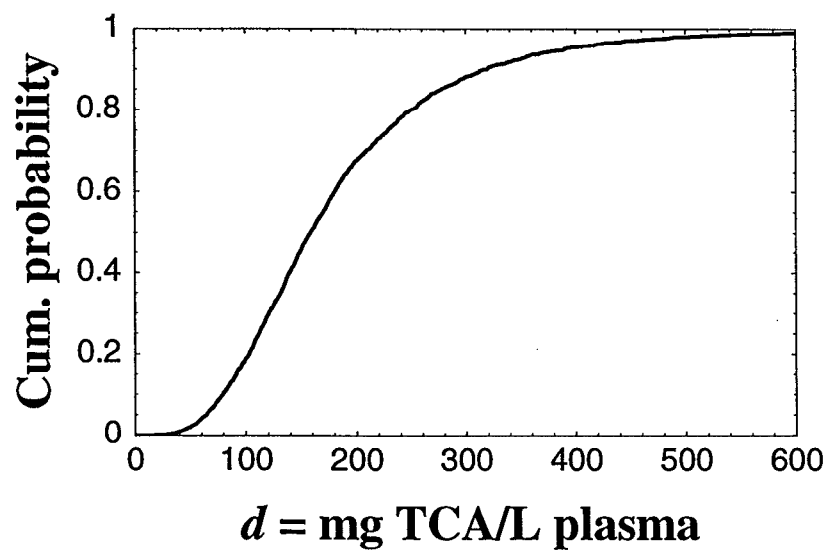
Figure 7. Risk of cytotoxic response estimated from mouse cytotoxicity data of Larson and Bull (1992a) on TCA-induced TBARS elevation, as a function of acute administered TCA dose d.
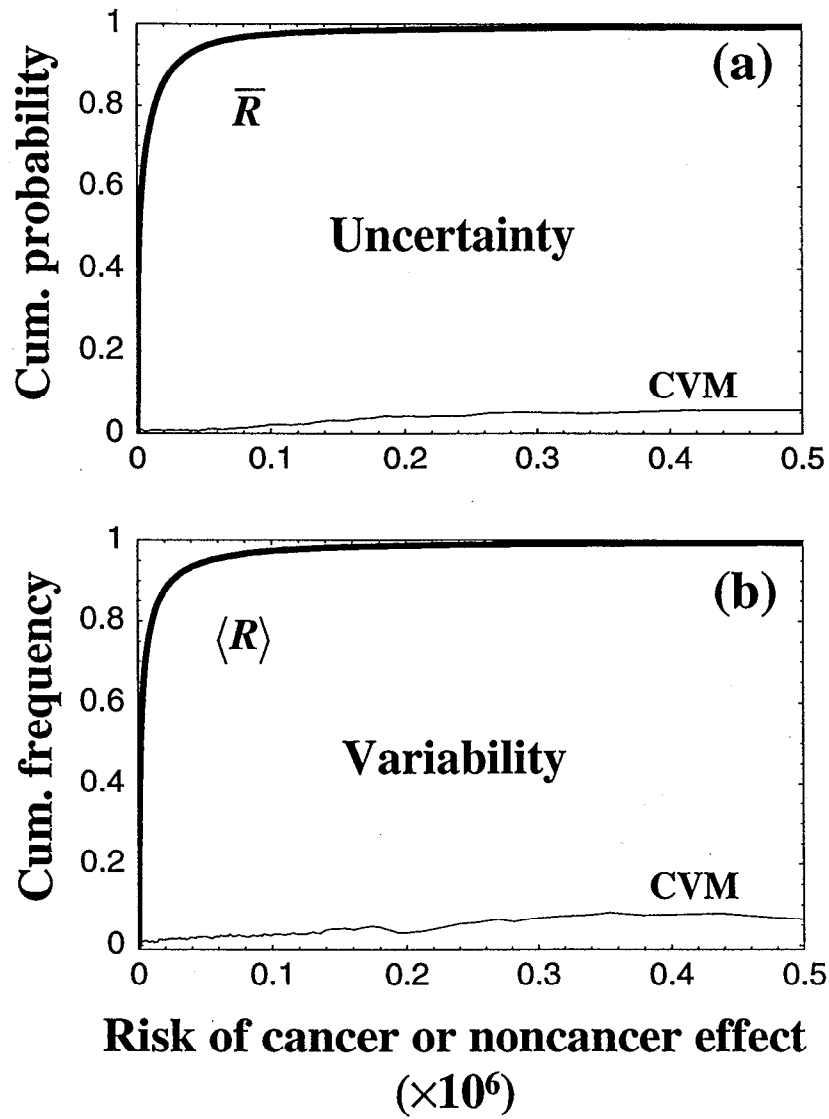
Figure 8. Uncertainty in (a) population-average risk, $\overline{R}$, and (b) interindividual variability in expected risk, $\langle R \rangle$, predicted for hypothetical individuals exposed to TCE in ground water from Site LF-13. In each plot, the Monte-Carlo relative-sampling error of the x-axis value of each point on the bold cdf curve is indicated by the corresponding y-axis value (labeled CVM) of the light curve shown. For example, from plot (a) the 99th percentile value of $\overline{R}$ is estimated to be $\sim 0.29 \times 10^{-6}$, which estimate has a CVM of ~ 0.051, indicating a sampling error of about $\pm 5\%$.
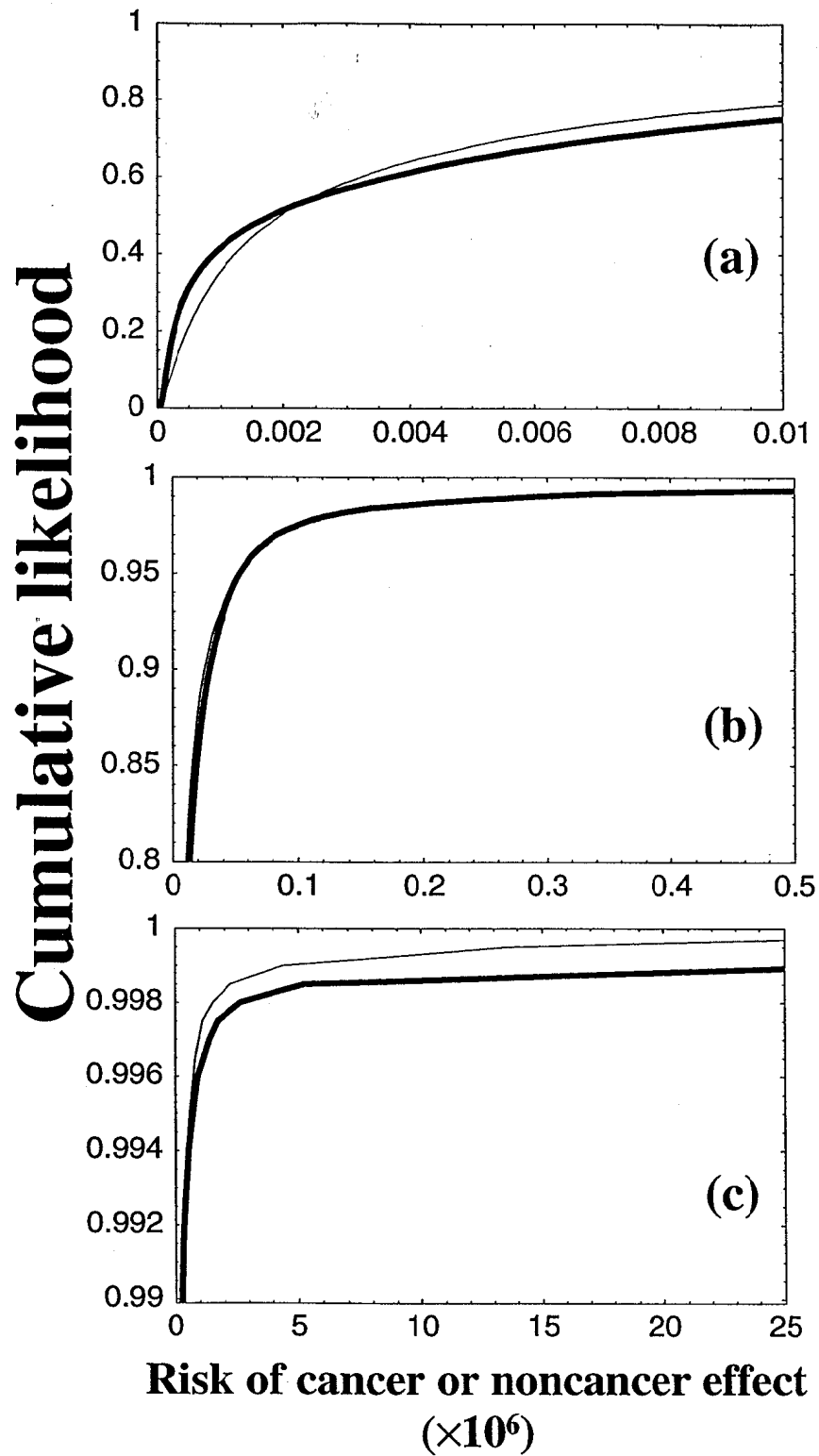
Figure 9. Comparison of $\overline{R}$ (bold curves) vs. $\langle R \rangle$ (light curves) over different ranges of predicted risk: **(a)** $R \leq 0.01 \times 10^{-6}$, **(b)** $R \leq 0.5 \times 10^{-6}$, and **(c)** $R \leq 25 \times 10^{-6}$. The relationship is not consistent over these risk ranges, and both cdfs are highly skewed.
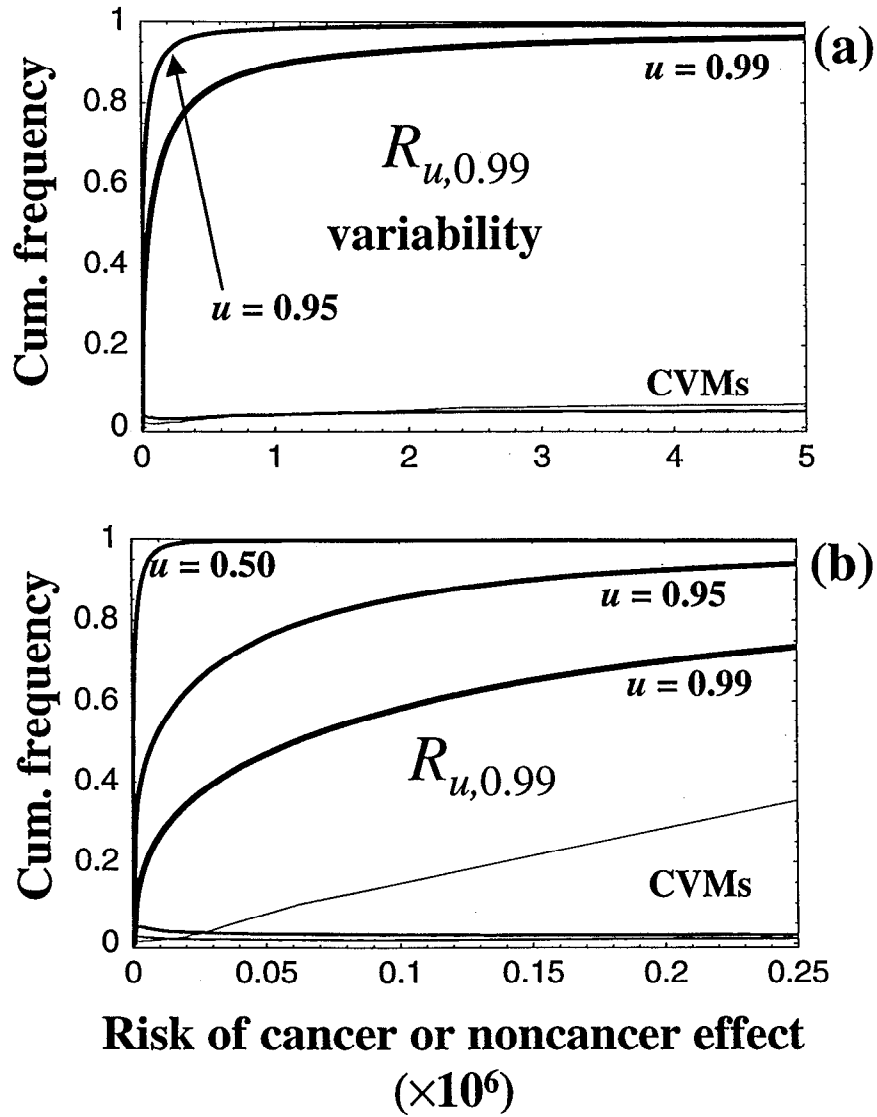
Figure 10. Comparison of estimators, $R_{u,v}$, o f joint uncertainty and variability in risk, over different ranges fo risk, where u and v refer to fractiles with respect to uncertainty and variability, respectively, and where the upper-bound value $v = 0.99$ was used. In (a), $R_{u,0.99} \leq 5\times10^{-6}$, an d in (b) $R_{u,0.99} \leq 0.25\times10^{-6}$. CVM cu rves denote corresponding relative error, as in Figure 8. The CVM that exceeds 0.20 where $R_{u,0.99} = 0.25\times10^{-6}$ corresponds to value of $u = 0.50$ (median uncertainty), conditional on w hich, for example, $R_{0.5,0.99} = 0.017\times10^{-6}$. The CVM > 0.20 therefore pertains to a very unlikely level of risk.

55

conditional on specified confidence bounds (u) on uncertainty, for $u = 0.50$, 0.95, and 0.99. The nested Monte-Carlo calculations required to estimate these three $R_{u,v}$ cdfs took a total of 10.6 h to perform.

Table 4 provides a comparison of an upper variability bound ($v = 0.99$) on these cdfs to mean and upper-bound values of $\overline{R}$ and $\langle R \rangle$, as well as to traditional point-estimates of risk ($\hat{R}_{RME}$ and $\hat{R}_{High}$) taken from Daniels et al. (1999). CVM values were all about 10% or less, except for a CVM value of 23% for the expected value of $\overline{R}$. These CVM values indicate reliability in the result obtained that the estimated mean and upper-bound values of $\overline{R}$ and $\langle R \rangle$ are all $< 10^{-6}$, and that both JUV estimators are $< 5 \times 10^{-5}$.

Corresponding estimates of population risk (i.e., the uncertain number N of cases of cancer or TCE-induced toxicity) depend on the assumed size n of the total exposed population (including all immigrants to and emigrants from areas hypothetically served by Site LF-13 water), for an arbitrarily assumed total period equal to one average lifetime (taken to be 70 y), during which total or partial lifetime exposures would hypothetically occur (see Daniels et al., 1999). Expected population risk $\langle N \rangle$ conditional on various assumptions concerning population size n are listed in Table 5, together with estimates of the corresponding likelihood ($1 - p_0$) of one or more cases, and the likelihood (p_0) of zero cases, being attributable to TCE in groundwater at Site LF-13 over the 70-y period of consideration.

Table 5. Population risk associated with multipathway exposures to TCE-contaminated ground water at Beale Air Force Base in California[a]

Total exposed population over 70 y n	Exposed population during 7.6 y n_{res}	Prob($N = 0$)[b] P_0	Prob($N \geq 0$)[b] $1 - P_0$	Expected value[b] of N $\langle N \rangle = n \times \langle \overline{R} \rangle$
100	11	0.99998	0.00002	0.0000022
1,000	109	0.99981	0.00019	0.00022
2,000	217	0.99967	0.00033	0.00044
10,000	1,086	0.99919	0.00081	0.0022
30,000	3,257	0.99863	0.00137	0.0066
100,000	10,857	0.99717	0.00283	0.022
1,000,000	108,571	0.98453	0.01547	0.22
310,795,000	33,743,457	0.50	0.50	68.

[a]N = population risk, i.e., the predicted number of cases (i.e., individuals with) a cancer or noncancer endpoint due to exposure to TCE from Site LF-13; n = the total number of individuals assumed to incur the population-average risk $\overline{R}$ within a 70-y period of consideration; n_{res} = mean number of exposed people at any given moment assumed to be served by ground water from Site LF-13, assuming a mean 7.6-y duration of residence (see Daniels et al., 1999).

[b]Probabilities were arbitrarily rounded to 5 decimal places so complimentary values listed sum to 1; no more than 2 significant figures are implied.

4. DISCUSSION

A unified probabilistic approach was applied to estimate the aggregate risk of cancer and noncancer endpoints for hypothetical future residents exposed to TCE from ground water at an inactive landfill site at Beale U.S. Air Force Base. The approach developed is superior to previous related efforts (Baird et al., 1996; Butterworth and Bogdanffy, 1999; Carlson-Lynch et al., 1999; Gaylor et al., 1999; Lewis, 1993; Slob and Pieters, 1998), insofar as it is the first to provide an integrated, consistent treatment of: (a) cancer as well as noncancer endpoints, (b) two disparate yet plausible mechanisms of carcinogenic action in the case TCE (genotoxic vs. cytotoxic), (c) pharmacokinetic considerations, and (d) quantitative analysis of JUV in model inputs and corresponding characterized risk. The approach incorporates some of the probabilistic methods suggested previously, but modifies others in important ways. For example, the human-variability factor V_{tdyn} (that has an AM of 1) and the acute-to-chronic uncertainty factor $(1+U_{chron})$ (that by definition is >1) used here differed fundamentally from analogous factors recommended by Slob and Pieters (1998), in order for these factors to fit logically within a unified approach capable of adressing points (a)-(d). Application of the approach to the case of TCE also highlighted and addressed key technical issues never before considered in this context, such as the practical requirement for analytic low-risk (extreme-value) extrapolation of any relation between response probability and effective dose that is—e.g., as suggested by Slob and Pieters (1998)—bootstrapped from experimental toxicity data.

All estimates of individual risk obtained in this study (Table 4) are far less than corresponding upper-bound point estimates of individual risk, $\hat{R}_{RME}$ and $\hat{R}_{High}$, that were obtained for comparison by Daniels et al. (1999) using standard, traditional deterministic methods (namely, algebraic substitution of upper-bound and/or default parameter values into equations used to estimate risk). A similar result was obtained by Daniels et al. (1999), who did not consider JUV in pharmacokinetic and dose-response relations pertaining to TCE risk. In the present study, application of a unified probabilistic approach to consider JUV in pharmacokinetic and dose-response relations pertaining to TCE had a substantial impact on predicted risk for Site LF-13. This impact can be assessed by comparing the risk summary in Table 4 of the present study with

that in Table 3 of Daniels et al. (1999). The upper-bound risk estimators $\overline{R}_{0.95}$ and $\langle R \rangle_{0.95}$ obtained in the present study are about 50- and 100-fold less, respectively, than the value of these estimators obtained by Daniels et al. (1999).

Even the JUV-estimator $R_{0.95,0.95}$ approximated in Daniels et al. (1999) is (slightly) *greater* than the value (of ~2×10^6) obtained here using a nested Monte-Carlo procedure for the *more conservative* JUV-estimator $R_{0.95,0.99}$. Only the relatively more conservative JUV-estimator, $R_{0.99,0.99}$, was predicted to have a value (~40×10^6) substantially greater than 10^{-6}. While the latter value is less than the deterministically (hence, relatively easily) calculated $\hat{R}_{RME}$ value of (~60×10^6), the two values are fairly close, indicating that $\hat{R}_{RME}$ in this case provides a credible estimate of the more precisely defined estimator $R_{0.99,0.99}$ (namely, the 99th percentile on uncertainty in risk to the person who is at the 99th percentile of risk relative to others at risk). Furthermore, $\hat{R}_{RME}$ is relatively easily calculated, whereas $R_{0.99,0.99}$ required about 10 h of computation in the present study. It might therefore be preferable to use $\hat{R}_{RME}$ to optimize risk reduction relative to an upper-bound JUV estimator (such as $R_{0.99,0.99}$).

Upper-bound JUV estimators allow explicit consideration of equity in the distribution of interindividual variability in imposed risk. Point estimates such as $\hat{R}_{RME}$ cannot do this explicitly, because they cannot generally be interpreted in any precise manner with respect to variability *per se* or to uncertainty *per se*. In the present case study, both $\hat{R}_{RME}$ and $R_{0.99,0.99}$ are < 5×10^{-4}, which indicates (vaguely via $\hat{R}_{RME}$, explicitly by $R_{0.99,0.99}$) the *de minimis* nature of predicted upper-bound risks plausibly due to TCE at Site LF-13 hypothetically faced by those who would be among most at risk relative to others exposed to ground water from that site. However, such risk estimates do not necessarily correspond to the magnitude of health consequences predicted to be associated with such exposure. Such effects can *only* be addressed by quantitatively considering *uncertainty* in *population* risk, which in turn can only be accomplished by quantitative JUV analysis that characterizes uncertainty in population-average risk $\overline{R}$ conditional on population size n (e.g., via Equation 22) (Bogen, 1986,1990b; Bogen and Spear, 1987).

60

Interesting results concerning population risk were obtained in this study via quantitative JUV analysis addressing multiple health endpoints and multiple mechanisms concerning TCE-induced health risk. Earlier results by Daniels et al. (1999) indicated that exposure to TCE from ground water at Site LF-13 would be *unlikely* to cause a single occurrence of a TCE-related health impact provided that $n < {\sim}30{,}000$. Results from the present, more comprehensive analysis (Table 5) indicate that a single case is *unlikely* to occur even if the population served by ground water from Site LF-13 were $>10^6$. That is, the new results indicate that a single case is unlikely to occur under *any* realistic assumption concerning population size. Moreover, results obtained in the present study indicate that, under the assumptions used, there is a *>99% chance* that TCE-related mitigation of Site LF-13 would confer *no (i.e., zero) public-health benefit* if as many as 10,000 or fewer people were residentially served by the site's TCE-contaminated water (assuming the concentration of TCE never were to increase above levels measured in 1997). Therefore, under this population scenario, any resources directed at mitigating the site are *virtually certain* to be wasted from a public-health perspective. Even this hypothetical scenario is conservative, because it is likely that current TCE contamination in ground water at Site LF-13 (due to a finite mass of TCE contamination) could not persist for 70 y if that water were to serve 10,000 hypothetical residents throughout this period. Dilution of the source mass is expected, and the magnitude of this dilution is expected to be proportional to the water flow rate into and away from the source; indeed, this is the basis for pump-and-treat site-mitigation strategies. Water service to that many people from this single goundwater source—if even possible—would also induce some (perhaps substantial) infiltration of non-contaminated water, again causing dilution of residentially delivered TCE concentrations.

5. REFERENCES

Abbas, R., and J.W. Fisher. 1997. A physiologically based pharmacokinetic model for trichloroethylene and its metabolites, chloral hydrate, trichloroacetate, dichloroacetate, trichloroethanol, and trichloroethanol glucuronide in B6C3F1 mice. *Toxicol. Appl. Pharmacol.* 147:15-30.

Acharya, S., K. Mehta, S. Rodriguez, J. Pereira, S. Krishnan, and C.V. Rao. 1997. A histopathological study of liver and kidney in male Wistar rats treated with subtoxic doses of t-butyl alcohol and trichloroacetic acid. *Exper. Toxicol. Pathol.* 49:369-373.

Aitchison, J., and J.A.C. Brown. 1957. The Lognormal Distribution. Cambridge U. Press, New York.

Allen, B.C., and J.W. Fisher. 1993. Pharmacokinetic modeling of trichloroethylene and trichloroacetic acid in humans. *Risk Anal.* 15:71-86.

Ames, B., and L.S. Gold. 1990a. Too many rodent carcinogens: Mitogenesis increases mutagenesis. *Science.* 249:970-972.

Ames, B.N., and L.S. Gold. 1990b. Chemical carcinogenesis: Too many rodent carcinogens. *Proc. Natl. Acad. Sci.* 87:7772-7776.

Ames, B.N., L.S. Gold, and W.C. Willett. 1995. The causes and prevention of cancer. *Proc. Natl. Acad. Sci.* 92:5258-5265.

Ames, B.N., M.K. Shigenaga, and L.S. Gold. 1993. DNA lesions, inducible DNA repair, and cell division: Three key factors in mutagenesis and carcinogenesis. *Environ. Health Perspect.* 101(Suppl. 5):35-44.

Andersen, M.E., H.A. Barton, R. Bull, and I. Schultz. 1998. DCA dosimetry: Interpreting DCA-induced liver cancer dose-response and the potential for DCA to contribute to TCE-induced liver cancer, AL-OE-DR-TR-1998-0009. United States Air Force Armstrong Laboratory, Brooks Air Force Base, TX.

Anderson, E.L., R.E. Albert, R. McGaughy, L. Anderson, S. Bayard, D. Bayliss, C. Chen, M. Chu, H. Gibb, B. Haberman, C. Hiremath, D. Singh, and T. Thorslund. 1983. Quantitative approaches in use to assess cancer risk. *Risk Anal.* 3:277-295.

Armitage, P., and R. Doll. 1957. A two-stage theory of carcinogenesis in relation to the age distribution of human cancer. *Br. J. Cancer.* 11:161-169.

Baird, S.J.S., J.T. Cohen, J.D. Graham, A.I. Shlyakter, and J.S. Evans. 1996. Noncancer risk assessment: A probabilistic alternative to current practice. *Human Ecol. Risk Assessment.* 2:79-102.

Bell, Z.G., K.J. Olsen, and T.J. Benya. 1978. Final Report of Audit Findings of the Manufacturing Chemists Association (MCA): Administered Trichloroethylene (TCE) Chronic Inhalation Study at Industrial Bio-Test Laboratories, Inc., Decator, Illinois. Unpublished study reported in EPA (1985).

Bogen, K.T. 1986. Uncertainty in Environmental Health Risk Assessment: A Framework for Analysis and an Application to a Chronic Exposure Situation Involving a Chemical Carcinogen. *In* School of Public Health. University of California, Berkeley. 195.

Bogen, K.T. 1988. Pharmacokinetics for regulatory risk assessment: The case of trichloroethlyene. *Regulatory Toxicol. Pharmacol.* 8:447-466.

Bogen, K.T. 1989. Cell proliferation kinetics and multistage cancer risk models. *J. National Cancer Inst.* 81:267-277.

Bogen, K.T. 1990a. Risk extrapolation for chlorinated methanes as promoters vs initiators of multistage carcinogenesis. *Fund. Appl. Toxicol.* 15:536-557.

Bogen, K.T. 1990b. Uncertainty in Environmental Health Risk Assessment. Garland Publishing, Inc., New York.

Bogen, K.T. 1992. RiskQ: An interactive approach to probability, uncertainty, and statistics for use with Mathematica. Lawrence Livermore National Laboratory, Livermore, CA UCRL-MA-110232;.

Bogen, K.T. 1994. Cancer potencies of heterocyclic amines found in cooked foods. *Fd. Chem. Toxicol.* 32:505-515.

Bogen, K.T. 1995. Methods to approximate joint uncertainty and variability in risk. *Risk Anal.* 15:411-419.

Bogen, K.T., and L.S. Gold. 1997. Trichloroethylene cancer risks: Simplified calculation of PBPK-based MCLs for cytotoxic endpoints. *Regulatory Toxicol. Pharmacol.* 25:26-42.

Bogen, K.T., and L.C. Hall. 1989. Pharmacokinetics for regulatory risk assessment: The case of 1,1,1-trichloroethane (Methyl chloroform). *Regulatory Toxicol. Pharmacol.* 10:26-50.

Bogen, K.T., L.C. Hall, T.E. McKone, D.W. Layton, and S.E. Patton. 1988. Health Risk Assessment of Trichloroethylene in California Drinking Water. Report prepared for the California Public Health Foundation and California Department of Health Services. Lawrence Livermore National Laboratory, Livermore, CA.

Bogen, K.T., and R.C. Spear. 1987. Integrating uncertainty and interindividual variability in environmental risk assessment. *Risk Anal.* 7:427-436.

Brown, L.P., D.G. Farrar, and C.G. DeRooij. 1990. Health risk assessment of environmental exposure to trichloroethylene. *Regulatory Toxicol. Pharmacol.* 11:24-41.

Bull, R.J., I.M. Sanchez, M.A. Nelson, J.L. Larson, and A.J. Lansing. 1990. Liver tumor induction in B6C3F1 mice by dichloroacetate and trichloroacetate. *Toxicology.* 63:341-359.

Butterworth, B.E., and M.S. Bogdanffy. 1999. A comprehensive approach for integration of toxicity and cancer risk assessments. *Regulatory Toxicol. Pharmacol.* 29:23-36.

California Environmental Protection Agency (CalEPA). 1996. Air Toxics Hot Spots Program Risk Assessment Guidelines Part IV, Technical Support Document: Exposure Assessment and Stochastic Analysis (December 1998). CalEPA Office of Health Hazard Assessment, Berkeley, CA.

Carlson-Lynch, H., P.S. Price, J.C. Swartout, M.L. Dourson, and R.E. Keenan. 1999. Application of quantitative information on the uncertainty in the RfD of Noncarcinogenic risk assessments. *Human Ecol. Risk Assess,.* 5:527-546.

Cohen, S.M., and L.B. Ellwein. 1990. Cell proliferation in carcinogenesis. *Science.* 249:1007-1011.

Cohen, S.M., and L.B. Ellwein. 1991. Genetic errors, cell proliferation, and carcinogenesis. *Cancer Res.* 51:6493-6505.

Daniels, J., K.T. Bogen, and L. Hall. 1999. Procedures for addressing uncertainty and variability in exposure to characterize potential health risk from trichloroethylene contaminated groundwater at Beale Air Force Base in California. Lawrence Livermore National Laboratory, Livermore, CA.

DeAngelo, A.B., F.B. Daniel, B.M. Most, and G.R. Olson. 1997. Failure of monochloroacetic acid and trichloroacetic acid administered in the drinking water to produce liver cancer in male F344/N rats. *J. Toxicol. Environ. Health.* 52:425-445.

DeAngelo, A.B., F.B. Daniel, J.A. Stober, and G.R. Olsen. 1991. The carcinogenicity of dichloroacetic acid in the male B6C3F1 mouse. *Fund. Appl. Toxicol.* 16:337-347.

Dees, C., and C. Travis. 1994. Trichloroacetate stimulation of liver DNA synthesis in male and female mice. *Toxicol. Lett.* 70:343-355.

Dourson, M.L., S.P. Felter, and D. Robinson. 1996. Evolution of science-based uncertainty factors in noncancer risk assessment. *Regulatory Toxicol, Pharmacol.* 24:108-120.

Eyre, R.J., D.K. Stevens, J.C. Parker, and R.J. Bull. 1995. Renal activation of trichloroethylnene and S-(1,2-dichlorovinyl)-L-cysteine and cell proliferative responses in the kidneys of F344 rats and B6C3F1 mice. *J. Toxicol. Environ. Health.* 46:465-481.

Fahrig, R., S. Madle, and H. Baumann. 1995. Genetic toxicology of trichloroethylene. *Mutat. Res.* 340:1-36.

Finley, B., D. Proctor, P. Scott, N. Harrington, D. Paustenback, and P. Prince. 1994. Recommended distributions for exposure factors frequently used in health risk assessment. *Risk Anal.* 14:533-553.

Fisher, J.W., and B.C. Allen. 1993. Evaluating the risk of liver cancer in humans exposed to trichloroethylene using physiological models. *Risk Anal.* 15:87-95.

Fisher, J.W., M.L. Gargas, B.C. Allen, and M.E. Andersen. 1991. Physiologically based pharmacokinetic modeling with trichloroethylene and its metabolite, trichloroacetic acid, in the rat and the mouse. *Toxicol. Appl. Pharmacol.* 109:183-195.

Fisher, J.W., D. Mahle, and R. Abbas. 1998. A human physiologically based pharmacokinetic model for trichloroethylene and its metabolites, trichloroacetic acid and free trichloroethanol. *Toxicol. Appl. Pharmacol.* 152:339-359.

Gaylor, D.W., R.L. Kodell, J.J. Chen, and D. Krewski. 1999. A unified approach to risk assessment for cancer and noncancer endpoints based on benchmark doses. *Regulatory Toxicol. Pharmacol.* 29:151-157.

Harrington-Brock, K., C.L. Doerr, and M.M. Moore. 1998. Mutagenicity of three disinfection by-products: Di- and trichloroacetic acid and chloral hydrate in L5178Y/TK +/- (-)3.7.2C mouse lymphoma cells. *Mutat. Res.* 413:265-276.

Herren-Freund, S.L., M.A. Pereira, M.D. Khoury, and G. Olson. 1987. The carcinogenicity of trichloroethylene and its metabolites, trichloroacetic and dichloroacetic acid, in mouse liver. *Toxicol. Appl. Pharmacol.* 90:183-189.

Iman, R.L., and W.J. Conover. 1982. A distribution-free approach to inducing rank correlation among input variates. *Commun. Statist. (Ser. B) Simulation and Computation.* 11:311-334.

Jennrich, R.I. 1970. An asymptotic χ^2 test for the equality of two correlation matrices. *J. Am. Stat. Assoc.* 65:904-912.

Larson, J.L., and R.J. Bull. 1992a. Metabolism and lipoperoxidative activity of trichloroacetate and dichloroacetate in rats and mice. *Toxicol. Appl. Pharmacol.* 115:268-277.

Larson, J.L., and R.J. Bull. 1992b. Species differences in the metabolism of trichoroethylene to the carcinogenic metabolites trichloroacetate and dichloroacetate. *Toxicol. Appl. Pharmacol.* 115:278-285.

Lewis, S.C. 1993. Reducing uncertainty with adjustment factors: Improvements in quantitative noncancer risk assessment. *Fund. Appl. Toxicol.* 20:2-4.

Lipscomb, J.C., J.W. Fisher, P.D. Confer, and J.Z. Byczkowski. 1998. *In vitro* to *in vivo* extrapolation for trichloroethylene metabolism in humans. *Toxicol. Appl. Pharmacol.* 152:376-387.

Maltoni, C., G. Lefemine, and G. Cotti. 1986. Archives of Research on Industrial Carcinogenesis. Vol. V. Experimental Research of Trichloroethylene Carcinogenesis. Princeton University Press, Princeton, N.J.

Merdink, J.L., A. Gonzalez-Leon, R.J. Bull, and I.R. Schultz. 1998. The extent of dichloroacetate formation from trichloroethylene, chloral hydrate, trichloroacetate, and trichloroethanol in B6C3F1 mice. *Toxicol. Sci.* 45:33-41.

Moolgavkar, S.H. 1983. Model for human carcinogenesis: Action of environmental agents. *Environ. Health Perspect.* 50:285-291.

Moolgavkar, S.H., A. Dewanji, and D.J. Venzon. 1988. A stochastic two-stage model for cancer risk assessment: The hazard function and the probability of tumor. *Risk Anal.* 8:383-392.

Moolgavkar, S.H., and A.G. Knudson. 1981. Mutation and cancer: A model for human carcinogenesis. *J. Natl. Cancer Inst.* 66:1037-1052.

National Cancer Institute (NCI). 1976. Carcinogeneiss Bioassay of Trichloroethylene. NCI-CG-TR-2, DHEW Publ. No. (NIH) 76-802. U.S. Government Printing Office, Washington, DC.

National Research Council (NRC). 1994. *Science and Judgment in Risk Assessment.* NRC Committee on Risk Assessment of Hazardous Air Pollutants, National Academy Press, Washington, DC.

National Toxicology Program (NTP). 1988. *Toxicology and Carcinogenesis Studies of Trichloroethylene (CAS No. 79-01-6) in Four Strains of Rats (ACI, August, Marshall, Osborne-Mendel) (Gavage Studies).* NIH Pub No. 88-2529, NTP Tech. Rep. Ser. No. 273. National Institutes of Health, NTP, Research Triangle Park, NC.

National Toxicology Program (NTP). 1990. *Carcinogenesis Studies of Trichloroethylene (Without Epichlorohydrin) (CAS No. 79-01-6) in F344/N Rates and B3C3F1 Mice (Gavage Studies).* NIH Pub No. 90-1799. National Institutes of Health, NTP, Research Triangle Park, NC.

Ni, Y.C., T.Y. Wong, R.V. Llyoyd, T.M. Heinze, S. Shelton, D. Caciano, F.F. Kadlubar, and P.P. Fu. 1996. Mouse liver microsomal metabolism of chloral hydrate, trichloroacetic acid, and trichloroethanol leading to induction of lipid peroxidation vai a free radical mechanism. *Drg. Metab. Disposition.* 24:81-90.

Pereira, M.A. 1996. Carcinogenic activity of dichloroacetic acid and trichloroacetic acid in the liver of female B6C3F1 mice. *Fund. Appl. Toxicol.* 31:192-199.

Pereira, M.A., and J.B. Phelps. 1996. Promotion by dichloroacetic acid and trichloroacetic acid of N-methyl-N-nitrosourea-initiated cancer in the liver of female B6C3F1 mice. *Cancer Lett.* 102:133-141.

Press, W.H., S.A. Teukolsky, W.T. Vetterling, and B.P. Flannery. 1992. Numerical Recipes in FORTRAN — The Art of Scientific Computing. Cambridge University Press, New York, pp. 650-700.

Renwick, A.G. 1993. Data derived safety factors for the evaluation of food additives and environmental contaminants. *Food Add. Contam.* 10:275-305.

Slob, W., and M.N. Pieters. 1998. A probabilistic approach for deriving acceptable human intake limits and human health risks from toxicological studies: General framework. *Risk Anal.* 18:787-798.

Stenner, R.D., J.L. Merdink, J.W. Fisher, and R.J. Bull. 1998. Physiologically-based pharmacokinetic model for trichloroethylene considering enterohepatic recirculation of major metabolites. *Risk Anal.* 18:261-269.

Templin, M.V., J.C. Parker, and R.J. Bull. 1993. Relative formation of dichloroacetate and trichloroacetate from trichloroethylene in male B6C3F1 mice. *Toxicol. Appl. Pharmacol.* 123:1-8.

U.S. Environmental Protection Agency (EPA). 1985. *Health Assessment Document for Trichloroethylene.* EPA/600/8-82/006F. U.S. EPA Office of Research and Development, Office of Health and Environmental Assessment, Environmental Criteria and Assessment Office, Research Triangle Park, NC.

U.S. Environmental Protection Agency (EPA). 1987a. Technical Analysis of New Methods and Data Regarding Dichloromethane Hazard Assessments. EPA/600/8-87/029A (June 1987). U.S. EPA Office of Health and Environmental Assessment, Washington, DC.

U.S. Environmental Protection Agency (EPA). 1987b. Addendum to the Health Assessment Document for Trichloroethylene: Updated Carcinogenicity Assessment for Trichloroethylene. EPA/600/8-82/006FA. U.S. EPA Office of Research and Development, Office of Health and Environmental Assessment, Environmental Criteria and Assessment Office, Research Triangle Park, NC.

U.S. Environmental Protection Agency (EPA). 1992. Draft report: A cross-species scaling factor for carcinogen risk assesment based on equivalence of $mg/kg^{3/4}/day$. *Fed. Register.* 57(No. 109, June 5):24152-24172.

U.S. Environmental Protection Agency (EPA). 1996. Proposed Guidelines for Carcinogen Risk Assessment. EPA/600/P-92/003C. U.S. EPA Office of Research and Development, Washington, DC.

U.S. Environmental Protection Agency (EPA). 1998. Ambient Water Quality Criteria Methodology: Human Health [EPA/822-Z-98-001, U.S. EPA Office of Water]. *Fed. Regist.* 63(No. 157, Aug. 14):43755-43828.

URS Greiner Woodward Clyde (URSGWC). 1998. Management Action Plan, Beale Air Force Base, California. December 1998. Prepared for Headquarters Air Combat Command (ACC), Langley Air Force Base, VA, under contract to US Air Force Center for Environmental Excellence (AFCEE), Brooks Air Force Base, TX, Project No. ACCH19987544 [obtain from Chief, Environmental Restoration (M.E. O'Brien), Beale Air Force Base, California]. URSGWC, Omaha, NE.

Weil, C.S. 1972. Statistics vs. safety factors and scientific judgment in the evaluation of safety for man. *Toxicol. Appl. Pharmacol.* 21:454-463.

Wolfram, S. 1996. The Mathematica Book. Cambridge University Press, Cambridge, UK.

Wright, S. 1992. Adjusted p-values for simultaneous inference. *Biometrics.* 48:1005-1013.

Appendix 1.

Method of Moments for Lognormal Variates

Given a normally distributed variate Y with arithmetic mean (AM) μ_Y standard deviation (SD) σ_Y, and corresponding coefficient of variation (CV = SD/AM) $\gamma_Y = (\sigma_Y / \mu_Y)$, the variate $X = e^Y$ has a lognormal (LN) distribution with geometric mean (GM) e^{μ_Y} and geometric standard deviation (GSD) e^{σ_Y}, where $e = \ln^{-1}(1)$ and ln denotes natural logarithm. These assumptions are efficiently denoted $Y \sim N(\mu_Y, \sigma_Y)$ and $X \sim LN(\mu_Y, \sigma_Y)$. The method of moments may be used to relate given AM, SD, and CV values of X (μ_X, σ_X, and γ_X, respectively) to those of Y; in particular, the AM/GM ratio for X, $\rho = (\mu_X / e^{\mu_Y})$, is equal to $e^{\sigma_Y^2/2}$ where $\sigma_Y^2 = \ln \rho^2 = \ln(1 + \gamma_X^2)$ (Aitchison and Brown, 1957).

LN moment relations conveniently imply that the ratio of any given percentile of X relative to its GM or AM corresponds to a unique set of LN parameters. Let $X_p = e^{\mu_Y + \sigma_Y z_p}$ denote the $100p$th percentile of X, where $0 \le p \le 1$, $z_p = \Phi^{-1}(p)$, and Φ is the cumulative normal probability distribution function. Now let $q_p = X_p / e^{\mu_Y}$ and $r_p = X_p / \mu_X$ denote the ratios of X_p to the GM and AM of X, respectively. Conditional on e^{μ_Y} and the ratio q_p, it follows immediately (by solving for μ_Y and σ_Y) that $X \sim LN(\mu_Y, \ln q_p^{1/z_p})$. Conditional on μ_X and the ratio r_p, it follows that $X \sim LN[\ln(\mu_X) - (\sigma_Y^2/2), \sigma_Y]$, where σ_Y is the positive σ_Y-root of $\sigma_Y^2 - 2z_p\sigma_Y + 2 \ln r_p = 0$; i.e., $\sigma_Y = z_p + \sqrt{z_p^2 - \ln r_p^2}$ for all $r_p \le e^{z_p^2}/2$ (larger values of r_p are not possible conditional on z_p).

LN moment relations also imply that for any independent LN variates $X_i = e^{Y_i}$, $i = 1,...,n$, with corresponding CVs γ_i, the CV γ_Z of the product $Z = \prod_{i=1}^{n} X_i$ is conveniently ralated as follows to the CVs γ_i of X_i:

$$\gamma_Z = \sqrt{e^{\sigma_{\ln Z}^2} - 1} = \sqrt{-1 + \exp\left(\sigma_{\Sigma_{i=1}^n Y_i}^2\right)}$$

$$= \sqrt{-1 + \exp\left(\sum_{i=1}^n \sigma_{Y_i}^2\right)} = \sqrt{-1 + \exp\left(\sum_{i=1}^n \ln\left(1 + \gamma_i^2\right)\right)}$$

$$= \sqrt{-1 + \prod_{i=1}^n \left(1 + \gamma_i^2\right)} \quad .$$

Conditional on known γ_Z and γ_i for $i \neq j$ and $1 \leq j \leq n$, inverting the latter equation

readily yields the unknown CV of X_j as

$$\gamma_j = \sqrt{\frac{1 + \gamma_Z^2}{\prod_{i \neq j}^n \left(1 + \gamma_i^2\right)} - 1} \quad .$$

If γ_j is obtained in this way and a single additional X_j-parameter among the set {AM, SD, GM, GSD} is known, all three remaining X_j-parameters are easily obtained via the moment relations described above. For example, if the AM of X_j equals 1, it follows that $X_j \sim LN(-\sigma^2/2, \sigma)$ where $\sigma^2 = \ln(1 + \gamma_j^2)$.

Appendix 2.

Mathematica 3.0® Notebooks Documenting Calculations

All calculations were performed on a 400-MHz PowerMac G3 using the programs *Mathematica*® 3.0 (Wolfram, 1996) and *RiskQ* (Bogen, 1992). Documentation of these calculations appears in Appendices 2.A through 2.I which follow, in which calculations and related comments are organized by topic. Appendices 2.A (Concentration), 2.B (Intakes), and 2.C (Fraction of Lifetime at One Local Residence) all document the derivation or re-derivation of exposure-related input variates explained in Daniels et al. (1999), which were used to calculate TCE exposures as explained above (Section 2.2). Appendices 2.D (Effective Genotoxic Dose) and 2.E (Effective Cytotoxic Dose) document the calculation of corresponding biologically effective (TCE or TCA) doses. Note that calculations pertaining to the definition or characterization of variates V_w, V_{Vmax}, $V_{fm,ing}$, V_{fd}, $(f_{deq}/V_{t,P})$ and V_e all appear in Appendix 2.E. Appendix 2.F (Effective Dose Correlations) documents calculations made to estimate rank correlations among MA- and pathway-specific normalized biologically effective doses. Appendix 2.G (Potency) documents all calculations made pertaining to modeled dose-response under both mechanisms of carcinogenic action considered (MA_G and MA_C). Appendix 2.H (TCE Risk) documents all calculations made pertaining to corresponding predicted risk. Note that calculations pertaining to the definition of variates U_{chron}, U_{tdyn}, and V_{tdyn} appear in Appendix 2.H. Finally, Appendix 2.I (Functions Used) briefly describes all *Mathematica*® and *RiskQ* functions used to carry out calculations documented in Appendices 2.A-2.H.

Please note that more detailed explanation of *Mathematica*®, *RiskQ*, and JUV analysis is beyond the scope of this report, and is provided in references cited.

Appendix 2.A

Concentration
of TCE @ BAFB (mg/L)

$Y = Log[X]$

```
con = {.018, .021, .028}; (*mg/L*)
{{my, sdmy} = {EV[Log[con]], SD[Log[con]] / Sqrt[3]},
{mx, sdmx} = {EV[con], SD[con] / Sqrt[3]}}

{{-3.81872, 0.129473}, {0.0223333, 0.00296273}}


{cv = sdmx / mx, E^sdmx}

{0.13266, 1.00297}


t0 = tt /. Solve[mx + tt * sdx == 0, tt][[1]]

-4.35212


RQ[C, T, 2, t0]

0.0244757


tsim = SimulateCdf[{T, 2}, 2000];

Sort[tsim][[{1, 2, 3, 1998, 1990, 1999, 2000}]]

{-31.607, -22.3327, -18.2209, 18.2209, 9.45819, 22.3327, 31.607}


c = E^(0 + sdmy * tsim);
{{mc = EV[c], SD[c]}, {EV[Log[c]], SD[Log[c]]}, Idf[Cdf[c], {.5, .95}]}

{{1.08122, 1.43409}, {1.10724 x 10^-17, 0.32201}, {0.999908, 1.45641}}
```

simulated conc. values

```
scon = (mx / mc) c;
{{mcon = EV[scon], SD[scon]}, {EV[Log[scon]], SD[Log[scon]]},
 Idf[cdf = Cdf[scon], {.5, .95}]}

{{0.0223333, 0.0296222}, {-3.87976, 0.32201}, {0.0206538, 0.0300832}}


Take[Sort[scon], -10]

{0.074688, 0.0801479, 0.0871134, 0.0963267, 0.109112, 0.128074, 0.159096,
 0.218571, 0.372219, 1.23676}
```

```
PlotCdf[cdf, Xmin -> -.001, Xmax -> .05];
```
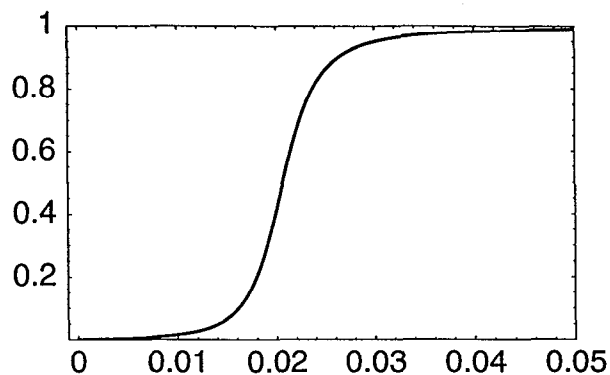


```
scdf = StandardizeCdf[cdf, 404];

WriteMatrix["BogenHD:Desktop Folder:concentration.txt", N[scdf]];
```

■ Log-Transform Utility Functions (where X = LogY)

```
MSDx[GMx_, GSDx_] := Module[{mux, sigy},
   sigy = Log[GSDx];
   mux = GMx E ^ ((sigy^2) / 2);
   mux {1, Sqrt[E ^ (sigy^2) - 1]}]

GMGSDx[Mx_, SDx_] := Module[{muy, sigy},
   sigy = Sqrt[Log[1 + (SDx / Mx) ^ 2]];
   muy = Log[Mx] - (sigy^2) / 2;
   E ^ {muy, sigy}]
```

end

Appendix 2.B

Intakes

2-17-99 (updated 4-26-99)

```
<< RiskQ`;
```

■ Log-Transform Utility Functions

```
GMGSDx::usage = "GMGSDx[Mx,SDx] returns the  geometric mean and geometric sdandard
    deviation of a lognormal variate X that also has the specified arithmetic mean Mx
    and arithmetic sdandard deviation SDx, based on the method of moments.";

MSDx::usage = "MSDx[GMx,GSDx] returns the arithmetic mean and arithmetic sdandard
    deviation of a lognormal variate X that also has the specified geometric mean GMx
    and geometric sdandard deviation GSDx, based on the method of moments.";

GMGSDx1::usage = "GMGSDx1[cvWant,cv2] returns the GM and GSD of a lognormal variate
    X1, such that the product X1*X2 has the desired coefficient of variation (CV) =
    cvWant, conditional on the lognormal variate X2 having an arithmetic
    mean and CV equal to 1 and cv2, respectively, based on the method of moments.";

MSDx[GMx_, GSDx_] := Module[{mux, sigy},
    sigy = Log[GSDx];
    mux = GMx E^((sigy^2) / 2);
    mux {1, Sqrt[E^(sigy^2) - 1]}]

GMGSDx[Mx_, SDx_] := Module[{muy, sigy},
    sigy = Sqrt[Log[1 + (SDx / Mx)^2]];
    muy = Log[Mx] - (sigy^2) / 2;
    E^{muy, sigy}]

GMGSDx1[cvWant_, cv2_] := Module[{muy1},
```

$$muy1 = Log\left[Sqrt\left[\frac{cv2^2 + 1}{cvWant^2 + 1}\right]\right];$$

```
    E^{muy1, Sqrt[-2 muy1]}
    ] /; cvWant >= cv2
```

■ Data on 1998 U.S. Population

```
dat =
  Partition[{5, 18983, 10, 19928, 15, 19268, 20, 19535, 25,  17768, 30, 18545, 35, 20014,
      40, 22602, 45, 21962, 50, 18978, 55, 15907, 60, 12587, 65, 10332, 70, 9530, 75, 8782,
    80, 7227, 85, 4739, 90, 2554, 95, 1105, 100, 322, 105, 64}, 2];
  TBL[data = Data[dat, {Age, temp}, Append -> {Pop, 1000 * temp},
    Drop -> temp, Append -> {{Fpop, 1. Pop / (Plus @@ Pop)}, 1},
      {CFpop, SUM[Fpop], 1}}]]
```

Age	Pop	Fpop	CFpop
5	18983000	0.0701173	0.0701173
10	19928000	0.0736078	0.143725
15	19268000	0.07117	0.214895
20	19535000	0.0721562	0.287051
25	17768000	0.0656295	0.352681
30	18545000	0.0684995	0.42118
35	20014000	0.0739255	0.495106
40	22602000	0.0834848	0.578591
45	21962000	0.0811208	0.659711
50	18978000	0.0700988	0.72981
55	15907000	0.0587555	0.788566
60	12587000	0.0464925	0.835058
65	10332000	0.0381632	0.873221
70	9530000	0.0352009	0.908422
75	8782000	0.032438	0.94086
80	7227000	0.0266943	0.967555
85	4739000	0.0175044	0.985059
90	2554000	0.00943368	0.994493
95	1105000	0.00408153	0.998574
100	322000	0.00118937	0.999764
105	64000	0.000236396	1.

```
tpop = Plus @@ Data[data, Pop]
```

270732000

12 years and over: 200899000

```
{plo, phi} = Data[data, CFpop] [[{2, 3}]];
pwant = plo + (phi - plo) 2 / 5;
{plo, pwant, phi}
```

{0.143725, 0.172193, 0.214895}

```
{f12 = pwant, f12p = 1 - f12, f12 + f12p}
```

{0.172193, 0.827807, 1.}

18 years and over: 200899000

```
f2 = 2 Data[data, CFpop] [[1]] / 5;
f18p = 200899000. / tpop;
f18 = 1 - f2 - f18p;
{w1, w2, w3, ww} = {f2, f18, f18p, f2 + f18 + f18p}
```

{0.0280469, 0.229895, 0.742059, 1.}

■ Ingestion (L/kg-d) Ershow and Cantor, 1989, Table 36 p. 76

```
age = {1, 10, 20, 65, 65 plus};
w = {87.7, 1127.2, 1197.8, 3960.7, 697.0} / 7070.4;
ingest = {53.2, 38.7, 18.4, 21.4, 23.1} / 1000;
sd = {50.9, 23.8, 10.7, 12.2, 9.7} / 1000;
gmgsd = MapThread[GMGSDx[#1, #2]&, {ingest, sd}]
```

{{0.0384398, 2.23934}, {0.032965, 1.76188}, {0.0159061, 1.71553}, {0.0185911, 1.69976},
 {0.0212984, 1.49628}}

```
Plus@@w
```

1.

```
cdfs = LogNormalCdf[#[[1]], #[[2]], 1000]&/@Log[gmgsd];
```

```
adf = AverageCdf[cdfs, Weights -> w];
Dimensions[adf]
```

{5001, 2}

```
sim = SimulateCdf[cdfs, 5000, Report -> False];
cdfTWA = Cdf[Plus@@ (w * sim)];
```

```
cdfTWAcorrected = Cdf[Plus@@ ({1, 10, 9, 45, 5} * sim / 70)];
```

```
{gm, gsd} = GMGSDx[24.2 / 1000, 17 / 1000];
{{gm, gsd}, Log[{gm, gsd}], 17 / 24.2}
```

{{0.0198023, 1.88387}, {-3.92196, 0.63333}, 0.702479}

```
cdfErCan = LogNormalCdf[-3.92195619921997042`, 0.633330172027946325`, 200];
```

```
PlotCdf[{cdfTWA, adf, cdfErCan}, Xmin -> -.0001, Xmax -> .06];
```
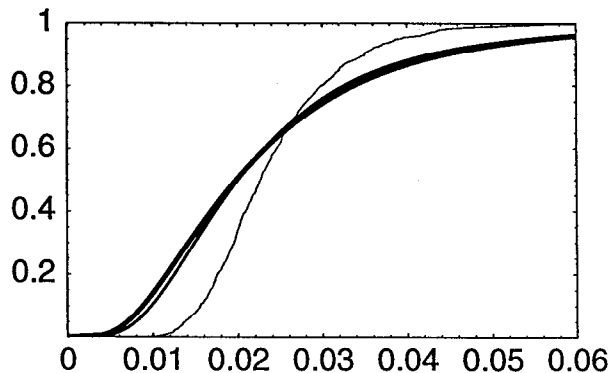
```
PlotCdf[{cdfTWA, cdfTWAcorrected}, Xmin → -.0001, Xmax → .06];
```
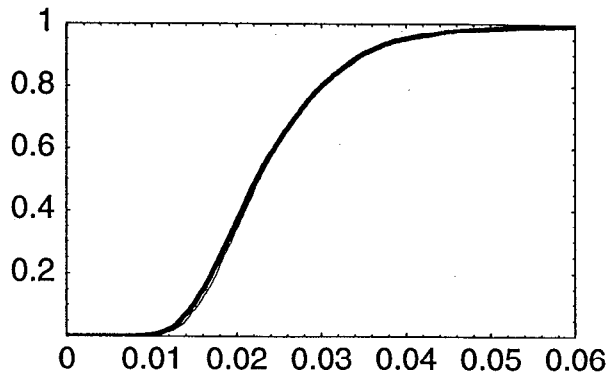


```
{EV[#], SD[#], Idf[#, {.5, .95}]}&/@{cdfTWA, cdfTWAcorrected, adf, cdfErCan}
```

```
{{0.0241953, 0.00802976, {0.0227623, 0.0390576}}, {0.0240441, 0.00862608,
  {0.0223285, 0.0398658}}, {0.024215, 0.0170167, {0.0200231, 0.054078}},
  {0.0242229, 0.0170924, {0.0198023, 0.0561224}}}
```

end

■ SABW Ratio calculations

■ Distribution of Body Surface Area to Body Weight (cm2/kg) Ratio (Phillips et al., 1993)

```
pp = {0, 5, 10, 25, 50, 75, 90, 95, 100} / 100.;
ratio = {
  {421, 470, 507, 563, 617, 719, 784, 846, 1142},
  {268, 291, 328, 376, 422, 454, 501, 594, 670},
  {200, 238, 244, 270, 286, 302, 316, 329, 351}} * 1.;
cdfs = Transpose[{#, pp}]&/@ratio;
PlotCdf[cdfs];
```
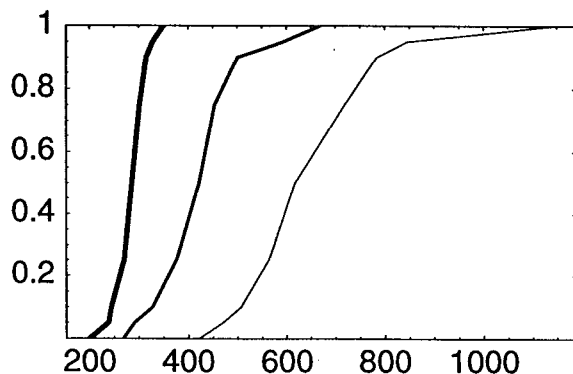
◾ sabwALL

```
adf = AverageCdf[cdfs, Weights -> {w1, w2, w3}];
PlotCdf[adf, Xmin -> -.01, Xmax -> 800];
```
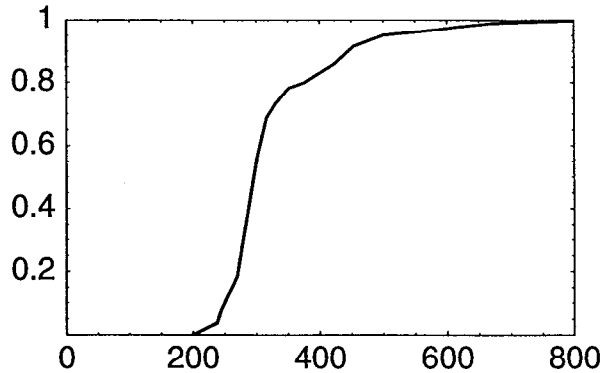


```
TBL[adf]
```

```
200.    0
238.    0.0371029
244.    0.0742059
268.    0.176952
270.    0.186514
286.    0.380025
291.    0.440497
302.    0.571456
316.    0.687114
328.    0.725091
329.    0.728664
351.    0.781572
376.    0.799532
421.    0.855756
422.    0.857034
454.    0.915424
470.    0.927621
501.    0.951541
507.    0.95251
563.    0.963639
594.    0.971495
617.    0.97796
670.    0.98962
719.    0.992988
784.    0.997195
846.    0.998598
1142.   1.
```

```
{EV[adf], Idf[adf, .95]}
```

```
{325.881, 499.003}
```

```
WriteMatrix["BogenHD:Desktop Folder:sabwratioALL.txt", adf];
```

```
{x, y} = Transpose[Rest[Drop[adf, -1]]]
```

```
{{238., 244., 268., 270., 286., 291., 302., 316., 328., 329., 351., 376.,
  421., 422., 454., 470., 501., 507., 563., 594., 617., 670., 719., 784., 846.},
 {0.0371029, 0.0742059, 0.176952, 0.186514, 0.380025, 0.440497, 0.571456, 0.687114,
  0.725091, 0.728664, 0.781572, 0.799532, 0.855756, 0.857034, 0.915424, 0.927621,
  0.951541, 0.95251, 0.963639, 0.971495, 0.97796, 0.98962, 0.992988, 0.997195, 0.998598}}
```

```
xy = Transpose[{NormalCdf[y, Inv], x}]
```

{{-1.78534, 238.}, {-1.44516, 244.}, {-0.927042, 268.},
  {-0.890815, 270.}, {-0.305415, 286.}, {-0.149709, 291.}, {0.180083, 302.},
  {0.487687, 316.}, {0.598033, 328.}, {0.608776, 329.}, {0.777512, 351.},
  {0.839952, 376.}, {1.06145, 421.}, {1.06709, 422.}, {1.37493, 454.},
  {1.4583, 470.}, {1.65998, 501.}, {1.66969, 507.}, {1.79457, 563.}, {1.90324, 594.},
  {2.01334, 617.}, {2.31232, 670.}, {2.45666, 719.}, {2.76978, 784.}, {2.98837, 846.}}

```
PlotData[xy];
```
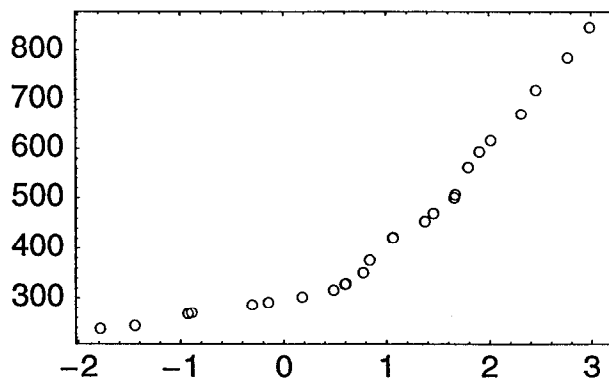

end

■ sabwTWA

```
{nsam, nsim} = {2000, 10};
Clear[fxn];
fxn[a1_, a2_, a3_] := Plus@@({a1, a2, a3} {
     2, 16, 52}/70)
```

```
Timing[{jen, cdf, cvm} = QUAnalyze[cdfs, fxn, nsam, nsim];]
```

{233.983 Second, Null}

```
TBL/@jen
```

Mean[Δr]	Max[|Δr|]	JennrichChi2	DegFr	Pval
-0.000142045	0.017043	0.775025	3	0.855431

Fractile	Value	CVM(%)
0.01	259.77	0.362611
0.05	279.448	0.0700455
0.5	326.046	0.0251131
0.95	373.11	0.0744586
0.99	393.457	0.15432
Mean	325.884	$0. + 4.93556 \times 10^{-7}$ I
Variance	777.661	0.230742

```
PlotCdf[{cvm, cdf}, Ymin → -.01, Xmin → 225, Xmax → 430];
```
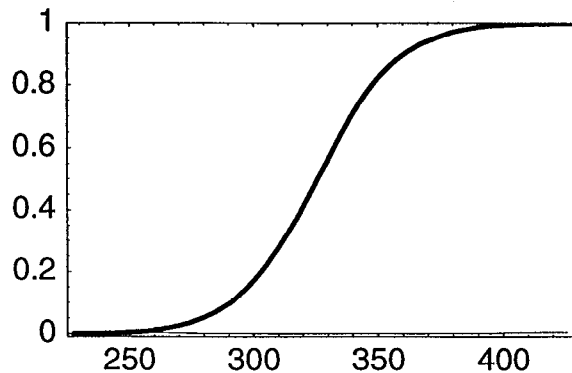


```
Sqrt[777.660703210145509]
```

27.8865685090537002

```
{EV[cdf, Empirical -> True], SD[cdf, Empirical -> True], Idf[cdf, {.5, .95}]}
```

{325.884, 27.8746, {326.046, 373.11}}

```
sdf = StandardizeCdf[cdf, 404];
```

```
{EV[sdf, Empirical -> True], Idf[sdf, {.5, .95}]}
```

{325.875, {326.046, 373.235}}

```
WriteMatrix["Bogen's:Desktop Folder:sabwratioTWA.txt", sdf];
```

```
{x, y} = Transpose[Rest[Drop[cdf, -1]]];
```

```
xy = Transpose[{NormalCdf[y, Inv], x}];
fit = FIT[xy, {1, X}, X, Report → True];
```

Coef	LS Est.	SD	95%LCL	95%UCL
q[0]	325.884	0.0240524	325.837	325.931
q[1]	27.9467	0.0241325	27.8994	27.994

R^2 = 0.998512

$F(1,1998)$ = 1.34108×10^6 2-tail p= $3.7487211392 \times 10^{-2827}$

```
PlotData[xy, FitTo → {fit . {1, X}, X}];
```
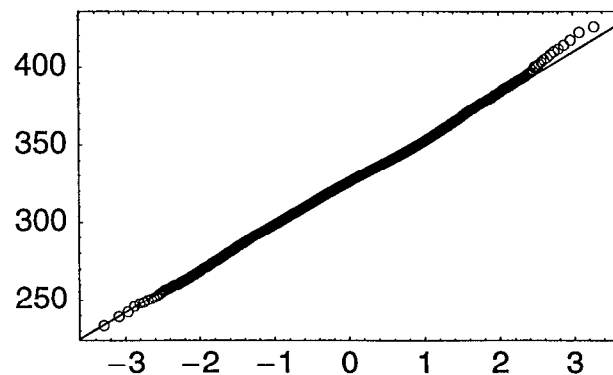
end

end

■ Inhalation (L/kg-d) OHEA. 1996. Stochastic Analysis, p. 3-31 - 3-32.

```
pval = .01 {1, 5, 10, 25, 50, 75, 90, 95, 99, 100 (1 - 1579⁻¹)};
zval = NormalCdf[pval, Inverse];
yAdult = {112.8, 171.4, 179.7, 185.2, 206, 245.6, 295.1, 366.6, 494, 638.8};
yChild = {342.5, 364.5, 375, 401.5, 441, 489.5, 540.5, 580.5, 663.3, 747.5};
{zyA, zyC} = Transpose[{zval, Log[#]}]& /@ {yAdult, yChild};
```

Option 1 (Not Used): Calculate lognormal parameters from OHEA data

```
Clear[x];
{my, sy} = FIT[zyA, {1, x}, x];
{gm, gsd} = E ^ {my, sy};
{{gm, gsd}, MSDx[gm, gsd]}
```

```
{{231.574, 1.32974}, {241.172, 70.1495}}
```

```
PlotData[zyA, FitTo -> {my + sy * x, x}];
```
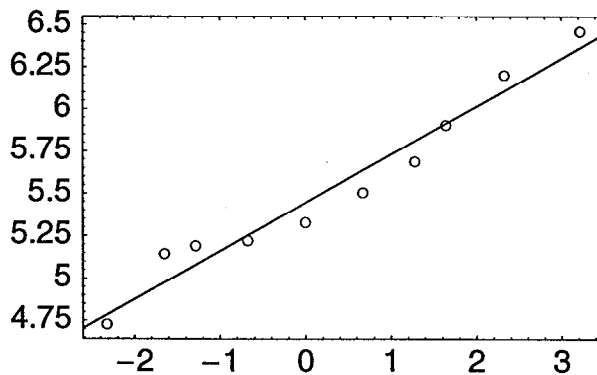


```
{my, sy} = FIT[zyC, {1, x}, x];
{gm, gsd} = E ^ {my, sy};
{{gm, gsd}, MSDx[gm, gsd]}
```

```
{{456.675, 1.15697}, {461.555, 67.6548}}
```

```
PlotData[zyC, FitTo -> {my + sy * x, x}];
```
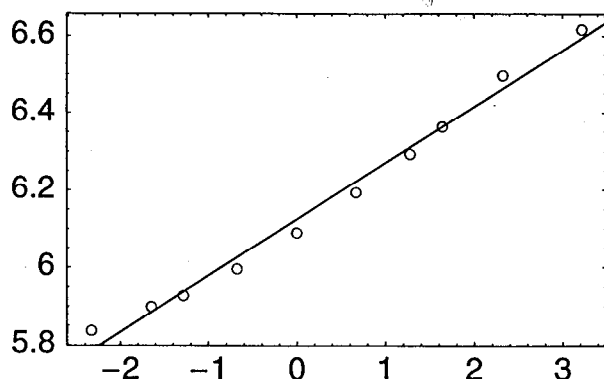

Option2 (Used): Use lognormal parameters derived from reported OHEA mean and SD values for Adult and Child distributions

```
{mA, sdA, mC, sdC} = {225.2, 64.634, 452, 67.73};
{{gmA, gsdA} = GMGSDx[225.2, 64.634],
{gmC, gsdC} = GMGSDx[452, 67.73],
{cvA, cvC} = {sdA / mA, sdC / mC}}
```

```
{{216.461, 1.32491}, {447.009, 1.16069}, {0.287007, 0.149845}}
```

```
{inhA, inhC} = SimulateCdf[{{{LN, Log[{gmA, gsdA}]}, {LN, Log[{gmC, gsdC}]}}, 5000];
cdfs = Cdf /@ {inhA, inhC};
PlotCdf[Reverse[cdfs]];
```

```
Output-Sample Rank-Correlation Matrix:
```

```
1.          0.000314
0.000314  1.
```

```
Jennrich's Asymptotic Chi-Square Test of Homogeneity

   Between Input & Target Correlation Matrices

   For 5000 2-Variate Normal Samples:

Chi2(1)= 0.000492816    1-tail p= 0.982289 (NS)
```
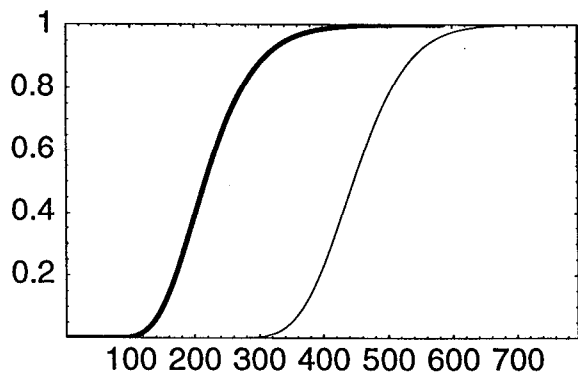

From Finley et al. 1994 (CalEPA 1996, p. 10-7), the BW distribution for adult males & females is ~LN and CV[BW] = ~0.22:

```
{ev, sd} = {71., 15.9};
{cv = sd / ev, {BWgm, BWgsd} = GMGSDx[ev, sd], Log[{BWgm, BWgsd}]}
```

```
{0.223944, {69.2839, 1.24759}, {4.23821, 0.22121}}
```

From CalEPA/OHEA (1996, Stochastic Analysis, p. 3-31 - 3-32; cit. above), cvA = CV[24*Q/BW] = CV[Qtot/BW] = ~ 0.3, where Q denotes total ventilation rate in L/h. From Allen and Fisher (1993), alveolar ventilation rate in L/h is modeled as Q ~ 12.9*BW^0.7, and Qtot ~ kQ for some constant k. Now let VQ be LN-distributed with an arithmetic mean of 1, where VQ represents variation in Q not attributable to that in BW. Thus, Q ~ 12.9*VQa*BW^.7, whence Q/BW ~ 12.9*VQ*BW^-0.3. It follows from the method of moments that CV[BW^-.3] = CV[BW^.3] = 0.06644, whence CV[VQ] = 0.2919, GM[VQ] = 0.9599, GSD[VQ] = 1.331, Log[{GM[VQ], GSD[VQ]}] = {-0.0408868, 0.285961}.

```
{{o1, o2} = MSDx[a BWgm^-.3, BWgsd^-.3], cvBW3 = o2 / o1}
```

```
{{0.281039 a, 0.0186711 a}, 0.066436}
```

```
{o = GMGSDx1[0.3, cvBW3], {muyX, sdyX} = Log[o]}
```

```
{{0.959938, 1.33104}, {-0.0408868, 0.285961}}
```

```
{{mX, sdX} = MSDx@@o, cvX = sdX / mX}
```

```
{{1., 0.291908}, 0.291908}
```

```
(* By definition, the CV of (BW^.3 * X) = *)
{Sqrt[E^ (sdyX^2 + Log[BWgsd^.3]^2) - 1],
 ((1 + cvBW3^2) (1 + cvX^2) - 1)^.5}
```

```
{0.3, 0.3}
```

■ InhaleALL

```
{f12, f12p}
```

```
{0.172193, 0.827807}
```

```
adf = AverageCdf[cdfs, Weights -> {f12p, f12}];
sadf = N[StandardizeCdf[adf, 404]];
```

```
PlotCdf[sadf, Xmin -> -.001, Ymin -> -.001];
```
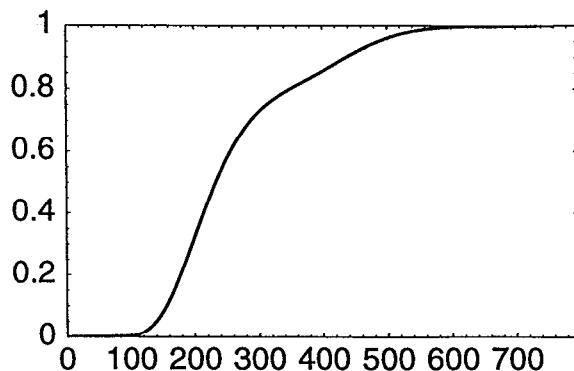
```
{EV[#], SD[#], Idf[#, {.5, .95}]}&/@{adf, sadf}
```

```
{{264.165, 107.491, {233.106, 487.138}}, {264.165, 108.051, {233.106, 487.146}}}
```

```
N[{{pA, pC} = Edf[#, 487.138]&/@cdfs, wp = {f12p*pA, f12*pC}, Plus@@wp}, 10]
```

```
{{0.9982290631, 0.7181436766}, {0.8263408411, 0.1236594327}, 0.9500002739}
```

$$\left(f12p \; \text{NormalCdf}\left[\frac{\text{Log}[x / \text{gmA}]}{\text{Log}[\text{gsdA}]} \right] + f12 \; \text{NormalCdf}\left[\frac{\text{Log}[x / \text{gmC}]}{\text{Log}[\text{gsdC}]} \right] \right) \; /. \; x \to \text{Range}[487.3, 487.4, .01]$$

```
{0.949947, 0.949956, 0.949964, 0.949972, 0.949981, 0.949989, 0.949997, 0.950006,
 0.950014, 0.950023}
```

$$N\left[\text{FindRoot}\left[f12p \; \text{CDF}\left[\text{NormalDistribution}[0, 1], \frac{\text{Log}[x / \text{gmA}]}{\text{Log}[\text{gsdA}]} \right] + \right.\right.$$

$$\left.\left. f12 \; \text{CDF}\left[\text{NormalDistribution}[0, 1], \frac{\text{Log}[x / \text{gmC}]}{\text{Log}[\text{gsdC}]} \right] == 95 / 100, \{x, 485, 480, 490\} \right], \right.$$

$$16\Big]$$

```
{x → 487.3630111243049}
```

```
WriteMatrix["BogenHD:Desktop Folder:inhaleALL.txt", sadf];
```

■ InhaleTWA

```
{{f12p, f12}, {f12p, f12} 70}
```

```
{{0.827807, 0.172193}, {57.9465, 12.0535}}
```

```
{nsam, nsim} = {2000, 10};
Clear[fxn];
fxn[a1_, a2_] := Plus@@ ({a1, a2} {
     58, 12} / 70)
```

```
Timing[{jen, cdf, cvm} = QUAnalyze[cdfs, fxn, nsam, nsim];]
```

```
{143.533 Second, Null}
```

```
TBL/@jen
```

Mean[Δr]	Max[|Δr|]	JennrichChi2	DegFr	Pval
0.0010747	0.00945733	0.178882	1	0.672335

Fractile	Value	CVM(%)
0.01	166.336	0.275487
0.05	187.965	0.14204
0.5	257.154	0.0674972
0.95	362.928	0.17087
0.99	424.294	0.272136
Mean	263.865	7.46556×10^{-7}
Variance	2937.4	0.0463849

```
PlotCdf[{cvm, cdf}, Ymin → -.01, Xmin → 95, Xmax → 430];
```
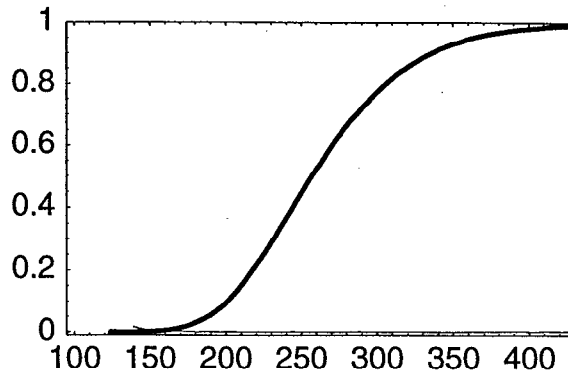


```
{EV[cdf, Empirical -> True], SD[cdf, Empirical -> True], Idf[cdf, {.5, .95}]}

{263.865, 54.1887, {257.154, 362.928}}


sdf = StandardizeCdf[cdf, 404];
{EV[sdf, Empirical -> True], SD[sdf, Empirical -> True], Idf[sdf, {.5, .95}]}

{263.752, 53.5784, {257.154, 362.847}}


WriteMatrix["Bogen's:Desktop Folder:inhaleTWA.txt", sdf];
```

Appendix 2.C

Fraction of Lifetime at One Local Residence

```
<< RiskQ`;

HardDrive = "Bogen";
PathName[filename_, hardDrive_String: HardDrive] := Module[{file = filename},
   If[Head[file] =!= String, file = ToString[file]];
   StringJoin[hardDrive, ":Ken:TCE Air Force:Data:", file]
   ];
```

■ Israeli, M., and C. Nelson. 1992. Distribution and expected time of residence for U.S. housholds. *Risk Anal.* 12, 65-72.

$$St = E^{-(a1*b1\,(1-E^{\wedge}(-t/b1))+a2\,t+a3*b3\,(E^{\wedge}(t/b3)-1))};$$

$$pt = St\,((a1 * (E^{\wedge} - (t/b1))) + a2 + (a3 * (E^{\wedge}(t/b3))));$$

$$Rt = \frac{pt}{a1 + a2 + a3};$$

Coefficients a and b all have units of y^{-1} and y, respectively, from Israeli and Nelson Table II (All households, W-Rgn)

■ All households

```
ruleA = Rule@@#& /@ Transpose[{{a1, b1, a2, a3, b3}, {.1503, 1.88, .0679, .0015, 13.3}}];

{St, Rt, RtrA = (Rt /. ruleA)}
```

$$\left\{E^{-a1\,b1\left(1-E^{-\frac{t}{b1}}\right)-a3\,b3\left(-1+E^{\frac{t}{b3}}\right)-a2\,t},\; \frac{E^{-a1\,b1\left(1-E^{-\frac{t}{b1}}\right)-a3\,b3\left(-1+E^{\frac{t}{b3}}\right)-a2\,t}\left(a2 + a1\,E^{-\frac{t}{b1}} + a3\,E^{\frac{t}{b3}}\right)}{a1 + a2 + a3},\; 4.55166\right.$$

$$\left. E^{-0.282564\,(1-E^{-0.531915\,t})-0.01995\,(-1+E^{0.075188\,t})-0.0679\,t}\;(0.0679 + 0.1503\,E^{-0.531915\,t} + 0.0015\,E^{0.075188\,t})\right\}$$

```
({St, pt, Rt} /. Append[ruleA, t -> #])& /@ {0, 50}
```

```
{{1, 0.2197, 1.}, {0.0109554, 0.00144923, 0.00659639}}
```

```
Plot[Log[10, Evaluate[St /. ruleA]], {t, 0, 50},
AxesOrigin -> {0, -3.01}, PlotRange -> {{0, 50}, {-3.01, 0}}, Frame -> True];
```
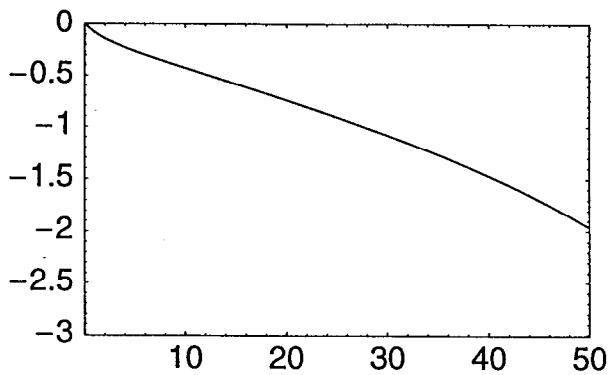


```
Plot[Log[10, Evaluate[RtrA]], {t, 0, 50},
AxesOrigin -> {-0.01, -3.01}, PlotRange -> {{-.01, 50}, {-3.01, 0}}, Frame -> True];
```
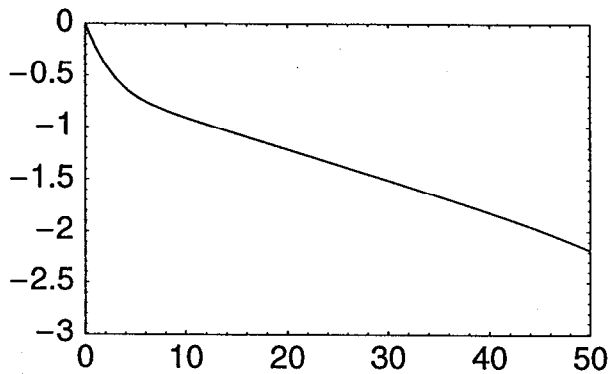

■ Western Region

```
ruleW = Rule@@#&/@Transpose[{{a1, b1, a2, a3, b3}, {.2029, 1.74, .0832, .0008, 10.3}}]
```

$\{a1 \rightarrow 0.2029, b1 \rightarrow 1.74, a2 \rightarrow 0.0832, a3 \rightarrow 0.0008, b3 \rightarrow 10.3\}$

```
RtrW = (Rt /. ruleW)
```

$3.48554 \, E^{-0.353046 \, (1-E^{-0.574713 \, t}) - 0.00824 \, (-1+E^{0.0970874 \, t}) - 0.0832 \, t} \, (0.0832 + 0.2029 \, E^{-0.574713 \, t} + 0.0008 \, E^{0.0970874 \, t})$

```
({St, pt, Rt} /. Append[ruleW, t -> #])&/@{0, 50}
```

$\{\{1, 0.2869, 1.\}, \{0.0038411, 0.00071383, 0.00248808\}\}$

```
Plot[Evaluate[Log[10, (St /. #)&/@{ruleA, ruleW}]], {t, 0, 50},
AxesOrigin -> {0, -3.01}, PlotRange -> {{0, 50}, {-3.01, 0}}, Frame -> True];
```
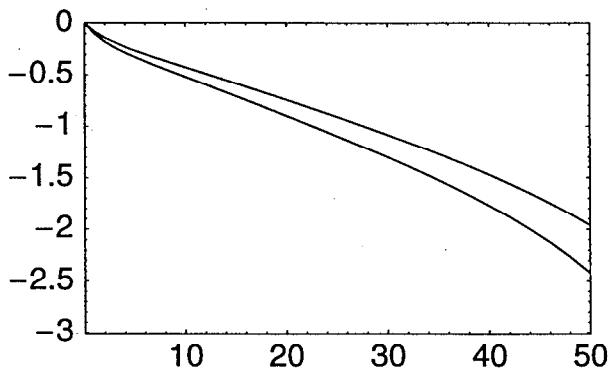


```
Plot[Evaluate[Log[10, {RtrA, RtrW}]], {t, 0, 50},
AxesOrigin -> {-0.01, -3.01}, PlotRange -> {{-.01, 50}, {-3.01, 0}}, Frame -> True];
```
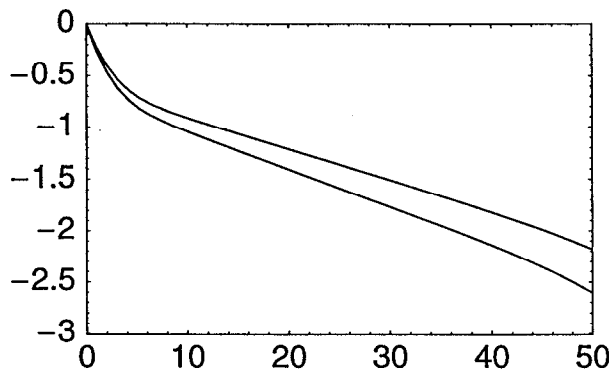

■ Adaptation of model to account for fraction Fm of moves that are out of a Western-region water distribution system

```
{RtrW, (RtrW /. t -> #)&/@{0, 50, 70}}
```

$$\{3.48554$$
$$E^{-0.353046\ (1-E^{-0.574713\ t})-0.00824\ (-1+E^{0.0970874\ t})-0.0832\ t}\ (0.0832 + 0.2029\ E^{-0.574713\ t} + 0.0008\ E^{0.0970874\ t}),$$
$$\{1., 0.00248808, 3.67283\times 10^{-6}\}\}$$

$$\left\{ fmLo = \frac{1}{3} + \sqrt{\frac{2}{3}\frac{1}{3}\ 0.05}\ ,\ fmHat = \frac{2}{3}\right\}$$

$$\left\{0.438743,\ \frac{2}{3}\right\}$$

```
time = Join[Range[0, 10, .1], Range[11, 50], Range[55, 70, 5]];
Mt = ((1 - RtrW^1) /. t -> time);
MtFmHat = ((1 - RtrW^fmHat) /. t -> time);
MtFmLo = ((1 - RtrW^fmLo) /. t -> time);

{cdfTR, cdfTRFmHat, cdfTRFmLo} =
 Append[Drop[Transpose[{time, #}], -1], {70, 1}]&/@{Mt, MtFmHat, MtFmLo};
```

```
RtrW /. t -> 1
```

0.544555

```
PlotData[{cdfTRFmLo, cdfTRFmHat, cdfTR}, Xmin -> -.01, Xmax -> 70, Ymin -> 0, Ymax -> 1,
  DotSize -> {.0001, .008, .0125}, Style -> O,
  JoinPoints -> True, FitTo -> {RtrW, t}];
```
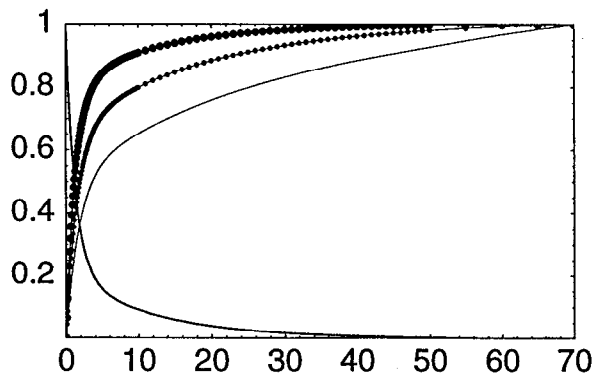


```
{EV[cdfTR], Sqrt[Var[cdfTR]], Idf[cdfTR, {.025, .5, .95, .975}]}
```

```
{3.48741, 6.83815, {0.0378193, 1.16603, 17.0596, 25.4481}}
```

```
{EV[cdfTRFmHat], Sqrt[Var[cdfTRFmHat]], Idf[cdfTRFmHat, {.025, .5, .95, .975}]}
```

```
{7.02862, 11.8589, {0.0560921, 1.9295, 35.0626, 46.1341}}
```

```
{EV[cdfTRFmLo], Sqrt[Var[cdfTRFmLo]], Idf[cdfTRFmLo, {.025, .5, .95, .975}]}
```

```
{12.9946, 17.7241, {0.0845741, 3.63964, 55.2843, 61.7931}}
```

```
Rt = (RtrW /. t -> time);
xy = Append[Drop[Transpose[{time, Rt}], -1], {70, 0}];
IRt = Interpolation[xy, InterpolationOrder -> 1];
```

```
10.5 / 16. (* = US fraction moving to same county *)
```

0.65625

```
fms = SimulateCdf[{Tri, {1 / 3, 2 / 3, 1}}, 2000];
Idf[Cdf[fms], .05]
```

0.438716

```
PlotCdf[Cdf[fms]];
```
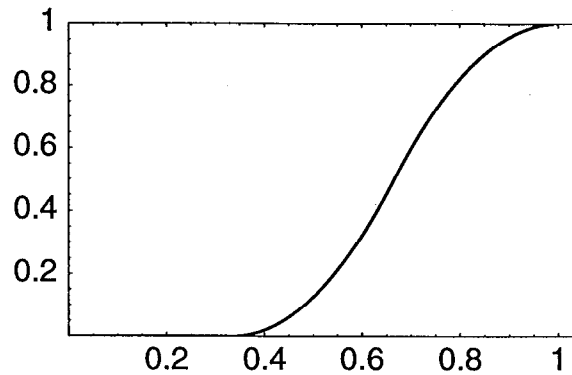


```
tRange = Prepend[time, t];

Tbar = NIntegrate[IRt[t]^#, Evaluate[tRange]]&/@fms;

cdfTbar = Cdf[Tbar];

PlotCdf[cdfTbar, Xmin -> -.01, Xmax -> 16];
```
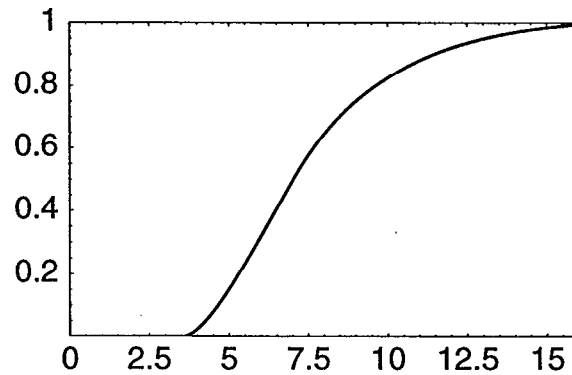


```
{EV[Tbar], Sqrt[Var[Tbar]], Idf[cdfTbar, {.025, .5, .975}]}

{7.5984, 2.67068, {4.00903, 7.03101, 14.2792}}

D[a^Fm, {Fm, 2}]

a^Fm Log[a]^2

cdfFm = TriangularCdf[1 / 3, 2 / 3, 1, 500];
{EV[cdfFm], Var[cdfFm]}

{0.666667, 0.0185294}

cdfFm = TriangularCdf[1 / 3, 2 / 3, 1, 10000];
{EV[cdfFm], Var[cdfFm]}

{0.666667, 0.0185186}
```

```
0.0185186464965580999^-1
```

```
53.999626818615568
```

```
Rti = Transpose[xy][[2]];
fmBar = 2 / 3;
fmVar = 1 / 54;
```

$$pi = 1 - \left((Rti \wedge fmBar) \left(1 + \frac{Log[Rti]^2}{2} fmVar \right) \right);$$

```
pi = Append[Drop[pi, -1], 1];
```

```
cdfTangbr = Transpose[{time, pi}];
```

```
PlotCdf[cdfTangbr, Xmin -> -.01, Xmax -> 70];
```
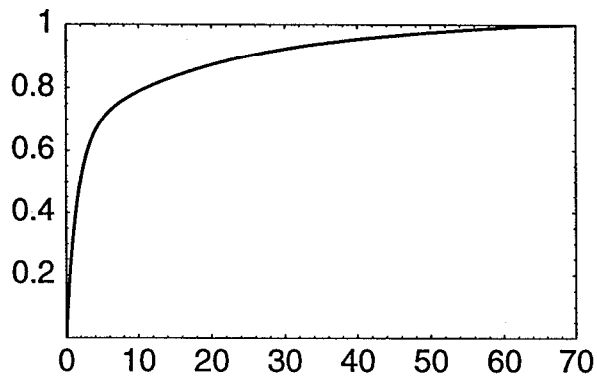


```
PlotCdf[{cdfTangbr, cdfTbar}, Xmin -> -.01, Xmax -> 70];
```
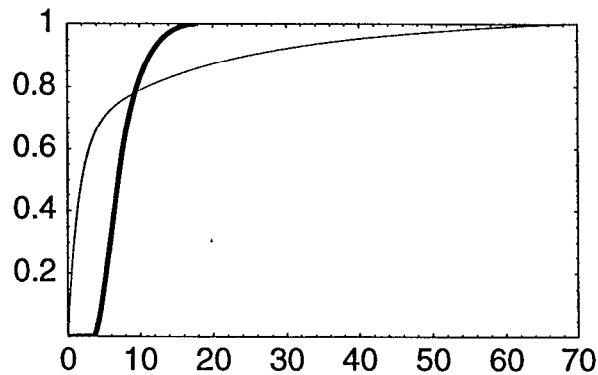


```
{EV[cdfTangbr], Sqrt[Var[cdfTangbr]], Idf[cdfTangbr, {.025, .5, .975}]}
```

```
{7.55321, 12.748, {0.0561443, 1.96772, 49.7245}}
```

```
sdfTbar = StandardizeCdf[cdfTbar, time];
```

```
TBL[out = Prepend[Transpose[{time, N[Last /@ sdfTbar, 8],
    N[Last /@ cdfTangbr, 8]}], {Time, FTbar, FTangbr}]]
```

Time	FTbar	FTangbr
0	0	0.
0.1	0.000014065155	0.044528152
0.2	0.00002813031	0.085900584
0.3	0.000042195465	0.12439054

0.4	0.00005626062	0.16024284
0.5	0.000070325776	0.19367728
0.6	0.000084390931	0.22489166
0.7	0.000098456086	0.25406435
0.8	0.00011252124	0.2813565
0.9	0.0001265864	0.30691402
1.	0.00014065155	0.33086927
1.1	0.00015471671	0.35334255
1.2	0.00016878186	0.37444339
1.3	0.00018284702	0.39427172
1.4	0.00019691217	0.41291884
1.5	0.00021097733	0.43046832
1.6	0.00022504248	0.4469968
1.7	0.00023910764	0.46257462
1.8	0.00025317279	0.47726652
1.9	0.00026723795	0.49113209
2.	0.0002813031	0.50422633
2.1	0.00029536826	0.51660002
2.2	0.00030943341	0.52830013
2.3	0.00032349857	0.53937017
2.4	0.00033756372	0.54985047
2.5	0.00035162888	0.55977846
2.6	0.00036569403	0.56918892
2.7	0.00037975919	0.57811422
2.8	0.00039382434	0.58658448
2.9	0.0004078895	0.59462778
3.	0.00042195465	0.60227029
3.1	0.00043601981	0.60953645
3.2	0.00045008496	0.61644911
3.3	0.00046415012	0.62302958
3.4	0.00047821527	0.62929784
3.5	0.00049228043	0.63527256
3.6	0.0013753219	0.64097123
3.7	0.0046798441	0.64641023
3.8	0.0097212226	0.65160492
3.9	0.016294389	0.6565697
4.	0.024222899	0.66131805
4.1	0.033351911	0.66586267
4.2	0.043545234	0.67021542
4.3	0.054682977	0.67438749
4.4	0.066658284	0.67838933
4.5	0.079376907	0.68223081
4.6	0.092754949	0.68592116
4.7	0.10671755	0.68946908
4.8	0.12119799	0.69288271
4.9	0.13613655	0.69616975
5.	0.15147976	0.69933738
5.1	0.16717972	0.70239239
5.2	0.18319323	0.70534116
5.3	0.19948154	0.70818966
5.4	0.21600975	0.71094353
5.5	0.23274635	0.71360807
5.6	0.24966287	0.71618824
5.7	0.26673362	0.71868873
5.8	0.28393535	0.72111394
5.9	0.30124702	0.72346801
6.	0.31864953	0.72575483
6.1	0.33612562	0.72797806
6.2	0.3536596	0.73014114
6.3	0.37123722	0.73224731
6.4	0.38884558	0.73429961
6.5	0.40647292	0.7363009
6.6	0.4241086	0.73825388
6.7	0.44174292	0.74016109
6.8	0.45936707	0.74202489
6.9	0.47697308	0.74384753
7.	0.49455365	0.74563113
7.1	0.51196343	0.74737765
7.2	0.52877535	0.74908897
7.3	0.54498488	0.75076684
7.4	0.56061815	0.75241291
7.5	0.57570017	0.75402873
7.6	0.59025445	0.75561577
7.7	0.60430319	0.75717539
7.8	0.61786745	0.7587089
7.9	0.63096716	0.7602175
8.	0.6436211	0.76170234
8.1	0.65584727	0.76316451
8.2	0.66766265	0.76460501
8.3	0.67908339	0.7660248
8.4	0.69012475	0.76742478

```
8.5    0.70080134        0.76880579
8.6    0.71112707        0.77016864
8.7    0.72111508        0.77151407
8.8    0.73077791        0.7728428
8.9    0.74012765        0.77415548
9.     0.74917561        0.77545275
9.1    0.75793282        0.77673519
9.2    0.7664095         0.77800336
9.3    0.77461566        0.7792578
9.4    0.78256085        0.78049899
9.5    0.79025397        0.7817274
9.6    0.79770389        0.78294347
9.7    0.80491887        0.78414763
9.8    0.81190674        0.78534025
9.9    0.81867513        0.78652171
10.    0.82523141        0.78769236
11     0.88053089        0.79886871
12     0.9207822         0.80923462
13     0.9498595         0.81893815
14     0.97047554        0.82807078
15     0.98457918        0.83669313
16     0.99360366        0.84484873
17     0.99861864        0.8525714
18     1.                0.85988918
19     1.                0.86682654
20     1.                0.87340553
21     1.                0.8796464
22     1.                0.88556805
23     1.                0.89118824
24     1.                0.89652371
25     1.                0.90159033
26     1.                0.90640318
27     1.                0.91097659
28     1.                0.91532422
29     1.                0.91945913
30     1.                0.92339381
31     1.                0.9271402
32     1.                0.9307098
33     1.                0.93411365
34     1.                0.93736239
35     1.                0.94046627
36     1.                0.9434352
37     1.                0.94627875
38     1.                0.94900617
39     1.                0.9516264
40     1.                0.95414801
41     1.                0.95657927
42     1.                0.95892806
43     1.                0.96120185
44     1.                0.96340761
45     1.                0.9655518
46     1.                0.96764026
47     1.                0.96967807
48     1.                0.97166952
49     1.                0.97361794
50     1.                0.97552559
55     1.                0.98444368
60     1.                0.99193758
65     1.                0.99706939
70     1.                1.
```

```
Put[out, PathName[Tbarang]];
```

Appendix 2.D

Effective Genotoxic Dose

```
<< RiskQ`;

HardDrive = "Bogen";
PathName[filename_, hardDrive_String: HardDrive] := Module[{file = filename},
  If[Head[file] =!= String, file = ToString[file]];
  StringJoin[hardDrive, ":Ken:TCE Air Force:Data:", file]
];
```

■ Input Empirical (Derived) Distributions

Recreate Input Distributions from Phase I study. Exposure in mg/kg-d.

■ Log-Transform Utility Functions

```
GMGSDx::usage = "GMGSDx[Mx,SDx] returns the  geometric mean and geometric sdandard
    deviation of a lognormal variate X that also has the specified arithmetic mean Mx
    and arithmetic sdandard deviation SDx, based on the method of moments.";

MSDx::usage = "MSDx[GMx,GSDx] returns the arithmetic mean and arithmetic sdandard
    deviation of a lognormal variate X that also has the specified geometric mean GMx
    and geometric sdandard deviation GSDx, based on the method of moments.";

GMGSDx1::usage = "GMGSDx1[cvWant,cv2] returns the GM and GSD of a lognormal variate
    X1, such that the product X1*X2 has the desired coefficient of variation (CV) =
    cvWant, conditional on the lognormal variate X2 having an arithmetic
    mean and CV equal to 1 and cv2, respectively, based on the method of moments.";

MSDx[GMx_, GSDx_] := Module[{mux, sigy},
  sigy = Log[GSDx];
  mux = GMx E ^ ((sigy^2) / 2);
  mux {1, Sqrt[E ^ (sigy^2) - 1]}]

GMGSDx[Mx_, SDx_] := Module[{muy, sigy},
  sigy = Sqrt[Log[1 + (SDx / Mx) ^ 2]];
  muy = Log[Mx] - (sigy^2) / 2;
  E ^ {muy, sigy}]
```

$$GMGSDx1[cvWant\_, cv2\_] := Module\Big[\{my1\},$$

$$muy1 = Log\Big[Sqrt\Big[\frac{cv2^2 + 1}{cvWant^2 + 1}\Big]\Big];$$

$$E \wedge \{muy1, Sqrt[-2\, muy1]\}$$

$$\Big] \; /; \; cvWant >= cv2$$

```
SABW = ToExpression[ReadList[PathName["sabwratioALL.txt"], Word, RecordLists -> True]];
Inhale = ToExpression[ReadList[PathName["inhaleALL.txt"], Word, RecordLists -> True]];
    (*Note: Inhale in L/kg-d *)
Conc = ToExpression[ReadList[PathName["concentration.txt"], Word, RecordLists -> True]];
    (*Note: Conc in mg/L *)
Tbarang = Rest[Get[PathName[Tbarang]]];
TresBar = #[[{1, 2}]]&/@Tbarang;
TresAng = #[[{1, 3}]]&/@Tbarang;
Dimensions/@{SABW, Inhale, Conc, TresBar, TresAng}

{{27, 2}, {405, 2}, {405, 2}, {145, 2}, {145, 2}}


EV/@{SABW, Inhale, Conc, TresBar, TresAng}

{325.881, 264.032, 0.0229323, 7.59939, 7.55321}


{BW, Vmet, VQ} =
  {{LN, {4.23821, 0.22121}},
   {LN, {-0.15154, 0.550528}}, {LN, {-0.0408868, 0.285961}}};
```

■ **Constants**

```
{TresBarAng, TresAngBar} = EV[#, Empirical -> True]&/@{TresBar, TresAng}

{7.59939, 7.55321}
```

$$\text{inhalebar} = 12.9 * 71^{0.74-1} * \frac{24}{1000} \qquad (* \ m3/kg\text{-}d \ *)$$

```
0.102205
```

```
EFcon    =     350;      (* d/y  *)
ATcon    =   25550;      (* d    *)
ConcAng  =   0.0223;     (* mg/L *)
IngestBar=   0.0242;     (* L/kg-d *)
InhaleBar =  0.102;      (* m3/kg-d *)
SABWBar  =   325.881;    (* cm2/kg *)
TresBarAng= 7.59358;     (* y *)
TresAngBar= 7.55321;     (* y *)
```

end

■ Fractions metabolized (summary–see "E. Effective Cytotoxic Dose")

Correlation between Vmet and Fmo = 0.86
Correlation between VQ and Fmr = -0.75
Correlation between Vmet and Fmr = 0.45

```
Fmo = Get[PathName[Fmo]]; Fmr = Get[PathName[Fmr]];
CdfQ/@{Fmo, Fmr}

{True, True}


{FmoBar, FmrBar} = {0.888543, 0.6732836};
```

end

Note:
All distributions below are multiplied by Scale→1000

■ Ingestion

■ EingBar = Uncertainty in Population-Average Level

{TresBar,Conc} = uncertain variates

```
{nsam, nsim} = {2000, 10};
cdfs = {TresBar, Conc};
Clear[fxn];
                        EFcon
fxn[t_, c_] := IngestBar * t ——— c * FmoBar
                        ATcon

fxn[TresBarAng, ConcAng]
```

0.0000498795

```
Timing[{jen, cdf, cvm} = QUAnalyze[cdfs, fxn, nsam, nsim, Scale → 1000];]
```

{200.817 Second, Null}

```
TBL /@jen
```

					Fractile	Value	CVM(%)
					0.01	0.0143149	2.23118
					0.05	0.0230076	0.210285
Mean[Δr]	Max[|Δr|]	JennrichChi2	DegFr	Pval	0.5	0.0429802	0.168471
−0.00355814	0.0158828	0.504529	1	0.477517	0.95	0.0889072	0.414161
					0.99	0.134017	1.78008
					Mean	0.0507837	0.514653
					Variance	0.00710812	18.3718

```
{First[cdf], Last[cdf]}
```

{{0.000853119, 0}, {4.43688, 1}}

```
PlotCdf[{cvm, cdf}, Ymin → -.01, Xmin → -.0001, Xmax → .125];
```



```
Put[cdf, PathName[EingestBar]];
```

end

■ <Eing> = Variability in Expected Level

{Ingest,TresAng,Fmo} = heterogeneous variates

```
{nsam, nsim} = {2000, 10};
Ingest = {LN, {Log[.0198], Log[1.88]}};
cdfs = {Ingest, TresAng, Fmo};
Clear[fxn];
```

$$fxn[ing\_, t\_, f\_] := ing * t \frac{EFcon}{ATcon} ConcAng * f$$

```
fxn[IngestBar, TresAngBar, FmoBar]
```

```
0.0000496144
```

```
Timing[{jen, cdf, cvm} = QUAnalyze[cdfs, fxn, nsam, nsim, Scale → 1000];]
```
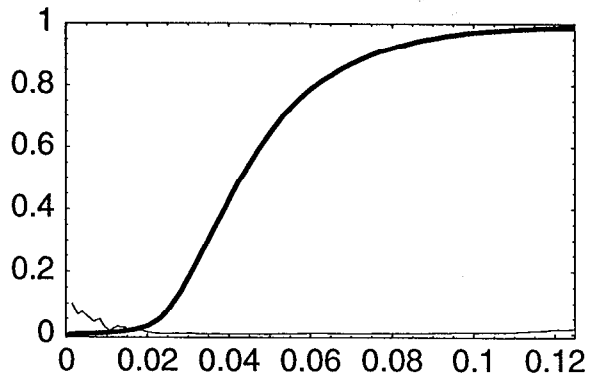
```
{47.8167 Second, Null}
```

```
TBL/@jen
```

Mean[Δr]	Max[|Δr|]	JennrichChi2	DegFr	P-adj
0.00168143	0.0152108	0.522666	3	0.995174

Fractile	Value	CVM(%)
0.01	0.000106569	3.27128
0.05	0.000509143	1.43336
0.5	0.0108513	0.866917
0.95	0.23658	1.24671
0.99	0.531411	4.21273
Mean	0.0491639	0.747214
Variance	0.0111399	5.47589

```
PlotCdf[{cvm, cdf}, Ymin → -.01, Xmin → -.0001, Xmax → .4];
```



```
Put[cdf, PathName[EingestAng]];
```

end

end

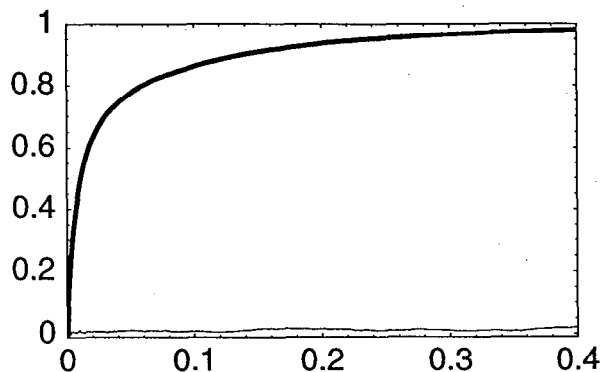# ■ Inhalation Exposure

■ EinhBar = Uncertainty in Population-Average Level

{TresBar,Conc} = uncertain variates

```
{AEshHBar, AEbaHBar, AEhHBar} = 1 / (EV /@ {
{1. / #[[1]], #[[2]]}&/@RQ[Cdf, U, {4, 20}, 2000],
{1. / #[[1]], #[[2]]}&/@RQ[Cdf, U, {10, 100}, 2000],
{1. / #[[1]], #[[2]]}&/@RQ[Cdf, U, {300, 1200}, 2000]})
```

```
{9.94136, 39.0865, 649.213}
```

```
cdfs = {TresBar, Conc};
```

$$
\text{fxn} \to \text{FmrBar} \left(\frac{12.9}{1000} * 71^{.74-1} * 1 \right) * t \; \frac{\text{EFcon}}{\text{ATcon}} \; c \; \frac{1}{24}
$$

$$
\left(480 \; (.76) \left(\frac{.129}{\text{AEshHBar}} + \frac{.33}{\text{AEbaHBar}} \right) + 42 \left(.76 \; \frac{.54}{.7} \right) \frac{14}{\text{AEhHBar}} \right)
$$

```
fxn → 0.0000136563 c t
```

```
Clear[fxn, jen, cdf, cvm];
fxn[t_, c_] := 0.0000136563095583647187` c t
```

```
fxn[t, c] /. {c → ConcAng, t → TresBarAng}
```

$$
2.31252 \times 10^{-6}
$$

```
Timing[{jen, cdf, cvm} = QUAnalyze[cdfs, fxn, 2000, 10, Scale → 1000];]
```

```
{205.55 Second, Null}
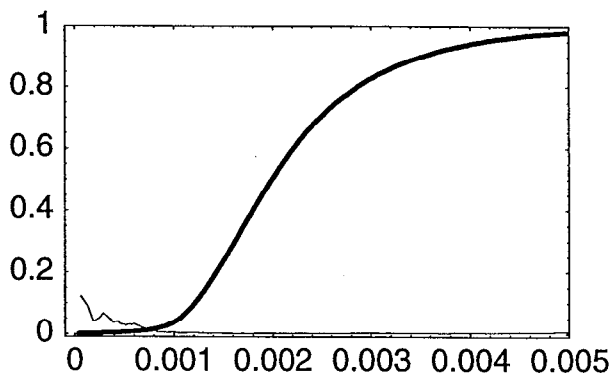```

**TBL/@jen**

```
{ Mean[Δr]      Max[|Δr|]   JennrichChi2  DegFr  Pval
{ 0.000642353   0.0113889   0.259415      1      0.610522 '
```

```
Fractile   Value         CVM(%)
0.01       0.000683362   2.05913
0.05       0.00106135    0.294054
0.5        0.00198916    0.19258
0.95       0.00412975    0.389326
0.99       0.00593213    1.01573
Mean       0.00235084    0.583042
Variance   0.0000146843  23.1052
```

{First[cdf], Last[cdf]}

```
{{0.0000407589, 0}, {0.209696, 1}}
```

PlotCdf[{cvm, cdf}, Ymin → -.01, Xmin → -.0001, Xmax → .005];

Put[cdf, PathName[EinhaleBar]];

end

■ <Einh> = Variability in Expected Level

{Inhale,TresAng,Wshower,Whouse,ETshower,ETbath,EThouse,AEshower,AEbath,AEhouse,
T13,T13,VQ,BW} = heterogeneous variates

gmgsd = GMGSDx@@#&/@N[{{480, 160}, {42, 15}, {.129, .052}, {.33, .22}}]

```
{{455.368, 1.38347}, {39.5532, 1.41408}, {0.119645, 1.47407}, {0.274577, 1.83382}}
```

{Wshower, Whouse, ETshower, ETbath} = ({LN, #}&/@Log[gmgsd])

```
{{LN, {6.12111, 0.324593}}, {LN, {3.67765, 0.346479}}, {LN, {-2.12323, 0.388026}},
 {LN, {-1.29253, 0.606403}}}
```

{AEshower, AEbath, AEhouse, EThouse} =
   ({U, #}&/@{{4, 20}, {10, 100}, {300, 1200}, {8, 20}})

```
{{U, {4, 20}}, {U, {10, 100}}, {U, {300, 1200}}, {U, {8, 20}}}
```

```
{InhaleBar, TresAngBar, ConcAng}

{0.102, 7.55321, 0.0223}

{VQ, BW}

{{LN, {-0.0408868, 0.285961}}, {LN, {4.23821, 0.22121}}}
```

Correlation between VQ and Fmr = -0.75 (see "E. Effective Cytotoxic Dose")

```
corr = Table[Table[0, {j}], {j, 13}];
corr = ReplacePart[Reverse[corr], -.75, {1, 1}]

{{-0.75, 0, 0, 0, 0, 0, 0, 0, 0, 0, 0, 0, 0}, {0, 0, 0, 0, 0, 0, 0, 0, 0, 0, 0, 0},
 {0, 0, 0, 0, 0, 0, 0, 0, 0, 0, 0}, {0, 0, 0, 0, 0, 0, 0, 0, 0, 0}, {0, 0, 0, 0, 0, 0, 0, 0, 0},
 {0, 0, 0, 0, 0, 0, 0, 0}, {0, 0, 0, 0, 0, 0, 0}, {0, 0, 0, 0, 0, 0}, {0, 0, 0, 0, 0},
 {0, 0, 0, 0}, {0, 0, 0}, {0, 0}, {0}}
```

```
Clear[fxn];
T13 = {T, 13};
cdfs = {Fmr, VQ, BW, TresAng, Wshower,
  Whouse, ETshower, ETbath, EThouse, AEshower, AEbath, AEhouse, T13, T13};
fxn[f_, vq_, bw_, t_, wsh_, wh_, etsh_, etba_, eth_, aesh_, aeba_, aeh_, t13sh_, t13h_] :=
```

$$ f * \left(\frac{12.9}{1000} * bw^{.74-1} * vq\right) t \ \frac{EFcon}{ATcon} \ ConcAng \ \frac{1}{24} \ \left($$

$$ wsh \ (.76 + .029 \ t13sh) \ \left(\frac{etsh}{aesh} + \frac{etba}{aeba}\right) + wh \ \left((.76 + .029 \ t13h) \ \frac{.54}{.7}\right) \frac{eth}{aeh} \right) $$

```
fxn[FmrBar, 1, 71, TresAngBar, 480, 42, .129, .33, 14, AEshHBar, AEbaHBar, AEhHBar, 0, 0]

2.30022 × 10⁻⁶
```

```
Timing[{jen, cdf, cvm} = QUAnalyze[cdfs, fxn, 2000, 10, Correlate → corr, Scale → 1000];]

{277.6 Second, Null}
```

```
TBL/@jen
```

Mean[Δr]	Max[|Δr|]	JennrichChi2	DegFr	P-adj
-0.000310836	0.0321802	10.4729	91	1.

Fractile	Value	CVM(%)
0.01	4.8772 × 10⁻⁶	2.95986
0.05	0.0000238177	1.50669
0.5	0.000489184	0.794377
0.95	0.010794	1.05828
0.99	0.0233732	2.245
Mean	0.00225019	0.501055
Variance	0.0000244482	5.8905

```
PlotCdf[{cvm, cdf}, Ymin → -.01, Xmin → -.0001, Xmax → .0125];
```
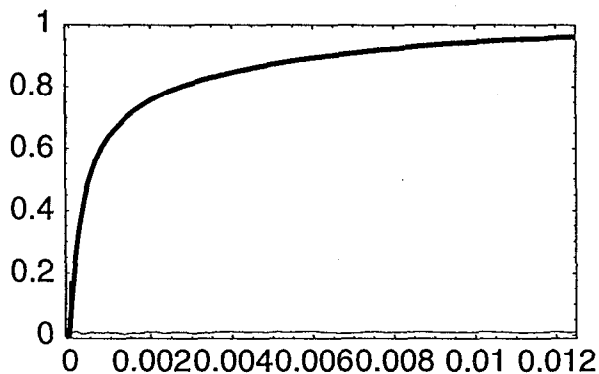


```
Put[cdf, PathName[EinhaleAng]];
```

end

end

■ Dermal Exposure

■ EdermalBar = Uncertainty in Population-Average Level

{TresBar,Conc} = uncertain variates

```
ETshower
```

```
{LN, {-2.12323, 0.388026}}
```

```
cdfs = {TresBar, Conc};
```

$$fxn \rightarrow FmrBar * SABWBar * .65 * .263 * .129 * t \; \frac{EFcon}{ATcon} \; c \left(1 - \frac{.76}{2}\right) 10^{-3}$$

```
fxn → 0.0000410946 c t
```

```
Clear[fxn];
fxn[t_, c_] := 0.0000410945965500063259` c t
```

```
fxn[t, c] /. {c → ConcAng, t → TresBarAng}
```

6.95883×10^{-6}

```
Timing[{jen, cdf, cvm} = QUAnalyze[cdfs, fxn, 2000, 10, Scale → 1000];]
```

```
{33.3833 Second, Null}
```

```
TBL/@jen
```

$$\left\{ \begin{array}{llllll} \text{Mean}[\Delta r] & \text{Max}[|\Delta r|] & \text{JennrichChi2} & \text{DegFr} & \text{P-adj} \\ -0.00280571 & 0.0144425 & 0.41717 & 1 & 0.929433 \end{array} \right\}$$

```
Fractile  Value       CVM(%)
0.01      0.00213724  1.34291
0.05      0.00318948  0.37956
0.5       0.005998    0.123699⎫
0.95      0.0123634   0.459695⎭
0.99      0.0187893   1.62332
Mean      0.0071258   0.269769
Variance  0.000136076 8.27214
```

```
PlotCdf[{cvm, cdf}, Ymin → -.01, Xmin → -.0001, Xmax → .015];
```
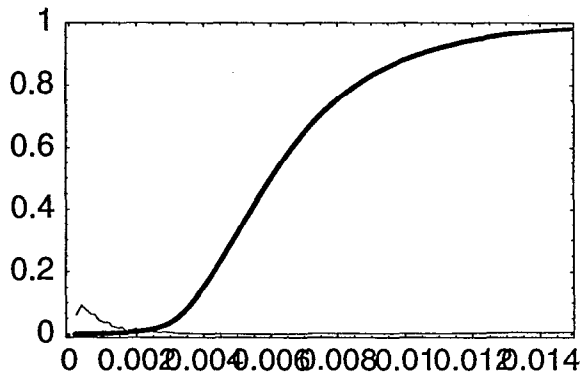


```
Put[cdf, PathName[EdermalBar]];
```

end

■ <Edermal> = Variability in Expected Level

{SABW,Fs,Kp,ETshower,TresAng,T13,Fmr} = heterogeneous variates

```
CdfQ/@{SABW, TresAng}
```

{True, True}

```
{ConcAng, Fs, Kp, ETshower, T13}
```

{0.0223, Fs, Kp, {LN, {-2.12323, 0.388026}}, {T, 13}}

```
T13 = {T, 13};
Fs = {U, {.4, .9}};
Kp = {N, {.263, .018}};
cdfs = {Fmr, SABW, Fs, Kp, ETshower, TresAng, T13};
Clear[fxn];
fxn[f_, sabw_, fs_, kp_, etsh_, t_, t13_] :=
```

$$f * sabw * fs * kp * etsh * t \frac{\text{EFcon}}{\text{ATcon}} \text{ConcAng} \left(1 - \frac{.76 + .029\ t13}{2}\right) 10^{-3}$$

```
fxn[FmrBar, SABWBar, .65, .263, .129, TresAngBar, 0]
```

6.92183×10^{-6}

```
Timing[{jen, cdf, cvm} = QUAnalyze[cdfs, fxn, 2000, 10, Scale → 1000];]
```

{131.933 Second, Null}

```
TBL/@jen
```

$$\left\{ \begin{array}{lllll} \text{Mean}[\Delta r] & \text{Max}[|\Delta r|] & \text{JennrichChi2} & \text{DegFr} & \text{P-adj} \\ -0.000538521 & 0.0183593 & 2.62117 & 21 & 1. \end{array} \right., $$

```
Fractile  Value            CVM(%)
0.01      0.0000165555     3.56479
0.05      0.0000796803     1.07369
0.5       0.00159787       0.732505
0.95      0.0331107        1.28518
0.99      0.0669827        1.42869
Mean      0.00684773       0.342052
Variance  0.000191493      1.74394
```

```
PlotCdf[{cvm, cdf}, Ymin → -.01, Xmin → -.0001, Xmax → .03];
```
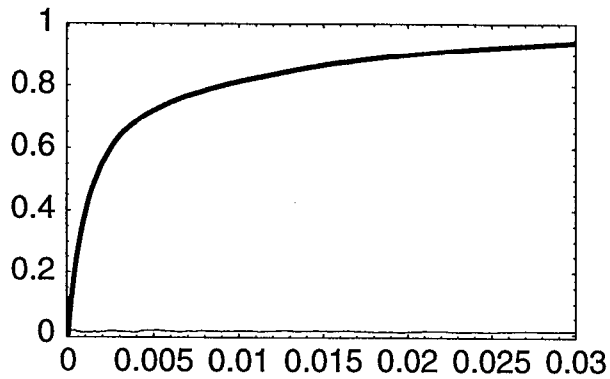


```
Put[cdf, PathName[EdermalAng]];
```

end

end

Appendix 2.E:

Effective Cytotoxic Dose

```
<< RiskQ`;

HardDrive = "Bogen";
PathName[filename_, hardDrive_String: HardDrive] := Module[{file = filename},
  If[Head[file] =!= String, file = ToString[file]];
  StringJoin[hardDrive, ":Ken:TCE Air Force:Data:", file]
  ];
```

Inputs

■ Log-Transform Utility Functions

```
GMGSDx::usage = "GMGSDx[Mx,SDx] returns the  geometric mean and geometric sdandard
    deviation of a lognormal variate X that also has the specified arithmetic mean Mx
    and arithmetic sdandard deviation SDx, based on the method of moments.";

MSDx::usage = "MSDx[GMx,GSDx] returns the arithmetic mean and arithmetic sdandard
    deviation of a lognormal variate X that also has the specified geometric mean GMx
    and geometric sdandard deviation GSDx, based on the method of moments.";

GMGSDx1::usage = "GMGSDx1[cvWant,cv2] returns the GM and GSD of a lognormal variate
    X1, such that the product X1*X2 has the desired coefficient of variation (CV) =
    cvWant, conditional on the lognormal variate X2 having an arithmetic
    mean and CV equal to 1 and cv2, respectively, based on the method of moments.";

MSDx[GMx_, GSDx_] := Module[{mux, sigy},
  sigy = Log[GSDx];
  mux = GMx E ^ ((sigy^2) / 2);
  mux {1, Sqrt[E ^ (sigy^2) - 1]}]

GMGSDx[Mx_, SDx_] := Module[{muy, sigy},
  sigy = Sqrt[Log[1 + (SDx / Mx) ^ 2]];
  muy = Log[Mx] - (sigy^2) / 2;
  E ^ {muy, sigy}]
```

$$GMGSDx1[cvWant\_, cv2\_] := Module\Big[\{my1\},$$
$$muy1 = Log\Big[Sqrt\Big[\frac{cv2^2 + 1}{cvWant^2 + 1}\Big]\Big];$$
$$E \wedge \{muy1, Sqrt[-2\ muy1]\}$$
$$\Big] /;\ cvWant >= cv2$$

■ Input Empirical (Derived) Distributions

```
Conc = ToExpression[
   ReadList[PathName["concentration.txt", HardDrive], Word, RecordLists -> True]];
ConcAng =  0.0223;   (* mg/L    *)


Ingest = {LN, {Log[.0198], Log[1.88]}};
IngestBar = 0.0242; (* L/kg-d  *)


SABW = ToExpression[
   ReadList[PathName["sabwratioALL.txt", HardDrive], Word, RecordLists -> True]];
SABWBar =  325.881; (* cm2/kg *)
Fs = {U, {.4, .9}};
Kp = {N, {.263, .018}};


InhaleBar = 12.9 * (71^.74);    (* L/h *)
VQ = {LN, Log[{.959938, 1.33104}]};
T13 = {T, 13};
AEshower = {U, {4, 20}};
AEshHBar = 1/EV[{1./#[[1]], #[[2]]}&/@RQ[Cdf, U, {4, 20}, 2000]];
{gmgsd = GMGSDx@@#&/@N[{{480, 160}, {.129, .052}}]],
{Wshower, ETshower} = ({LN, #}&/@Log[gmgsd])}

{{{455.368, 1.38347}, {0.119645, 1.47407}},
  {{LN, {6.12111, 0.324593}}, {LN, {-2.12323, 0.388026}}}}}
```

end

■ Feq (function)

$$\text{lim} = \text{Limit}\left[\frac{1 - E^{-kt}}{t(1 - E^{-k24})}, t \to 0\right]$$

$$\frac{k}{1 - E^{-24k}}$$

{limk = lim /. k -> .000000000001, 1 / limk}

{0.0416666, 24.}

$$\text{fx}[k\_, t\_] := \frac{1 - E^{-kt}}{t(1 - E^{-k24})}$$

```
Plot[{fx[k, .01], fx[k, .25], fx[k, .5], 24^-1 + .57 k}, {k, 0.0001, .1},
 AxesOrigin -> {0.0001, 0.04}, PlotRange -> {{0.0001, .1}, {0.04, .12}}];
```
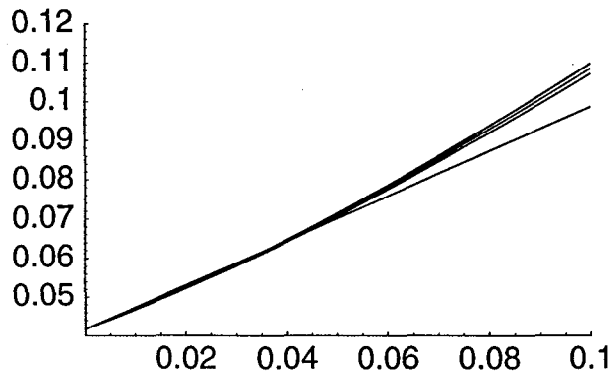


```
kval = Join[{.001}, Range[.005, .1, .0025]];
out = {fx[k, .01], fx[k, .25], fx[k, .5]} /. k → kval;
xy = Flatten[Transpose[{kval, #}] & /@ (out - 24^-1), 1];
fit = Fit[xy, {x, x^2}, x]  (* k = 0 - .1 *)
```

$$0.505316\, x + 1.66078\, x^2$$

```
fit[[2]] / fit[[1]]
```

$$3.28661\, x$$

```
zz = RQ[Q, N, {0, 1}, {.95, .99, .995}];
cv = 0.60;  (* = assumed CV for Vke; see below *)
gsd = E^Sqrt[Log[1 + cv^2]];  (* by method of moments *)
{ke = 0.028 * 71^-.3, gsd, ke * gsd^zz}
```

$$\{0.00779436, 1.74109, \{0.0194043, 0.028315, 0.032516\}\}$$

```
data = ({0, 24^-1} + #) & /@ Prepend[xy, {0, 0}];
PlotData[data, FitTo → {{24^-1 + fit, 24^-1 + 0.5053 x}, x},
Xmin → -.0001, Xmax → .1, Ymin → .0399, Ymax → .12, Style → OO, Dashed → {False, .025},
 DotSize → .0125];
```
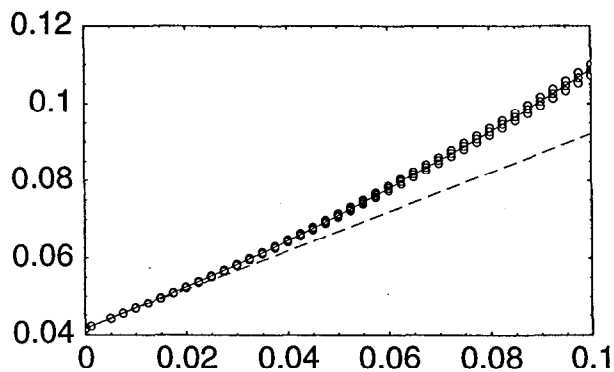
```
(* ~% relative error of linear approximation *)
Plot[100 ((24^-1 + fit) / (24^-1 + 0.5053 x) - 1), {x, 0, .06},
  AxesOrigin → {-.0001, -.0001}, PlotRange → {{-.0001, .06}, {-.0001, 10}},
  Frame → True, GridLines → {
    Range[.01, .05, .01], Range[2, 8, 2]}];
```
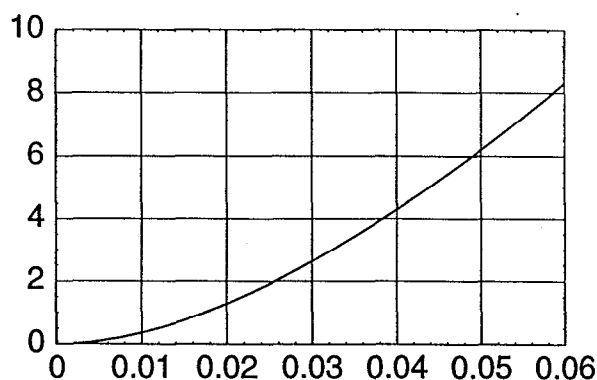

end

■ Body Weight (adult male + female), Vmax = Ve, and VQ

CV   = coefficient of variation

Qa   = alveolar ventilation rate = 12.9*BW^.74 (Allen & Fisher, 1993)

VVmax= Variability (unitless) in Vmax, where Vmax = 14.9*BW^.74 (in mg/h) (Allen & Fisher, 1993)

Vinhale= Variability (unitless) in Inhalation rate, where latter in L/h

VKe   = Variability (unitless) in Ke, where Ke = 0.028*BW^-.3 (in 1/h) (Allen & Fisher, 1993)

From Finley et al. 1994 (CalEPA 1996, p. 10-7), the BW distribution for adult males & females is ~LN and CV[BW] = ~0.22:

```
Clear[gsd];
{ev, sd} = {71., 15.9};
{cv = sd / ev, cvWant = 0.6, {BWgm, BWgsd} = GMGSDx[ev, sd],
Log[{BWgm, BWgsd}]}

{0.223944, 0.6, {69.2839, 1.24759}, {4.23821, 0.22121}}
```

CVwant = 0.60 for Vmax/BW assumed, based on Lipscombe et al. 1998 (Table 5). From Allen and Fisher (1993), the maximum metabolic rate in mg/h is modeled as Vmax ~ 14.9*BW^0.7. Now let VVmax be LN-distributed with an arithmetic mean of 1, where Vmet represents variation in Vmax not attributable to that in BW. Thus, Vmax ~ 14.9*Vmet*BW^.7, whence Vmax/BW ~ 14.9*Vmet*BW^-0.3. It follows from the method of moments that CV[BW^-.3] = CV[BW^.3] = 0.06644, whence CV[Vmet] = 0.5950, GM[Vmet] = 0.8594, GSD[Vmet] = 1.734, Log[{GM[Vmet], GSD[Vmet]}] = {-0.15154,0.550528}. CVwant = 0.60 for VKe is also assumed, based on Fisher et al. 1998 (Table 8); thus VKe = VVmax = Vmet.

```
{{o1, o2} = MSDx[a BWgm^-.3, BWgsd^-.3], cvCorr = o2 / o1}

{{0.281039 a, 0.0186711 a}, 0.066436}
```

```
{{o1, o2} = MSDx[a BWgm^-.3, BWgsd^.3], cvCorr = o2 / o1}
```

```
{{0.281039 a, 0.0186711 a}, 0.066436}
```

```
{o = GMGSDx1[cvWant, cvCorr], {muyVmet, sdyVmet} = Log[o]}
```

```
{{0.859383, 1.73417}, {-0.15154, 0.550528}}
```

```
MSDx@@o
```

```
{1., 0.594999}
```

```
(* By definition, the CV of (BW^.3 * Vmet) = *)
Sqrt[E^(sdyVmet^2 + Log[BWgsd^.3]^2) - 1]
```

```
0.6
```

```
{BW = {LN, Log[{BWgm, BWgsd}]}, Vmet = {LN, {muyVmet, sdyVmet}}}
```

```
{{LN, {4.23821, 0.22121}}, {LN, {-0.15154, 0.550528}}}
```

From CalEPA/OHEA (1996, Stochastic Analysis, p. 3-31 - 3-32; cit. above), cvA = CV[24*Q/BW] = CV[Qtot/BW] = ~ 0.3, where Q denotes total ventilation rate in L/h. From Allen and Fisher (1993), alveolar ventilation rate in L/h is modeled as Q ~ 12.9*BW^0.7, and Qtot ~ kQ for some constant k. Now let VQ be LN-distributed with an arithmetic mean of 1, where VQ represents variation in Q not attributable to that in BW. Thus, Q ~ 12.9*VQa*BW^.7, whence Q/BW ~ 12.9*VQ*BW^-0.3. It follows from the method of moments that CV[BW^-.3] = CV[BW^.3] = 0.06644, whence CV[VQ] = 0.2919, GM[VQ] = 0.9599, GSD[VQ] = 1.331, Log[{GM[VQ], GSD[VQ]}] = {-0.0408868, 0.285961}.

```
{{o1, o2} = MSDx[a BWgm^-.3, BWgsd^-.3], cvBW3 = o2 / o1}
```

```
{{0.281039 a, 0.0186711 a}, 0.066436}
```

```
{o = GMGSDx1[0.3, cvBW3], {muyX, sdyX} = Log[o]}
```

```
{{0.959938, 1.33104}, {-0.0408868, 0.285961}}
```

```
{{mX, sdX} = MSDx@@o, cvX = sdX / mX}
```

```
{{1., 0.291908}, 0.291908}
```

```
(* By definition, the CV of (BW^.3 * X) = *)
{Sqrt[E^(sdyX^2 + Log[BWgsd^.3]^2) - 1],
((1 + cvBW3^2) (1 + cvX^2) - 1)^.5}
```

```
{0.3, 0.3}
```

```
{BW,Vmet,VQ} =
  {{LN, {4.23821,0.22121}},
    {LN, {-0.15154,0.550528}},{LN, {-0.0408868,0.285961}}};
```

■ Fractions metabolized

■ Oral (fmo)

Heterogeneous variates ={Pb,Vmet,VQ}

```
{nsam, nsim} = {2000, 10};
Pb = NormalCdf[10.2, 1.6, 405];
cdfs = {Pb, VQ, Vmet};
Clear[fxn];
fxn[pb_, vq_, vmet_] := (1 + vq (vmet (.77 pb + 2.547))⁻¹)⁻¹
```

$$fxn[pb\_, vq\_, vmet\_] := (1 + vq\,(vmet\,(.77\,pb + 2.547))^{-1})^{-1}$$

```
fxn[10.2, 1, 1]

0.912288
```

```
sim = Table[SimulateCdf[cdfs, 500, TestCdf → False, Report → Append], {10}];
{sims, rval, jens} = Transpose[sim];
jen = Last[Sort[Last /@ jens]]    (* Max[chi2],df,pval *)

{0.398663, 3, 0.940519}
```

```
corr = First[Correlation[{#[[3]], fxn@@#& /@Transpose[#]},
    Type → Spearman, Report → False]]& /@sims;
Stats[corr, Report]
```

Mean	SD	CVM%	95%LCL	95%UCL	Min	Max	n
0.859935	0.00411002	0.1511	0.856994	0.862875	0.854597	0.868392	10

Correlation between Vmet and Fmo = 0.86

```
corr = First[Correlation[{#[[2]], fxn@@#& /@Transpose[#]},
    Type → Spearman, Report → False]]& /@sims;
Stats[corr, Report]
```

Mean	SD	CVM%	95%LCL	95%UCL	Min	Max	n
-0.43378	0.0133479	0.9731	-0.443329	-0.424232	-0.45298	-0.417722	10

Correlation between VQ and Fmo = -0.43

$$corr = First\left[Correlation\left[\left\{\left(1 + \frac{\#[[2]]}{\#[[1]]}\left(\frac{1.299}{\#[[3]]} + 3.307\right)\right)^{-1}, fxn@@#\&\,/@Transpose[\#]\right\}, \right.\right.$$
$$\left.\left. Type → Spearman, Report → False\right]\right]\&\,/@sims;$$
Stats[corr, Report]

Mean	SD	CVM%	95%LCL	95%UCL	Min	Max	n
0.825436	0.00851143	0.3261	0.819347	0.831524	0.81263	0.837117	10

Correlation between Fmr and Fmo = 0.83

```
Timing[{jen, cdf, cvm} = QUAnalyze[cdfs, fxn, nsam, nsim, Scale → 1];]

{1094.55 Second, Null}
```
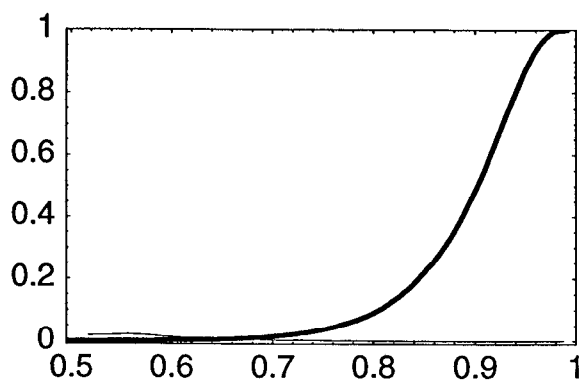
TBL/@jen

```
{ Mean[Δr]     Max[|Δr|]   JennrichChi2  DegFr  Pval
{ 0.00256474   0.0100917   0.390451      3      0.942208 '
```

```
Fractile   Value        CVM(%)
0.01       0.680326     0.395848
0.05       0.765428     0.103074
0.5        0.90237      0.0203722   }
0.95       0.963376     0.0237576   }
0.99       0.975746     0.0236983
Mean       0.888543     0.00239931
Variance   0.00395071   0.863083
```

{First[cdf], Last[cdf]}

{{0.476647, 0}, {0.99139, 1}}

PlotCdf[{cvm, cdf}, Ymin → -.01, Xmin → .495, Xmax → 1];

Fmo = StandardizeCdf[cdf, 405];

end

Inhalation and dermal (fmr)

Heterogeneous variates ={Pb,Vmet,VQ}

```
{nsam, nsim} = {2000, 10};
cdfs = {Pb, VQ, Vmet};
Clear[fxn];
```

$$fxn[pb\_, vq\_, vmet\_] := \left(1 + \frac{vq}{pb}\left(\frac{1.299}{vmet} + 3.307\right)\right)^{-1}$$

fxn[10.2, 1, 1]

0.68891

```
corr = First[Correlation[{#[[2]], fxn@@#&/@Transpose[#]},
   Type → Spearman, Report → False]]&/@sims;
Stats[corr, Report]
```

Mean	SD	CVM%	95%LCL	95%UCL	Min	Max	n
-0.753049	0.00720099	0.3024	-0.758201	-0.747898	-0.764949	-0.741702	10

Correlation between VQ and Fmr = -0.75

```
corr = First[Correlation[{#[[3]], fxn@@#&/@Transpose[#]},
   Type -> Spearman, Report -> False]]&/@sims;
Stats[corr, Report]
```

```
Mean       SD          CVM%      95%LCL    95%UCL    Min       Max        n
0.453276   0.00968226  0.6755    0.44635   0.460202  0.436792  0.466869   10
```

Correlation between Vmet and Fmr = 0.45

```
Timing[{jen, cdf, cvm} = QUAnalyze[cdfs, fxn, nsam, nsim, Scale -> 1];]
```

```
{1096.72 Second, Null}
```

```
TBL/@jen
```

					Fractile	Value	CVM(%)
					0.01	0.454963	0.559908
					0.05	0.527838	0.151762
{Mean[Δr]	Max[|Δr|]	JennrichChi2	DegFr	Pval	0.5	0.680315	0.0680913}
{0.001593	0.0140407	0.499243	3	0.919058'	0.95	0.794697	0.0632056}
					0.99	0.830531	0.090292
					Mean	0.673284	0.0011681
					Variance	0.00656651	0.240044

```
{First[cdf], Last[cdf]}
```

```
{{0.264383, 0}, {0.890069, 1}}
```

```
PlotCdf[{cvm, cdf}, Ymin -> -.01, Xmin -> -.0001, Xmax -> 1];
```
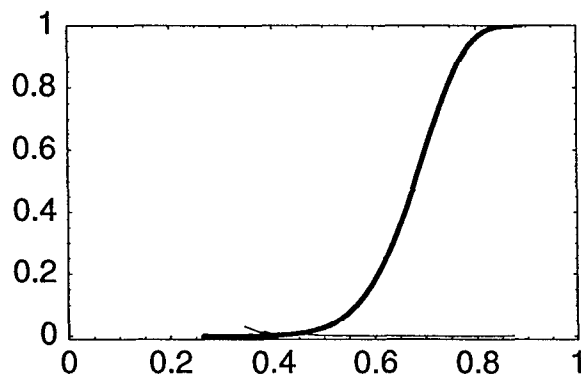


```
Fmr = StandardizeCdf[cdf, 405];
```

end

```
Put[Fmo, PathName["Fmo"]];
```

```
Put[Fmr, PathName["Fmr"]];
```

Correlation between Vmet and Fmo = 0.86
Correlation between VQ and Fmr = -0.75
Correlation between Vmet and Fmr = 0.45

```
Fmo = Get[PathName[Fmo]]; Fmr = Get[PathName[Fmr]];
CdfQ/@{Fmo, Fmr}

{True, True}

{FmoBar, FmrBar} = {0.888543, 0.6732836};

PlotCdf[{Fmr, Fmo}, Ymin -> -.001, Xmin -> .398, Xmax -> 1];
```
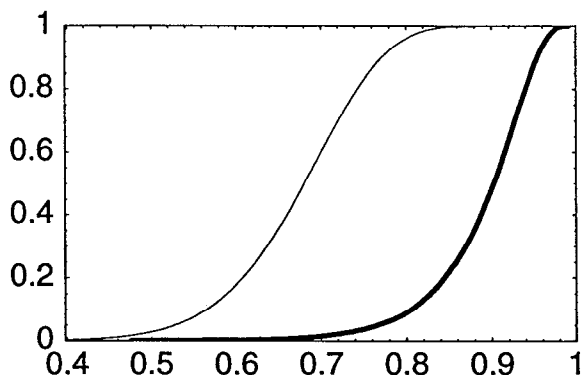

end

end

Note: All distributions below are *un*scaled

■ Ingestion Effective Dose (mg TCA/L plasma)

■ <ECingest> = Variability in Expected Level

{VolDist,BW,VKe,Fmo,Ingest} = heterogeneous variates
Correlation between VolDist and BW is assumed to be -.5
Correlation between Vmet =Ve and Fmo is assumed to be 0

```
{nsam, nsim} = {2000, 10};
Ingest = {LN, {Log[.0198], Log[1.88]}};
VolDist = {U, {.052, .152}}; (* L/kg *)
cdfs = {VolDist, BW, Vmet, Fmo, Ingest};
corr = {{-.5, 0, 0, 0}, {0, 0, 0}, {0, 0}, {0}};
Clear[fxn];

fxn[u_, bw_, vmet_, fmo_, ing_] := ing * ConcAng * fmo * (
```

$$\frac{.4104}{u}\left(\frac{1.488\, bw^{.3}}{vmet} + .5053\right)\right)$$

```
fxn[.1, 70, 1, .7, IngestBar]

0.00903536
```

```
Timing[{jen, cdf, cvm} = QUAnalyze[cdfs, fxn, nsam, nsim, Scale → 1, Correlate → corr];]
```

{85.7333 Second, Null}

```
TBL/@jen
```

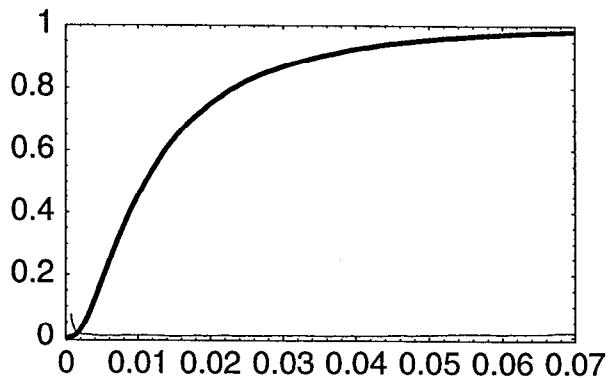|						Fractile	Value	CVM(%)
						0.01	0.00149497	1.41686
						0.05	0.00265397	0.846307
Mean[Δr]	Max[|Δr|]	JennrichChi2	DegFr	P-adj		0.5	0.0110646	0.571085
-0.000233837	0.0171728	1.5172	10	1.		0.95	0.0476501	0.587508
						0.99	0.0879985	2.44676
						Mean	0.0163479	0.171948
						Variance	0.000306492	3.01902

```
PlotCdf[{cvm, cdf}, Ymin → -.01, Xmin → -.0001, Xmax → .07];
```



```
sdf = StandardizeCdf[cdf, 404]; EV[sdf, Empirical -> True]
```

0.0161848

```
Put[sdf, PathName[ECingestAng]];
```

```
ECingestAng = Get[PathName[ECingestAng]];
```

```
ECingestAngBar=0.0161848;
```

end

■ ECingestBar = Uncertainty in Population-Average Level

{Conc} = uncertain variate

$$\text{cdf} = \left\{ \frac{\text{ECingestAngBar}}{\text{ConcAng}} \#[[1]], \#[[2]] \right\} \& /@ \text{Conc};$$

```
Put[cdf, PathName[ECingestBar]];
```

```
ECingestBar = Get[PathName[ECingestBar]];
```

end

end

■ Inhalation Effective Dose (mg TCA/L plasma)

■ <ECinhale> = Variability in Expected Level

{VolDist,BW,VKe,Fmr,Inhale,Wshower,ETshower,AEshower,T13} = heterogeneous variates
Correlation between Vmet = Ve and Fmr is assumed to be 0
Correlation between VolDist and BW is assumed to be -.5
Correlation between VQ and Fmr = -0.75

```
{InhaleBar, ConcAng}

{302.358, 0.0223}

{nsam, nsim} = {2000, 10};
Clear[fxn];
cdfs = {VolDist, BW, Vmet, VQ, Fmr, Wshower, ETshower, AEshower, T13};
corr = {{-.5, 0, 0, 0, 0, 0, 0, 0}, {0, 0, 0, 0, 0, 0, 0},
    {0, 0, 0, 0, 0, 0}, {-.75, 0, 0, 0, 0}, {0, 0, 0, 0}, {0, 0, 0}, {0, 0}, {0}};
```

$$fxn[u\_, bw\_, vmet\_, vq\_, fmr\_, wsh\_, etsh\_, aesh\_, t13\_] := \left(\frac{.4104}{u} \left(\frac{19.195}{vmet} + \frac{6.5145}{bw^{.3}} \right) \right) vq * ConcAng \left(\frac{wsh \; (.76 + .029 \; t13)}{1000 \; aesh} \right) fmr * etsh$$

```
fxn[.1, 70, 1, 1, .7, 480, .129, AEshHBar, 0]

0.00637328

Timing[{jen, cdf, cvm} = QUAnalyze[cdfs, fxn, nsam, nsim, Scale → 1, Correlate → corr];]

{179.167 Second, Null}

TBL/@jen
```

Mean[Δr]	Max[|Δr|]	JennrichChi2	DegFr	P-adj
-0.000248172	0.0207595	4.33342	36	1.

Fractile	Value	CVM(%)
0.01	0.000715826	1.62597
0.05	0.00126666	0.60722
0.5	0.00538319	0.46861
0.95	0.0259794	1.09888
0.99	0.0489231	1.70975
Mean	0.00844442	0.179915
Variance	0.0000944227	3.53902

```
PlotCdf[{cvm, cdf}, Ymin → -.01, Xmin → -.0001, Xmax → .05];
```
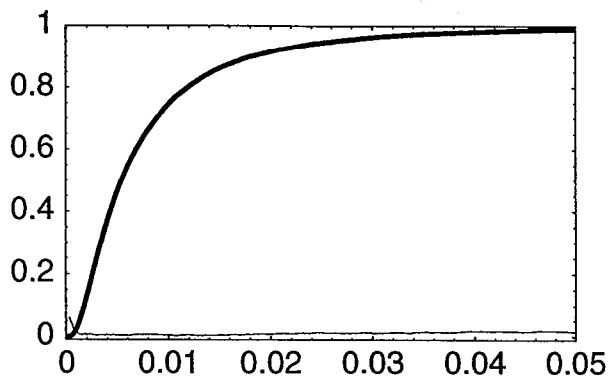


```
sdf = StandardizeCdf[cdf, 404]; EV[sdf, Empirical → True]

0.00835208

Put[sdf, PathName[ECinhaleAng]];

ECinhaleAng = Get[PathName[ECinhaleAng]];

ECinhaleAngBar = 0.0083520792794854834 5`;
```

end

■ ECinhaleBar = Uncertainty in Population-Average Level

{Conc} = uncertain variate

$$cdf = \left\{ \frac{ECinhaleAngBar}{ConcAng} \#[[1]], \#[[2]] \right\} \& /@Conc;$$

```
Put[cdf, PathName[ECinhaleBar]];

ECinhaleBar = Get[PathName[ECingestBar]];
```

end

end

■ Dermal Effective Dose (mg TCA/L plasma)

■ <Edermal> = Variability in Expected Level

{VolDist,BW,Vmet,Fmr,SABW,Fs,Kp,ETshower,T13} = heterogeneous variates
Correlation between Vmet = Ve and Fmr is assumed to be 0
Correlation between VolDist and BW is assumed to be -.5

```
{nsam, nsim} = {2000, 10};
corr = {{-.5, 0, 0, 0, 0, 0, 0, 0}, {0, 0, 0, 0, 0, 0, 0},
   {0, 0, 0, 0, 0, 0}, {0, 0, 0, 0, 0}, {0, 0, 0, 0}, {0, 0, 0}, {0, 0}, {0}};
cdfs = {VolDist, BW, Vmet, Fmr, SABW, Fs, Kp, ETshower, T13};
Clear[fxn];
fxn[u_, bw_, vmet_, fmr_, sabw_, fs_, kp_, etsh_, t13_] :=
```

$$
sabw * fs * kp * etsh * ConcAng \left(1 - \frac{.76 + .029\, t13}{2}\right) 10^{-3} * fmr * \left(
$$

$$
\frac{.4104}{u} \left(\frac{1.488\, bw^{.3}}{vmet} + .5053\right)\right)
$$

```
fxn[.1, 70, 1, .7, SABWBar, .65, .263, .129, 0]
```

0.00166356

```
(CdfQ[#] || RQ[Test, #[[1]], #[[2]]])&/@cdfs
```

{True, True, True, True, True, True, True, True, True}

```
Timing[{jen, cdf, cvm} = QUAnalyze[cdfs, fxn, nsam, nsim, Scale → 1, Correlate → corr];]
```

{173.433 Second, Null}

```
TBL/@jen
```

						Fractile	Value	CVM(%)
						0.01	0.000268902	0.97206
						0.05	0.000445612	0.780994
Mean[Δr]	Max[$|\Delta r|$]	JennrichChi2	DegFr	P-adj		0.5	0.00163022	0.369624
0.000459795	0.0212962	4.44316	36	1.		0.95	0.00625184	1.02696
						0.99	0.0111429	0.914124
						Mean	0.00228462	0.1228
						Variance	5.0004×10^{-6}	2.93471

```
PlotCdf[{cvm, cdf}, Ymin → -.01, Xmin → -.00001, Xmax → .01];
```
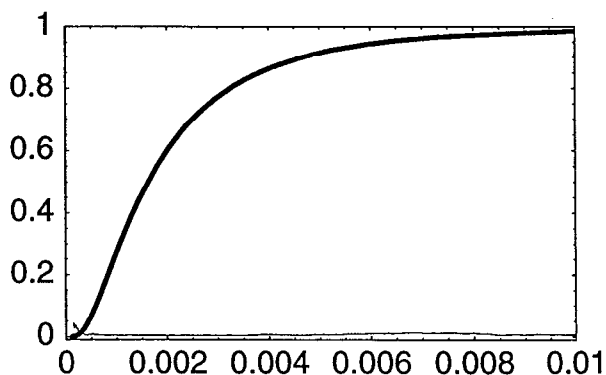


```
sdf = StandardizeCdf[cdf, 404]; EV[sdf, Empirical → True]
```

0.00226194

```
Put[sdf, PathName[ECdermalAng]];
```

```
ECdermalAng = Get[PathName[ECdermalAng]];
```

```
ECdermalAngBar = 0.00226194038376105455`;
```

end

■ EdermalBar = Uncertainty in Population-Average Level

{Conc} = uncertain variates

$$cdf = \left\{ \frac{ECdermalAngBar}{ConcAng} \ \#[[1]], \ \#[[2]] \right\} \& /@Conc;$$

```
Put[cdf, PathName[ECdermalBar]];

ECdermalBar = Get[PathName[ECdermalBar]];
```

end

end

Appendix 2.F

Effective Dose Correlations

```
<< RiskQ`;

HardDrive = "Bogen";
PathName[filename_, hardDrive_String: HardDrive] := Module[{file = filename},
  If[Head[file] =!= String, file = ToString[file]];
  StringJoin[hardDrive, ":Ken:TCE Air Force:Data:", file]
];
```

Inputs

■ Log-Transform Utility Functions

```
GMGSDx::usage = "GMGSDx[Mx,SDx] returns the  geometric mean and geometric sdandard
    deviation of a lognormal variate X that also has the specified arithmetic mean Mx
    and arithmetic sdandard deviation SDx, based on the method of moments.";

MSDx::usage = "MSDx[GMx,GSDx] returns the arithmetic mean and arithmetic sdandard
    deviation of a lognormal variate X that also has the specified geometric mean GMx
    and geometric sdandard deviation GSDx, based on the method of moments.";

GMGSDx1::usage = "GMGSDx1[cvWant,cv2] returns the GM and GSD of a lognormal variate
    X1, such that the product X1*X2 has the desired coefficient of variation (CV) =
    cvWant, conditional on the lognormal variate X2 having an arithmetic
    mean and CV equal to 1 and cv2, respectively, based on the method of moments.";

MSDx[GMx_, GSDx_] := Module[{mux, sigy},
  sigy = Log[GSDx];
  mux = GMx E ^ ((sigy^2) / 2);
  mux {1, Sqrt[E ^ (sigy^2) - 1]}]

GMGSDx[Mx_, SDx_] := Module[{muy, sigy},
  sigy = Sqrt[Log[1 + (SDx / Mx) ^ 2]];
  muy = Log[Mx] - (sigy^2) / 2;
  E ^ {muy, sigy}]

GMGSDx1[cvWant_, cv2_] := Module[{my1},
  muy1 = Log[Sqrt[ (cv2^2 + 1) / (cvWant^2 + 1) ]];
  E ^ {muy1, Sqrt[-2 muy1]}
] /; cvWant >= cv2
```

■ Input Empirical (Derived) Distributions

```
Clear[Tbarang, TresBar, TresAng];
Tbarang = Rest[Get[PathName[Tbarang]]];
TresBar = #[[{1, 2}]]&/@Tbarang;
TresAng = #[[{1, 3}]]&/@Tbarang;
TresBarAng =  7.59358; (* y *)
TresAngBar =  7.55321; (* y *)
EFcon  =  350;  (* d/y  *)
ATcon  =  25550; (* d     *)
Conc = ToExpression[
   ReadList[PathName["concentration.txt", HardDrive], Word, RecordLists -> True]];
ConcAng =  0.0223;  (* mg/L  *)


Ingest = {LN, {Log[.0198], Log[1.88]}};
IngestBar =  0.0242; (* L/kg-d *)
ECingestAngBar = 0.0161848;


SABW = ToExpression[
   ReadList[PathName["sabwratioALL.txt", HardDrive], Word, RecordLists -> True]];
SABWBar =  325.881; (* cm2/kg *)
Fs = {U, {.4, .9}};
Kp = {N, {.263, .018}};
ECdermalAngBar = 0.002261940;


Inhale = ToExpression[ReadList[PathName["inhaleALL.txt"], Word, RecordLists -> True]];
    (*Note: Inhale in L/kg-d *)
InhaleBarC = 12.9 * (71^.74);    (* L/h *)
InhaleBarG = 0.102;   (* m3/kg-d *)
ECinhaleAngBar = 0.0083520793;
{BW, Vmet, VQ} =
 {{LN, {4.23821, 0.22121}},
  {LN, {-0.15154, 0.550528}}, {LN, {-0.0408868, 0.285961}}};
VolDist = {U, {.052, .152}}; (* L/kg *)
T13 = {T, 13};


{AEshHBar, AEbaHBar, AEhHBar} = 1 / (EV/@{
{1./#[[1]], #[[2]]}&/@RQ[Cdf, U, {4, 20}, 2000],
{1./#[[1]], #[[2]]}&/@RQ[Cdf, U, {10, 100}, 2000],
{1./#[[1]], #[[2]]}&/@RQ[Cdf, U, {300, 1200}, 2000]});
gmgsd = GMGSDx@@#&/@N[{{480, 160}, {42, 15}, {.129, .052}, {.33, .22}}];
{Wshower, Whouse, ETshower, ETbath} = ({LN, #}&/@Log[gmgsd]);
{AEshower, AEbath, AEhouse, EThouse} =
  ({U, #}&/@{{4, 20}, {10, 100}, {300, 1200}, {8, 20}});
```

end

■ Fractions metabolized (summary–see Effective Cytotoxic Dose.nb)

Correlation between VolDist and BW = -0.50 (assumed approximation)
Correlation between Ve and Fmo =0, and between Ve and Fmr = 0
Correlation between VQ and Fmo = -0.43
Correlation between VQ and Fmr = -0.75
Correlation between Fmr and Fmo = 0.83

```
{FmoBar, FmrBar} = {0.888543, 0.6732836};
Clear[Fmo, Fmr];
Fmo = Get[PathName[Fmo]]; Fmr = Get[PathName[Fmr]];
CdfQ/@{Fmo, Fmr}

{True, True}
```

end

end

■ Effective Dose Uncertainty

```
cdfGingBar = {TresBar, Conc};
```

$$\text{fxnGingBar}[t\_, c\_] := \text{IngestBar} * t \; \frac{\text{EFcon}}{\text{ATcon}} \; c * \text{FmoBar};$$

```
cdfCingBar = {Conc};
```

$$\text{fxnCingBar}[c\_] := c \; \frac{\text{ECingestAngBar}}{\text{ConcAng}};$$

```
cdfGinhBar = {TresBar, Conc};
```

$$\text{fxnGinhBar}[t\_, c\_] := \text{FmrBar} \left(\frac{12.9}{1000} * 71^{.74-1} * 1\right) * t$$

$$\frac{\text{EFcon}}{\text{ATcon}} c \; \frac{1}{24} \left(480 \; (.76) \left(\frac{.129}{\text{AEshHBar}} + \frac{.33}{\text{AEbaHBar}}\right) + 42 \left(.76 \; \frac{.54}{.7}\right) \frac{14}{\text{AEhHBar}}\right);$$

```
cdfCinhBar = {Conc};
```

$$\text{fxnCinhBar}[c\_] := c \; \frac{\text{ECinhaleAngBar}}{\text{ConcAng}};$$

```
cdfGderBar = {TresBar, Conc};
```

$$\text{fxnGderBar}[t\_, c\_] := \text{FmrBar} * \text{SABWBar} * .65 * .263 * .129 * t \; \frac{\text{EFcon}}{\text{ATcon}} c \left(1 - \frac{.76}{2}\right) 10^{-3};$$

```
cdfCderBar = {Conc};
```

$$\text{fxnCderBar}[c\_] := c \; \frac{\text{ECdermalAngBar}}{\text{ConcAng}};$$

All 6 functions above are linear functions of either c or c*t; thus: all those involving just c are 100% correlated, all those involving just c*t are 100% correlated, and correlations between those involving c vs. c*t are given by:

```
cdfs = {TresBar, Conc};
sim = Table[SimulateCdf[cdfs, 500, TestCdf → False, Report → Append], {10}];
{sims, rval, jens} = Transpose[sim];
jen = Last[Sort[Last/@jens]]  (* Max[chi2],df,pval *)

{0.339124, 1, 0.560336}


corr = First[Correlation[{#[[2]], #[[1]] * #[[2]]},
   Type → Spearman, Report → False]]&/@sims;
Stats[corr, Report]
```

Mean	SD	CVM%	95%LCL	95%UCL	Min	Max	n
0.487765	0.0103941	0.6739	0.480329	0.4952	0.470525	0.506052	10

end

■ Effective Dose Variability

```
cdfGingAng = {Ingest, TresAng, Fmo};
```

$$fxnGingAng[ing\_, t\_, f\_] := ing * t \frac{EFcon}{ATcon} ConcAng * f;$$

```
cdfCingAng = {VolDist, BW, Vmet, Fmo, Ingest};
corCingAng = {{-.5, 0, 0, 0}, {0, 0, 0}, {0, 0}, {0}};
```

$$fxnCingAng[u\_, bw\_, vmet\_, fmo\_, ing\_] := ing * ConcAng * fmo * \left(\right.$$

$$\frac{.4104}{u} \left(\frac{1.488 \, bw^{.3}}{vmet} + .5053 \right) \Big);$$

```
cdfGinhAng = {Fmr, VQ, BW, TresAng, Wshower,
   Whouse, ETshower, ETbath, EThouse, AEshower, AEbath, AEhouse, T13, T13};
corr = Table[Table[0, {j}], {j, 13}];
corGinhAng = ReplacePart[Reverse[corr], -.75, {1, 1}]; fxnGinhAng[f_, vq_,
   bw_, t_, wsh_, wh_, etsh_, etba_, eth_, aesh_, aeba_, aeh_, t13sh_, t13h_] :=
```

$$f * \left(\frac{12.9}{1000} * bw^{.74-1} * vq \right) t \frac{EFcon}{ATcon} ConcAng \frac{1}{24} \left(\right.$$

$$wsh (.76 + .029 \, t13sh) \left(\frac{etsh}{aesh} + \frac{etba}{aeba} \right) + wh \left((.76 + .029 \, t13h) \frac{.54}{.7} \right) \frac{eth}{aeh} \Big);$$

```
cdfCinhAng = {VolDist, BW, Vmet, VQ, Fmr, Wshower, ETshower, AEshower, T13};
corCinhAng = {{-.5, 0, 0, 0, 0, 0, 0, 0}, {0, 0, 0, 0, 0, 0, 0},
   {0, 0, 0, 0, 0, 0}, {-.75, 0, 0, 0, 0}, {0, 0, 0, 0}, {0, 0, 0}, {0, 0}, {0}};
fxnCinhAng[
```

$$u\_, bw\_, vmet\_, vq\_, fmr\_, wsh\_, etsh\_, aesh\_, t13\_] := \left(\frac{.4104}{u} \left(\frac{19.195}{vmet} + \frac{6.5145}{bw^{.3}} \right) \right.$$

$$\Big) vq * ConcAng \left(\frac{wsh (.76 + .029 \, t13)}{1000 \, aesh} \right) fmr * etsh;$$

```
cdfGderAng = {Fmr, SABW, Fs, Kp, ETshower, TresAng, T13};
fxnGderAng[f_, sabw_, fs_, kp_, etsh_, t_, t13_] :=
```

$$f * sabw * fs * kp * etsh * t \frac{EFcon}{ATcon} ConcAng \left(1 - \frac{.76 + .029 \, t13}{2} \right) 10^{-3};$$

```
cdfCderAng = {VolDist, BW, Vmet, Fmr, SABW, Fs, Kp, ETshower, T13};
corCderAng = {{-.5, 0, 0, 0, 0, 0, 0, 0}, {0, 0, 0, 0, 0, 0, 0},
   {0, 0, 0, 0, 0, 0}, {0, 0, 0, 0, 0}, {0, 0, 0, 0}, {0, 0, 0}, {0, 0}, {0}};
fxnCderAng[u_, bw_, vmet_, fmr_, sabw_, fs_, kp_, etsh_, t13_] :=
```

$$sabw * fs * kp * etsh * ConcAng \left(1 - \frac{.76 + .029 \, t13}{2} \right) 10^{-3} * fmr * \left(\right.$$

$$\frac{.4104}{u} \left(\frac{1.488 \, bw^{.3}}{vmet} + .5053 \right) \Big);$$

Function {argument positions}:
fxnGingAng[ing_,t_,f_]
        {7,8,5}
fxnCingAng[u_,bw_,vmet_,fmo_,ing_]
        {1,2,3,5,7}

```
fxnGinhAng[f_,vq_,bw_,t_,wsh_,wh_,etsh_,etba_,eth_,aesh_,aeba_,aeh_,t13sh_,t13h_]
    {6,4,2,8,9,10,11,12,13,14,15,16,17,18}
fxnCinhAng[u_,bw_,vmet_,vq_,fmr_,wsh_,etsh_,aesh_,t13_]
    {1,2,3,4,6,9,11,14,17}
fxnGderAng[f_,sabw_,fs_,kp_,etsh_,t_,t13_]
    {6,19,20,21,11,8,17}
fxnCderAng[u_,bw_,vmet_,fmr_,sabw_,fs_,kp_,etsh_,t13_]
    {1,2,3,6,19,20,21,11,17}
```

```
    cdfs = {VolDist, BW, Vmet, VQ, Fmo, Fmr, Ingest, TresAng,
      Wshower, Whouse, ETshower, ETbath, EThouse, AEshower,
      AEbath, AEhouse, T13, T13, SABW, Fs, Kp}; (* n=21 *)
```

```
    (CdfQ[#] || RQ[Test, #[[1]], #[[2]]])&/@cdfs
```

```
    {True, True, True, True, True, True, True, True, True, True, True, True, True,
     True, True, True, True, True, True, True}
```

Correlation between VolDist and BW = -0.50 (assumed approximation)
Correlation between Ve and Fmo =0, and between Ve and Fmr = 0
Correlation between VQ and Fmo = -0.43
Correlation between VQ and Fmr = -0.75
Correlation between Fmr and Fmo = 0.83

```
    corr = Reverse[Table[Table[0, {j}], {j, 20}]];
    (corr = ReplacePart[corr, #[[1]], #[[2]]])&/@{
    {-.5, {1, 1}}, {-.43, {4, 1}}, {-.75, {4, 2}}, {.83, {5, 1}}};
```

```
    Clear[o];
    xx = {a, b, c, d, e, f, g,
      h, i, j, k, l, m, n, o, p, q, r, s, t, u, v, w, x, y, z}; xx
```

```
    {a, b, c, d, e, f, g, h, i, j, k, l, m, n, o, p, q, r, s, t, u, v, w, x, y, z}
```

Define fxns here each as a function of elements of the convenient dummy variate xx:

```
    fxns = {
    {fxnGingAng, {7, 8, 5}},
    {fxnCingAng, {1, 2, 3, 5, 7}},
    {fxnGinhAng, {6, 4, 2, 8, 9, 10, 11, 12, 13, 14, 15, 16, 17, 18}},
    {fxnCinhAng, {1, 2, 3, 4, 6, 9, 11, 14, 17}},
    {fxnGderAng, {6, 19, 20, 21, 11, 8, 17}},
    {fxnCderAng, {1, 2, 3, 6, 19, 20, 21, 11, 17}}};
    MapThread[#1@@xx[[#2]]&, Transpose[fxns]]
```

$$\left\{0.000305479\, e\, g\, h,\ \frac{0.00915192\left(0.5053 + \frac{1.488\, b^{0.3}}{c}\right) e\, g}{a},\right.$$

$$\frac{1.64195\times10^{-7}\, d\, f\, h\left(i\left(\frac{k}{n} + \frac{1}{o}\right)(0.76 + 0.029\, q) + \frac{0.771429\, j\, m\,(0.76+0.029\, r)}{p}\right)}{b^{0.26}},$$

$$\frac{9.15192\times10^{-6}\left(\frac{6.5145}{b^{0.3}} + \frac{19.195}{c}\right) d\, f\, i\, k\,(0.76 + 0.029\, q)}{a\, n},$$

$$3.05479\times10^{-7}\, f\, h\, k\left(1 + \frac{1}{2}\,(-0.76 - 0.029\, q)\right) s\, t\, u,$$

$$\left.\frac{9.15192\times10^{-6}\left(0.5053 + \frac{1.488\, b^{0.3}}{c}\right) f\, k\left(1 + \frac{1}{2}\,(-0.76 - 0.029\, q)\right) s\, t\, u}{a}\right\}$$

Select a series of 50 simulated-variate sets that each have a 21-variate correlation matrix (=corr, defined above) that is not significantly different than corr. Below, 20 of a total of 70 sets tried qualify for use using a p-value of <0.01 to reject:

```
Timing[
 sim = Table[(Prn[i]; SimulateCdf[cdfs, 500, Correlate → corr, Report → Append]), {i, 70}];
{sims, rval, jens} = Transpose[sim];
jen = Last[Sort[Last/@jens]]  (* Max[chi2],df,pval *)]
```

{3335. Second, {35.2754, 210, 1.}}

```
Dimensions[sims]
```

{70, 21, 500}

```
sel = Select[o = Last/@jens, Last[#] > 0.01&];
{pos = Position[o, #][[1, 1]]&/@sel, Length[pos]}
```

{{1, 2, 3, 4, 5, 6, 7, 8, 9, 10, 11, 12, 13, 14, 15, 16, 17, 18, 19, 20, 21, 22, 23, 24, 25, 26,
  27, 28, 29, 30, 31, 32, 33, 34, 35, 36, 37, 38, 39, 40, 41, 42, 43, 44, 45, 46, 47, 48, 49,
  50, 51, 52, 53, 54, 55, 56, 57, 58, 59, 60, 61, 62, 63, 64, 65, 66, 67, 68, 69, 70},
 70}

```
Union[Last/@Last/@jens]
```

{1.}

```
OKsims = sims[[Take[pos, 50]]]; nn = Length[OKsims]
```

50

```
corm = Table[First[Correlation[
      MapThread[#1@@OKsims[[i]][[#2]]&, Transpose[fxns]],
    Type → Spearman, Report → False]], {i, nn}];
```

Mean corr, SDM[corr], and CVM[corr] values for:

GingAng	CingAng	GinhAng	CinhAng	GderAng	CderAng

```
ev = Plus@@corm/nn; TBL[N[ev, 3]]
```

1.	0.233	0.878	-0.00269	0.894	0.000496
0.233	1.	-0.0088	0.421	0.00439	0.514
0.878	-0.0088	1.	0.187	0.918	0.035
-0.00269	0.421	0.187	1.	0.0766	0.649
0.894	0.00439	0.918	0.0766	1.	0.177
0.000496	0.514	0.035	0.649	0.177	1.

```
sdm = √(Plus@@(((# - ev)^2)&/@corm)) / (nn (nn - 1)); TBL[N[sdm, 3]]
```

0	0.0022	0.000722	0.00207	0.000508	0.0018
0.0022	0	0.00207	0.00183	0.00223	0.00171
0.000722	0.00207	0	0.0022	0.000564	0.00192
0.00207	0.00183	0.0022	0	0.00205	0.00159
0.000508	0.00223	0.000564	0.00205	0	0.00214
0.0018	0.00171	0.00192	0.00159	0.00214	0

```
cvm = Abs[100 sdm / ev]; TBL[N[cvm, 3]]

0        0.946   0.0822   76.7     0.0568   364.
0.946    0       23.5     0.435    50.8     0.333
0.0822   23.5    0        1.17     0.0614   5.49
76.7     0.435   1.17     0        2.68     0.245
0.0568   50.8    0.0614   2.68     0        1.21
364.     0.333   5.49     0.245    1.21     0
```

end

Appendix 2.G

Potency

```
<< RiskQ`;

<< Minimize`;
```

Multistage (Genotoxicity) Model

■ Multistage Potencies for TCE Cancer Bioassays

The *Mathematica* program "QFit" (by K.T. Bogen, LLNL—see "RiskQ Functions Used" section below) was used to obtain for each bioassay data set a distribution reflecting parameter-estimation uncertainty pertaining to the value of multistage-model "potency" (denoted q_1), that is, the value of the linear coefficient of dose D in the multistage model of cancer risk, which posits that cancer risk is essentially an exponentiated-polynomial function dose. Conditional on any sufficiently "upper-bound" (i.e., conservative) estimate (denoted $q_1^* > 0$) of the linear "potency" term (q_1), the multistage model guarantees that any small increase in cancer risk will be very nearly equal to the product: $q_1^* \times D$. Uncertainty distributions are derived corresponding to each of seven bioassay data sets considered below; one data set (data set #7 below concerning the study by Henchler et al., 1980, showing malignant lymphoma in female HAN:NMRI mice) is excluded for reasons noted below.

■ 1. NCI 1976 Mouse B6C3F1: M 34 g   HCC

```
xhi=800;
    doses = { 0, 370, 739}*1. (* mg/kg-d LTWAM *);
   ndosed = {20,   48,   40};
  nrespond = { 1,   26,   31};
```

```
qTCE1=QFit[doses, ndosed, nrespond,  500,
  PolyDegree->2, Exponentiated->True,
  ConfInterval->.90, Output->Q1,
  Xmin->-xhi/100,Xmax->1.01*xhi,Ymin->0,Ymax->1];
```

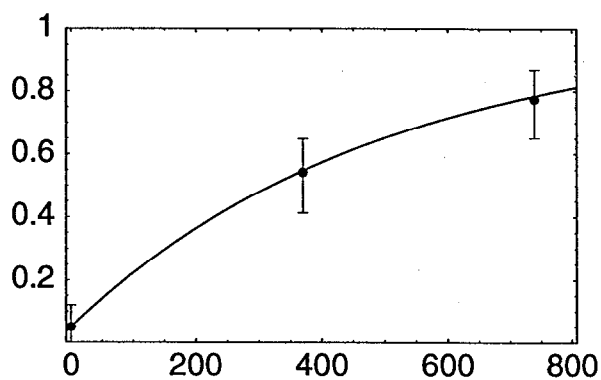The Optimized Function F of Dose d is:

$F(d) = 1 - \exp[-P(d)]$, where:

$P(d) = 0.0524116 + 0.00199086\,d + 2.72013 \times 10^{-8}\,d^2$

ChiSquare(1)= 0.032011   1-tailed p= 0.858003

$R^2 = 0.999488$

<div align="center">F(d) vs Data</div>

<div align="center">(& Bootstrap 90% Conf. Limits on Data)</div>

2. NCI 1976 Mouse B6C3F1: F 29 g   HCC

```
xhi=600;
    doses = { 0, 275, 550}*1. (* mg/kg-d LTWAM *);
   ndosed = {18, 42, 37};
nrespond = { 0,   4, 11};
```

```
qTCE2=QFit[doses, ndosed, nrespond,  500,
  PolyDegree->2, Exponentiated->True,
  ConfInterval->.90, Output->Q1,
  Xmin->-xhi/100,Xmax->1.01*xhi,Ymin->0,Ymax->1];
```

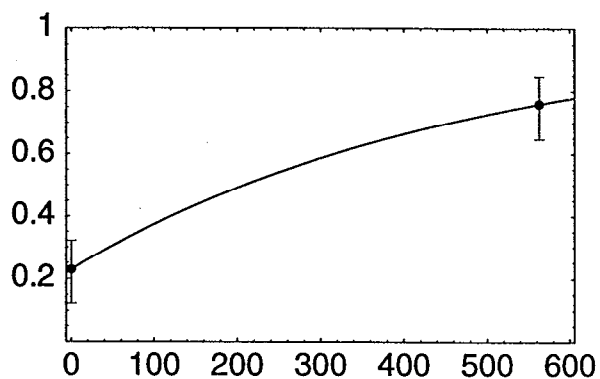The Optimized Function F of Dose d is:

$F(d) = 1 - exp[-P(d)]$, where:

$P(d) = 0.0000863863 \, d + 1.00929 \times 10^{-6} \, d^2$

ChiSquare(1) = 0. Perfect fit.

$R^2 = 1$.

F(d) vs Data

(& Bootstrap 90% Conf. Limits on Data)
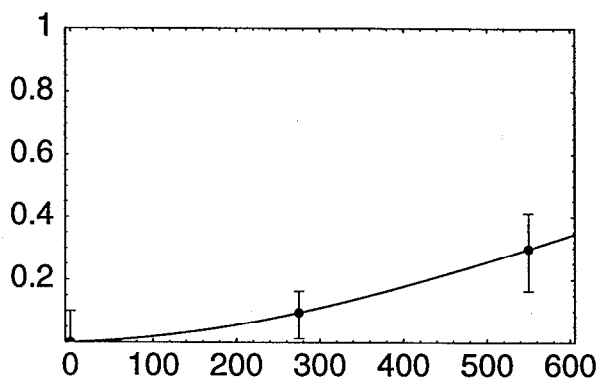
■ 3. NTP 1983 Mouse B6C3F1: M 37 g   HCC or HCA

```
xhi=600;
    doses = { 0, 563}*1. (* mg/kg-d LTWAM *);
  ndosed = {48, 50};
nrespond = {11, 38};
```

```
qTCE3=QFit[doses, ndosed, nrespond,  500,
  PolyDegree->1, Exponentiated->True,
  ConfInterval->.90, Output->Q1,
  Xmin->-xhi/100,Xmax->1.01*xhi,Ymin->0,Ymax->1];
```

The Optimized Function F of Dose d is:

$F(d) = 1 - \exp[-P(d)]$, where:

$P(d) = 0.260283 + 0.00207253\,d$

ChiSquare(0) = 0. Perfect fit.

$R^2 = 1$.

F(d) vs Data

(& Bootstrap 90% Conf. Limits on Data)

■ 4. NTP 1983 Mouse B6C3F1: F 33 g   HCC or HCA:

```
xhi=600;
    doses = { 0, 563}*1. (* mg/kg-d LTWAM *);
  ndosed = {41, 41};
nrespond = { 4, 19};
```

```
qTCE4=QFit[doses, ndosed, nrespond,  500,
  PolyDegree->1, Exponentiated->True,
  ConfInterval->.90, Output->Q1,
  Xmin->-xhi/100,Xmax->1.01*xhi,Ymin->0,Ymax->1];
```

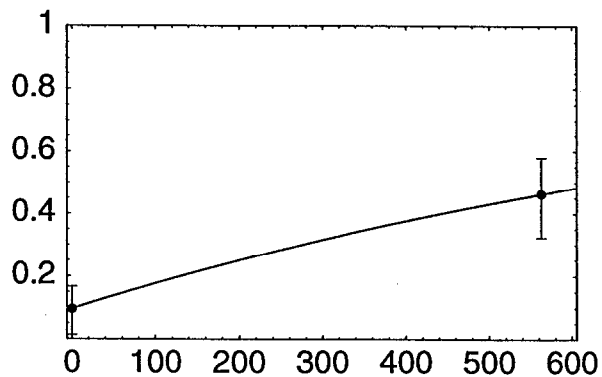The Optimized Function F of Dose d is:

F(d) = 1 - exp[-P(d)], where:

P(d) = 0.102654 + 0.000923402 d

ChiSquare(0) = 0. Perfect fit.

R^2 = 1.

                    F(d) vs Data

         (& Bootstrap 90% Conf. Limits on Data)

■ 5. NTP 1983 Rat F344/N: M 340 g   RenalTub Adenocarcinoma

```
xhi=300;
    doses = { 0, 198, 282}*1. (* mg/kg-d LTWAM *);
   ndosed = {33, 20, 16};
nrespond = { 0,  0,  3};
```

```
qTCE5=QFit[doses, ndosed, nrespond,  500,
   PolyDegree->2, Exponentiated->True,
   ConfInterval->.90, Output->Q1,
   Xmin->-xhi/100,Xmax->1.01*xhi,Ymin->0,Ymax->.5];
```

The Optimized Function F of Dose d is:

F(d) = 1 - exp[-P(d)], where:
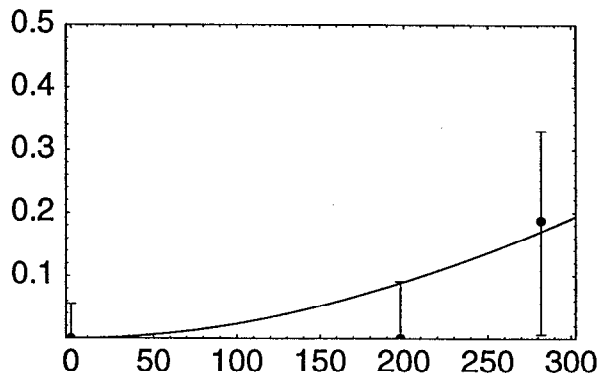
$P(d) = 2.35123 \times 10^{-6} d^2$

ChiSquare(2)= 1.96373   1-tailed p= 0.374612

R^2= 0.485332

                     F(d) vs Data

        (& Bootstrap 90% Conf. Limits on Data)

6. Bell et al. 1978 Mouse B6C3F1: M 35(?) g   HCC or HCA

```
xhi=300;
    doses = { 0, 42.3, 127, 254}*1. (* mg/kg-d LTWAM *);
   ndosed = {99, 95, 100, 97};
nrespond = {20, 35, 38, 53};
```

```
qTCE6=QFit[doses, ndosed, nrespond,  500,
   PolyDegree->3, Exponentiated->True,
   ConfInterval->.90, Output->Q1,
   Xmin->-xhi/100,Xmax->1.01*xhi,Ymin->0,Ymax->1];
```

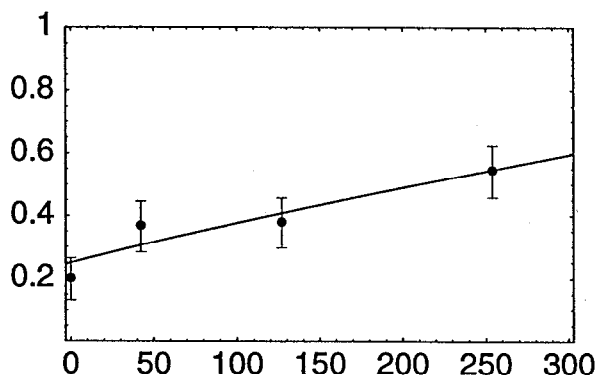The Optimized Function F of Dose d is:

$F(d) = 1 - \exp[-P(d)]$, where:

$P(d) = 0.287436 + 0.00181511\, d + 2.65261 \times 10^{-9}\, d^3$

ChiSquare(1) = 3.29871   1-tailed p = 0.0693345

$R^2 = 0.881871$

F(d) vs Data

(& Bootstrap 90% Conf. Limits on Data)

■ 7. Henchler et al. 1980 Mouse Han:NMRI: F 30(?) g   Malig. Lymphoma

Henchler did not consider this positive--called the study negative;
High spontaneous Malig. Lymphoma incidence is peculiar to this strain of mice in females (inborn
murine lymphoma virus)
p=0.03 by Fisher Exact for females (this data set); p=1 for males

```
xhi=200;
    doses = { 0, 33.2, 166}*1. (* mg/kg-d LTWAM *);
   ndosed = {29, 30,    28};
 nrespond = { 9, 17,    18};
```

```
qTCE7=QFit[doses, ndosed, nrespond,  500,
   PolyDegree->2, Exponentiated->True,
   ConfInterval->.90, Output->Q1,
   Xmin->-xhi/100,Xmax->1.01*xhi,Ymin->0,Ymax->1];
```

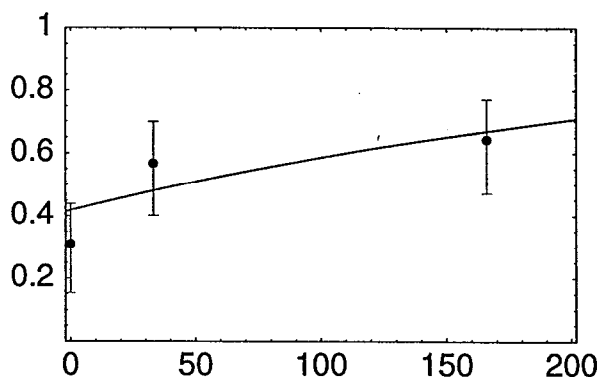The Optimized Function F of Dose d is:

$F(d) = 1 - \exp[-P(d)]$, where:

$P(d) = 0.54236 + 0.00338976\,d$

$\text{ChiSquare}(1) = 2.3744 \quad 1\text{-tailed } p = 0.123339$

$R^2 = 0.673392$

F(d) vs Data

(& Bootstrap 90% Conf. Limits on Data)

■ 8. Maltoni et al. 1986 Mouse Swiss: F 30(?) g Malig. Hepatoma

```
xhi=250;
    doses = { 0, 35.3, 106, 212}*1. (* mg/kg-d LTWAM *);
   ndosed = {90, 90, 90, 90};
nrespond = { 4, 2, 8, 13};
```

```
qTCE8=QFit[doses, ndosed, nrespond,  500,
  PolyDegree->3, Exponentiated->True,
  ConfInterval->.90, Output->Q1,
  Xmin->-xhi/100,Xmax->1.01*xhi,Ymin->0,Ymax->.25];
```

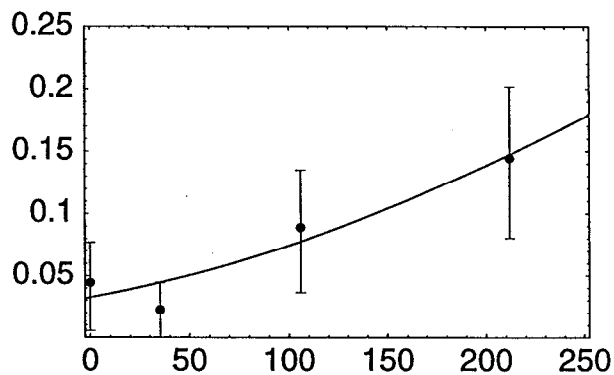The Optimized Function F of Dose d is:

$F(d) = 1 - \exp[-P(d)]$, where:

$P(d) = 0.0329504 + 0.000306602\,d + 1.36839 \times 10^{-6}\,d^2$

ChiSquare(1)= 1.62806   1-tailed p= 0.201971

R^2= 0.911347

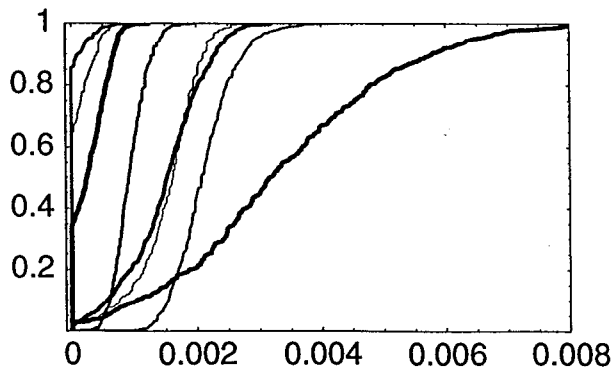F(d) vs Data

(& Bootstrap 90% Conf. Limits on Data)


```
qall = {qTCE1, qTCE2, qTCE3, qTCE4, qTCE5, qTCE6,
qTCE7, qTCE8};
```

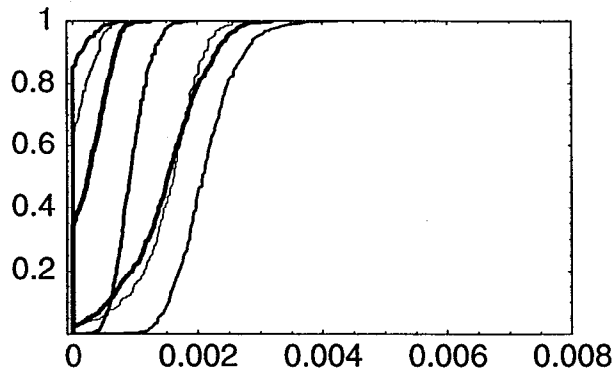# ■ Weighted-Average TCE Cancer Potency

■ Define qall

```
cdfs = Cdf /@qall;
```

```
PlotCdf[cdfs, Xmin -> -.0001, Xmax -> .008];
```
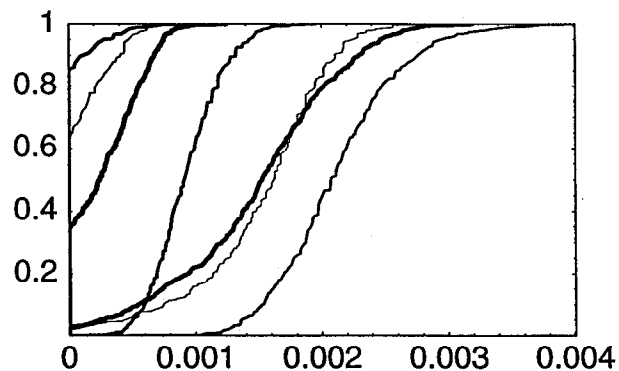
Remove Henchler lymphoma data, due to his determination that this was a negative study given the likelihood of murine lymphoma virus involvement:

```
cdf7 = Drop[cdfs, {7}]; CdfQ/@cdf7

{True, True, True, True, True, True, True}

PlotCdf[cdf7, Xmin -> -.0001, Xmax -> .008];
```


Replot to look nicer:

```
PlotCdf[cdf7, Xmin -> -10^-6, Xmax -> .00401];
```



```
o = {EV[#], Edf[#, 0], Idf[#, {.5, .95}]}&/@cdf7;

oo = Prepend[Transpose[Prepend[Transpose[Flatten/@o],
       Range[7]]], {"Study", Mean, P0, "50th%ile", "95th%ile"}];
TBL[oo]
```

Study	Mean	P0	50th%ile	95th%ile
1	0.00151724	0.018	0.00162322	0.00224792
2	0.000100304	0.624	0	0.000474276
3	0.0021167	0	0.00207564	0.00294787
4	0.000933588	0	0.000915365	0.00142873
5	0.0000371087	0.854	0	0.000283281
6	0.00148119	0.028	0.00152863	0.00246978
7	0.000282383	0.342	0.000246207	0.000755992

Study-Weighting Logic:
{Species, Strain, Sex, Site, Study}-specific data are equally likely, therefore:
Data sets {{{{1,3,6},{2,4}}, 8}, 5}={mouse,rat}={mouse{b6c3f1{m,f},swiss},rat}
get relative weights: {1,1} = { { {{1,1,1}, {1.5,1.5}}, 6}, 12}

(Note that Henchler lymphoma data was removed, due to his determination that this was a negative study given the likelihood of murine lymphoma virus involvement.)

```
ww = { { {{1, 1, 1}, {3/2, 3/2}}, 6}, 12} / 24;
studies = {{{{1, 3, 6}, {2, 4}}, 8}, 5};
bwg = {{{{34, 37, 35}, {29, 33}}, 30}, 340};
wt = Transpose[Flatten/@{studies, ww, bwg}];
swt = Sort[wt];
weights = #[[2]]&/@swt;
bwg = Last/@swt;
{ww, wt, swt, weights, bwg}
```

$$\left\{\left\{\left\{\left\{\left\{\tfrac{1}{24}, \tfrac{1}{24}, \tfrac{1}{24}\right\}, \left\{\tfrac{1}{16}, \tfrac{1}{16}\right\}\right\}, \tfrac{1}{4}\right\}, \tfrac{1}{2}\right\}, \left\{\left\{1, \tfrac{1}{24}, 34\right\}, \left\{3, \tfrac{1}{24}, 37\right\},\right.\right.$$

$$\left\{6, \tfrac{1}{24}, 35\right\}, \left\{2, \tfrac{1}{16}, 29\right\}, \left\{4, \tfrac{1}{16}, 33\right\}, \left\{8, \tfrac{1}{4}, 30\right\}, \left\{5, \tfrac{1}{2}, 340\right\}\right\}, \left\{\left\{1, \tfrac{1}{24}, 34\right\},\right.$$

$$\left\{2, \tfrac{1}{16}, 29\right\}, \left\{3, \tfrac{1}{24}, 37\right\}, \left\{4, \tfrac{1}{16}, 33\right\}, \left\{5, \tfrac{1}{2}, 340\right\}, \left\{6, \tfrac{1}{24}, 35\right\}, \left\{8, \tfrac{1}{4}, 30\right\}\right\},$$

$$\left\{\tfrac{1}{24}, \tfrac{1}{16}, \tfrac{1}{24}, \tfrac{1}{16}, \tfrac{1}{2}, \tfrac{1}{24}, \tfrac{1}{4}\right\}, \{34, 29, 37, 33, 340, 35, 30\}\right\}$$

Average the study-specific cdfs using the study-specific weights ("weights") defined above, plot the results, and get statistics for the resulting averaged cdf ("adfBW") based on a body-weight (i.e., using a mass-per-kg-body-weight) approach to interspecies scaling of equitoxic doses.

```
adfBW = AverageCdf[cdf7, Weights -> weights];

adfBW >> "BogenHD:Ken:Projects:TCE Air Force:QbwCdf";

PlotCdf[adfBW, Xmin -> -10^-6, Xmax -> .003, Ymin -> .499];
```
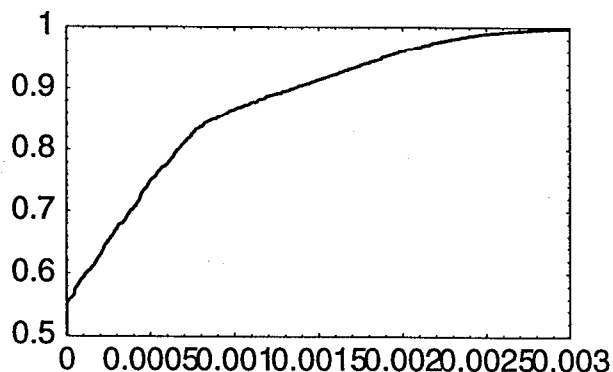


```
o1 = {Length[adfBW], EV[adfBW], Edf[adfBW, 0],
  Idf[adfBW, .95]};
TBL[{{Length, Mean, P0, "95th%ile"}, o1}]
```

```
Length    Mean          P0          95th%ile
1421.     0.000366899   0.553417    0.00187624
```

Multiply the abscissa of each cdf by $(Wh/BW)^{.25}$, where $Wh = 70$ kg and BW is rodent body weight in grams, i.e., scale using a $BW^{.75}$ scaling factor. Then re-average the cdfs using the same study-specific weights as used above, to obtain the resulting averaged cdf ("adf75") based on a (body weight)$^{.75}$ (i.e., using a mass-per-(kg body weight)$^{.75}$) approach to interspecies scaling of equitoxic doses.
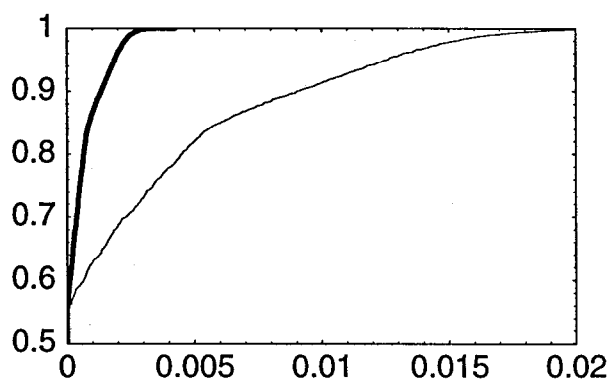
```
bwr75 = (70 * 1000 / bwg) ^ .25

{6.73604, 7.00931, 6.59514, 6.7865, 3.78795, 6.6874, 6.95015}


cdf75 =
 Transpose /@ ({#[[1, 1]] * #[[2]], #[[1, 2]]}& /@ Transpose[{Transpose /@ cdf7, bwr75}]);
Dimensions /@ #& /@ {cdf7, cdf75}

{{{298, 2}, {62, 2}, {143, 2}, {109, 2}, {22, 2}, {488, 2}, {309, 2}},
 {{298, 2}, {62, 2}, {143, 2}, {109, 2}, {22, 2}, {488, 2}, {309, 2}}}


adf75 = AverageCdf[cdf75, Weights -> weights];


PlotCdf[{adf75, adfBW}, Xmin -> -10^-6, Xmax -> .02, Ymin -> .499];
```



```
o2 = {Length[adf75], EV[adf75], Edf[adf75, 0],
 Idf[adf75, .95]};
TBL[{{Length, Mean, P0, "95th%ile"}, o2}]

Length  Mean        P0        95th%ile
1421    0.00242109  0.553417  0.0125937
```

Average the cdfs "adfBW" and "adf75" assuming equal likelihood, standardize, simplify, plot, get statistics, and save:
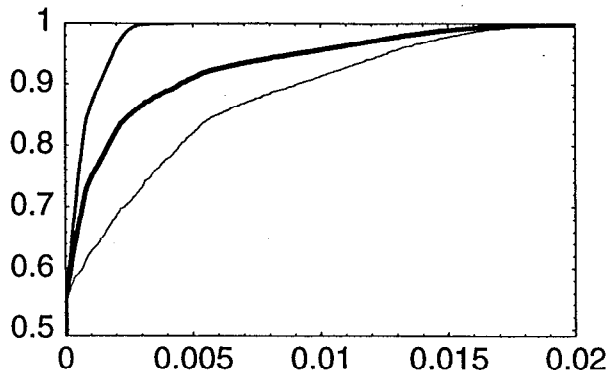
```
ade = AverageCdf[{adfBW, adf75}, Weights -> {.5, .5}];
ade = StandardizeCdf[ade, 500];
adf = SimplifyCdf[ade];


Dimensions /@ {ade, adf}

{{501, 2}, {226, 2}}
```

```
PlotCdf[{adf75, adfBW, adf}, Xmin -> -.00002, Xmax -> .02, Ymin -> .49];
```



```
o12 = {Length[adf], EV[adf], Edf[adf, 0], Idf[adf, .95]};
TBL[{{Length, Mean, P0, "95th%ile"}, o12}]
```

```
Length  Mean        P0     95th%ile
228     0.00140008  0.552  0.00902774
```

■ Define adf

```
WriteMatrix["BogenHD:Ken:Projects:TCE Air Force:Qcdf.txt", N[adf]];
```

TCE Threshold (Cytotoxicity) Model

■ TBARS dose-response in male B6C3F1 mice

27-g male B6C3F1 mice (Larson & Bull, 1992)
Dose in mg TCA per kg BW, vs. TBARS in nmol malondialdehyde equiv./g liver (n=4 @ ea. dose)

```
df = 3;
TBARScontrol = 40;
SDcontrol = 4;
dose = Log[10., {100, 300, 1000, 2000}];
tbars = {46, 67, 81, 108} - TBARScontrol;
sd = √{6, 7, 6, 7}² + 4² ;
dat = Transpose[{dose, #}]&/@{tbars + sd, tbars - sd, tbars};
{t95 = RQ[Q, T, 3, .95], TBARS95 = t95 * SDcontrol, TBARShi = Last[tbars]}

{2.35336, 9.41345, 68}

fxn[dose_, p_] := p[[1]] * NormalCdf[(dose - p[[2]]) / p[[3]]]
```

List "o" = {parameter estimates, corresponding SE values, {χ^2, df, p-value}}:

```
o = LSMin[dose, tbars, {140, 4, 1}, fxn,
  Weights → sd^-2, KnownVariances → True, Progress → True, Step → 10^-4, Output → CVM]
```

0 {{140., 4., 1.}, 29.8243}

1 {{140., 3.996, 1.00361}, 29.2399}

2 {{140., 3.95962, 1.03601}, 24.2432}

3 {{140.001, 3.77426, 1.17963}, 7.75091}

4 {{140.004, 3.49797, 1.11006}, 2.23287}

5 {{140.007, 3.3745, 0.864436}, 1.33394}

6 {{140.023, 3.38641, 0.882103}, 1.3235}

7 {{140.175, 3.38757, 0.882599}, 1.32304}

{{140.023, 3.38641, 0.882103},
 {{89321.2, 661.561, 283.881}, {661.561, 4.91457, 2.1214}, {283.881, 2.1214, 0.945736}},
 {1.32304, 1, 0.250047}}

```
vars = Diagonal[Sqrt[o[[2]]]];
vars = Table[vars[[i]] vars[[j]], {i, 3}, {j, 3}];
o[[2]] / vars
```

{{1., 0.998504, 0.976729}, {0.998504, 1., 0.983998}, {0.976729, 0.983998, 1.}}

```
Clear[fxn];
sdraw = √4 sd;
fxn[dose_, p_] := 100 * NormalCdf[(dose - p[[1]]) / p[[2]]]
```

```
o = LSMin[dose, tbars, {3, 1}, fxn, NYatX → {4, 4, 4, 4},
  SDY → sdraw, Weights → sdraw^-2, KnownVariances → True, Progress → True,
  Step → 10^-5, Output → CVM]
```

0 {{3., 1.}, 16.1584}

1 {{3.0001, 0.999935}, 16.1557}

2 {{3.00104, 0.999284}, 16.1294}

3 {{3.00964, 0.993005}, 15.8937}

4 {{3.05248, 0.944763}, 14.7945}

5 {{3.06417, 0.786705}, 13.6469}

6 {{3.05095, 0.731969}, 13.5613}

7 {{3.05227, 0.734029}, 13.5611}

{{3.05095, 0.731969}, {{0.0084548, 0.00477488}, {0.00477488, 0.0311052}},
 {13.5611, 14, 0.482896}}

```
vars = Diagonal[Sqrt[o[[2]]]];
vars = Table[vars[[i]] vars[[j]], {i, 2}, {j, 2}];
o[[2]] / vars
```

{{1., 0.294438}, {0.294438, 1.}}

```
{0.00845479840778034485`, 0.0311052466621742773`}^.5

{0.09195, 0.176367}

o = LSMin[dose, tbars, {3, 1}, fxn, NYatX → {4, 4, 4, 4},
    SDY → sdraw, Weights → sdraw^-2, KnownVariances → True, Progress → True, Step → 10^-5]

0 {{3., 1.}, 16.1584}

1 {{3.0001, 0.999935}, 16.1557}

2 {{3.00104, 0.999284}, 16.1294}

3 {{3.00964, 0.993005}, 15.8937}

4 {{3.05248, 0.944763}, 14.7945}

5 {{3.06417, 0.786705}, 13.6469}

6 {{3.05095, 0.731969}, 13.5613}

7 {{3.05227, 0.734029}, 13.5611}

{{3.05095, 0.731969}, {0.09195, 0.176367}, {13.5611, 14, 0.482896}}

o = {{3.05095121221202791`, 0.731969108012972302`},
    {0.0919499777475793855`, 0.176366795804012603`},
    {13.5610834321759421`, 14, 0.482895537121049489`}};

PlotData[dat, FitTo → {{fxn[d, o[[1]]], TBARS95 + 10^-6 * d}, d},
    Xmin → -.01, Xmax → 3.5, Ymin → -.01,
    Style → {M, J, M, OO}, DotSize → .015,
    Dashed → {False, .025}];
```
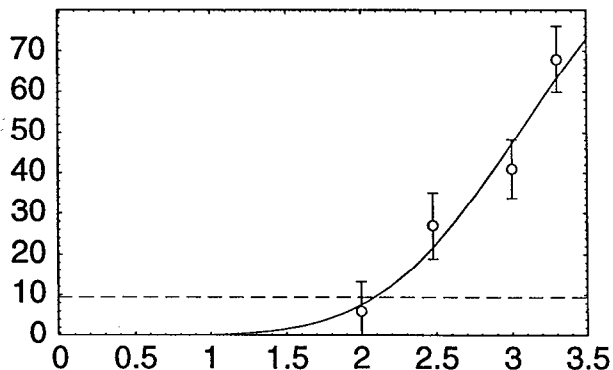


```
end
```

■ Effective acute TCA threshold dose (mg/kg) for TBARS elevation

Simulate 2 correlated T-distributions each with 2 degrees of freedom:

```
simT = SimulateCdf[{{T, 14}, {T, 14}}, 2000, Correlate → {{1, .294}, {.294, 1}}];
```

Output-Sample Rank-Correlation Matrix:

```
1.      0.293
0.293   1.
```

Jennrich's Asymptotic Chi-Square Test of Homogeneity

    Between Input & Target Correlation Matrices

    For 2000 2-Variate Normal Samples:

Chi2(1)= 0.00189492   1-tail p= 0.965279 (NS)

Construct 2000 simulated model-parameter sets, and 2000 corresponding values of d95 | fxn[{p1,p2},d95] = TBARS95, where d95 is dose on a log10(mg/kg) scale.
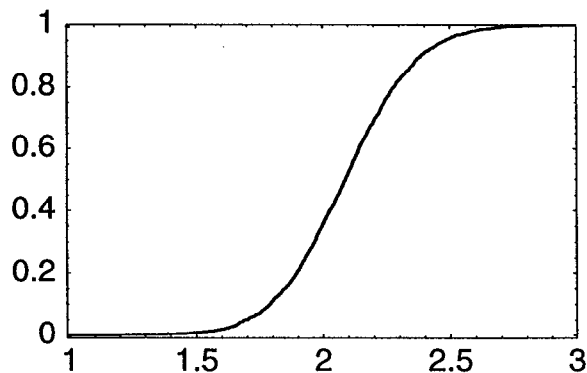
```
{{p1, p2} = o[[1]], {sdp1, sdp2} = o[[2]]}
```

```
{{3.05095, 0.731969}, {0.09195, 0.176367}}
```

```
p1s = p1 + sdp1 * simT[[1]];
p2s = p2 + sdp2 * simT[[2]];
```

```
{pval = TBARS95 / 100, zval = NormalCdf[TBARS95 / 100, Inv]}
```

```
{0.0941345, -1.31572}
```

```
d95 = p1s + p2s * zval;
cdf = Cdf[d95];
```

```
PlotCdf[cdf, Xmin → .99, Xmax → 3, Ymin → -.01];
```



```
cdf >> "BogenHD:Ken:Projects:TCE Air Force:Data:LnDose95";
```

```
cdf = << "BogenHD:Ken:Projects:TCE Air Force:LnDose95";
```

```
dat = {#[[1]], Log[10., #[[2]]]}&/@Rest[Take[cdf, 51]];
log10p = Fit[dat, {1, log10d}, log10d]
```

```
-7.60151 + 3.67626 log10d
```

```
FIT[dat, {1, log10d}, log10d, Report → True];
```

General Linear Model (GLM):

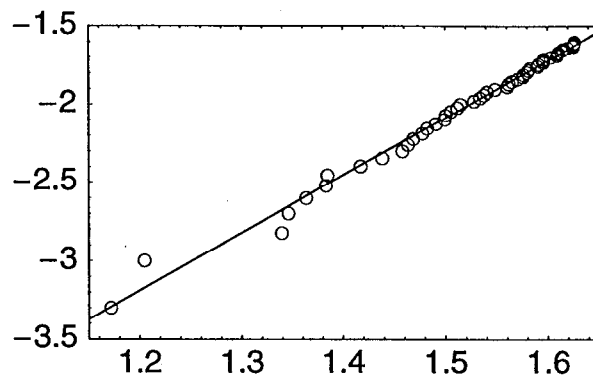$E[Y|log10d] = q[0] + log10d \, q[1]$

```
Coef      LS Est.      SD           95%LCL       95%UCL
q[0]      -7.60151     0.0794449    -7.76125     -7.44178
q[1]      3.67626      0.052125     3.57146      3.78106
```

$R^2 = 0.990442$

$F(1,48) = 4974.17$ 2-tail $p= 0.$

```
PlotData[dat, Xmin → 1.1499, Xmax → 1.65,
  Ymin → -3.501, Ymax → -1.499, Style → {OO}, DotSize → .02, FitTo → {log10p, log10d}];
```



```
logp = Range[-9, -3.5, .25];
logd = (log10d /. NSolve[log10p == #][[1]])&/@logp
```

```
{-0.38041, -0.312406, -0.244402, -0.176398, -0.108394, -0.0403904, 0.0276135,
 0.0956174, 0.163621, 0.231625, 0.299629, 0.367633, 0.435637, 0.503641, 0.571645,
 0.639648, 0.707652, 0.775656, 0.84366, 0.911664, 0.979668, 1.04767, 1.11568}
```

```
add = Transpose[{logd, 10^logp}];
```

■ **Define cdfD95 = Prob{significant TBARS elevation} | Effective TCA dose (mg/L plasma)**
(with abscissa units of mg TCA/L plasma based on Larson & Bull (TAP 115:268-277, 1992) using:
Vd = 15.0 mL
Cmax = 790 nmol TCA/mL plasma = 129.1 mg TCA/mL plasma
100 mg TCA in water administered by gavage)

```
cdfD95 = Prepend[{(10^#[[1]]) * (130./100), #[[2]]}&/@Join[add, Rest[cdf]], {0, 0}];
```

Take[cdfD95, 26]

$\{\{0, 0\}, \{0.541419, \frac{1}{1000000000}\}, \{0.633195, 1.77828 \times 10^{-9}\}, \{0.740528, 3.16228 \times 10^{-9}\},$
$\{0.866054, 5.62341 \times 10^{-9}\}, \{1.01286, 1. \times 10^{-8}\}, \{1.18455, 1.77828 \times 10^{-8}\},$
$\{1.38534, 3.16228 \times 10^{-8}\}, \{1.62017, 5.62341 \times 10^{-8}\}, \{1.89481, 1. \times 10^{-7}\},$
$\{2.21599, 1.77828 \times 10^{-7}\}, \{2.59163, 3.16228 \times 10^{-7}\}, \{3.03093, 5.62341 \times 10^{-7}\},$
$\{3.54471, 1. \times 10^{-6}\}, \{4.14557, 1.77828 \times 10^{-6}\}, \{4.84828, 3.16228 \times 10^{-6}\},$
$\{5.67011, 5.62341 \times 10^{-6}\}, \{6.63126, 0.00001\}, \{7.75532, 0.0000177828\},$
$\{9.06992, 0.0000316228\}, \{10.6074, 0.0000562341\}, \{12.4054, 0.0001\},$
$\{14.5083, 0.000177828\}, \{16.9675, 0.000316228\}, \{19.3012, \frac{1}{2000}\}, \{20.8328, \frac{1}{1000}\}\}$

PlotCdf[cdfD95, Xmin → -.01, Xmax → 600, Ymin → -.001];
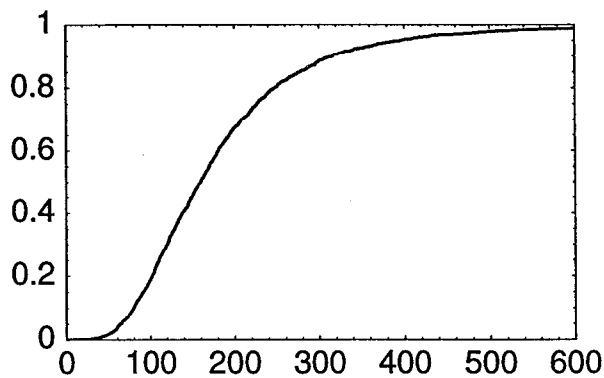
cdfD95 >> "BogenHD:Ken:Projects:TCE Air Force:Data:TBARSvTCA";

end

end

Appendix 2.H

TCE Risk

```
<< RiskQ`;

HardDrive = "BogenHD";
PathName[filename_, hardDrive_String: HardDrive] := Module[{file = filename},
   If[Head[file] =!= String, file = ToString[file]];
   StringJoin[hardDrive, ":Ken:TCE Air Force:Data:", file]
   ];
```

■ Log-Transform Utility Functions

```
GMGSDx::usage = "GMGSDx[Mx,SDx] returns the  geometric mean and geometric sdandard
     deviation of a lognormal variate X that also has the specified arithmetic mean Mx
     and arithmetic sdandard deviation SDx, based on the method of moments.";

MSDx::usage = "MSDx[GMx,GSDx] returns the arithmetic mean and arithmetic sdandard
     deviation of a lognormal variate X that also has the specified geometric mean GMx
     and geometric sdandard deviation GSDx, based on the method of moments.";

GMGSDx1::usage = "GMGSDx1[cvWant,cv2] returns the GM and GSD of a lognormal variate
     X1, such that the product X1*X2 has the desired coefficient of variation (CV) =
     cvWant, conditional on the lognormal variate X2 having an arithmetic
     mean and CV equal to 1 and cv2, respectively, based on the method of moments.";

MSDx[GMx_, GSDx_] := Module[{mux, sigy},
   sigy = Log[GSDx];
   mux = GMx E ^ ((sigy^2) / 2);
   mux {1, Sqrt[E^ (sigy^2) - 1]}]]

GMGSDx[Mx_, SDx_] := Module[{muy, sigy},
   sigy = Sqrt[Log[1 + (SDx / Mx) ^ 2]];
   muy = Log[Mx] - (sigy^2) / 2;
   E^ {muy, sigy}]
```

$$
\texttt{GMGSDx1[cvWant\_, cv2\_] := Module} \Big[\{my1\},
$$

$$
\texttt{muy1 = Log}\Big[\texttt{Sqrt}\Big[\frac{cv2^2 + 1}{cvWant^2 + 1}\Big]\Big];
$$

```
   E^ {muy1, Sqrt[-2 muy1]}
   ] /; cvWant >= cv2
```

■ Extrapolation Factors (cf. Slob & Pieters, *Risk Anal.*, 1998; EPA)

Assumed that median is central target for uncertain EF, expected value is central target for heterogeneous EF.

EFinterspTdyn: Uncertain (Median =1)

```
{{z95, z99} = RQ[Q, N, {0, 1}, {.95, .99}], sdy = Log[3 / 1] / z99, gsd = E ^ sdy}
```

```
{{1.64485, 2.32635}, 0.472248, 1.60359}
```

EFintraspTdyn: Heterogeneous (Mean = 1)

```
{Log[10 / 1] / z99, E ^ (Log[10 / 1] / z99)}
```

```
{0.989785, 2.69066, 4.1787}
```

```
rule = Solve[(mux / gmx) == E ^ (sigp * sigp / 2), gmx][[1]]
```

$$\left\{ gmx \to E^{-\frac{sigp^2}{2}} \; mux \right\}$$

```
Solve[sigp == (Log[xp / gmx] /. rule) / zp, sigp]
```

$$\left\{ \left\{ sigp \to zp - \sqrt{zp^2 - 2 \, Log\left[\frac{xp}{mux}\right]} \right\}, \; \left\{ sigp \to zp + \sqrt{zp^2 - 2 \, Log\left[\frac{xp}{mux}\right]} \right\} \right\}$$

```
10 ^ (2 / 3.)
```

```
4.64159
```

$$\left\{ sdy = z99 - \sqrt{z99^2 - 2 \, Log[5]} \; , \; muy = -sdy * sdy / 2, \; gmx = E ^ muy, \; gsdx = E ^ sdy \right\}$$

```
{0.845464, -0.357404, 0.69949, 2.32906}
```

```
{gmx * E ^ (sdy * z99), 5 / gmx}
```

```
{5., 7.14807}
```

(EF = 1+U): acute -> subchronic -> chronic EF, where EF>=1 and U is Uncertain (Median = 2x3 = 6)

$$\left\{ \{sdyA = Log[6 / 3] / z99, \; gsd = E ^ sdyA\}, \; \{sdyB = Log[10 / 2] / z99, \; E ^ sdyB\}, \right.$$

$$\left. \left\{ sdy = \sqrt{sdyA^2 + sdyB^2} \; , \; E ^ sdy \right\} \right\}$$

```
{{0.297955, 1.3471}, {0.69183, 1.99737}, {0.753264, 2.12392}}
```

```
EFinterspTdyn = {LN, Log[{1, 1.60359450162908601`}]};
EFintraspTdyn = {LN, Log[{0.700, 2.33}]};
EFacuteTosubchr = {LN, Log[{3, 1.34710131239470021`}]};
EFsubchrTochr = {LN, Log[{2, 1.99736804456840957`}]};
EFacuteTochr1 = {LN, Log[{5, 2.12392092140740462`}]};
```

```
frisk[cdf_] := RQ[Cdf, cdf[[1]], cdf[[2]], 2000];
{cdfEFinter, cdfEFintra, cdfEFchron1} =
  frisk /@ {EFinterspTdyn, EFintraspTdyn, EFacuteTochr1};
{EFinterspTdynAng, EFintraspTdynBar, EFacuteTochr1Ang} =
  (EV[#, Empirical -> True]& /@ {cdfEFinter, cdfEFintra, cdfEFchron1})
```

```
{1.11699, 0.997245, 6.62175}
```

```
EFintraspTdynBar = 1;
```

end

Effective Dose

■ Genotoxic effective dose (EgBar, EgAng)

Exposures are all in units of (mg/kg-d) x 1000 (see "D. Effective Genotoxic Dose"):

```
Clear[cdfEingestBar, cdfEingestAng,
  cdfEdermalBar, cdfEdermalAng, cdfEinhaleBar, cdfEinhaleAng,
  EingestBar, EingestAng, EdermalBar, EdermalAng, EinhaleBar, EinhaleAng, o,
EingestBarAng,
  EinhaleBarAng, EdermalBarAng, EingestAngBar, EinhaleAngBar, EdermalAngBar];

o = Get /@ (PathName[#1]&) /@
    {EingestBar, EingestAng, EdermalBar, EdermalAng, EinhaleBar, EinhaleAng};
{cdfEingestBar, cdfEingestAng, cdfEdermalBar,
  cdfEdermalAng, cdfEinhaleBar, cdfEinhaleAng} = o;
{EingestBarAng, EingestAngBar, EdermalBarAng,
   EdermalAngBar, EinhaleBarAng, EinhaleAngBar} = (EV[#, Empirical -> True]&/@o);
o = {{EingestBarAng, EinhaleBarAng, EdermalBarAng},
   {EingestAngBar, EinhaleAngBar, EdermalAngBar}}
```

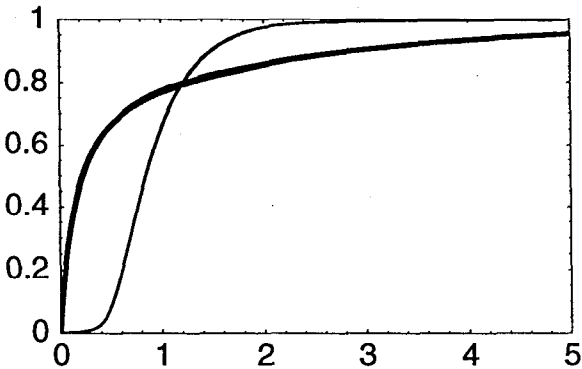{{0.0507837, 0.00235084, 0.0071258}, {0.0491639, 0.00225019, 0.00684773}}

```
Plus@@#&/@o
```

{0.0602603, 0.0582618}

```
cdfBar = {({EingestBarAng⁻¹, 1} #)&/@cdfEingestBar,
    ({EdermalBarAng⁻¹, 1} #)&/@cdfEdermalBar, ({EinhaleBarAng⁻¹, 1} #)&/@cdfEinhaleBar};
cdfAng = {({EingestAngBar⁻¹, 1} #)&/@cdfEingestAng,
    ({EdermalAngBar⁻¹, 1} #)&/@cdfEdermalAng, ({EinhaleAngBar⁻¹, 1} #)&/@cdfEinhaleAng};

PlotCdf[Join[cdfBar, cdfAng], Xmin -> -10⁻⁴, Xmax -> 5, Ymin -> -10⁻⁴];
```



```
Clear[EgBar, EgAng];
cdfBar = (Plus@@cdfBar) / 3;
cdfAng = (Plus@@cdfAng) / 3;
```

```
Put[cdfBar, PathName[EgBar]];
Put[cdfAng, PathName[EgAng]];

EgBar = cdfBar;
EgAng = cdfAng;

EgBar = Get[PathName[EgBar]];
EgAng = Get[PathName[EgAng]]; CdfQ/@{EgBar, EgAng}
```
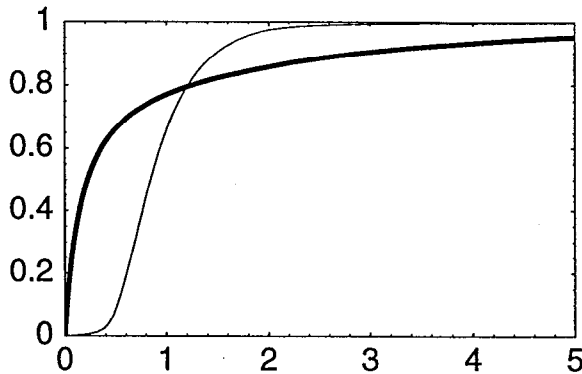
{True, True}

```
PlotCdf[{EgBar, EgAng}, Xmin → -10⁻⁴, Xmax → 5, Ymin → -10⁻⁴];
```



```
EV[#, Empirical → True]&/@{EgBar, EgAng}
```

{1., 1.}

```
Var[#, Empirical → True]&/@{EgBar, EgAng}
```

{2.45519, 4.42109}

```
{Edf[#, 1], Idf[#, {.5, .95, .99}]}&/@{EgBar, EgAng}
```

{{0.658518, {0.844739, 1.74748, 2.59973}}, {0.769714, {0.223819, 4.81475, 10.326}}}

```
{{EingestAngBar, EinhaleAngBar, EdermalAngBar}/
    (Plus@@{EingestAngBar, EinhaleAngBar, EdermalAngBar}),
 {EingestBarAng, EinhaleBarAng, EdermalBarAng}/
    (Plus@@{EingestBarAng, EinhaleBarAng, EdermalBarAng})}
```

{{0.843844, 0.038622, 0.117534}, {0.842738, 0.0390114, 0.11825}}

Redefine {EingestAngBar,EdermalAngBar, EinhaleAngBar} each as a mean of the corresponding AngBar and BarAng means, then derive relative contributions of {EingestAngBar,EdermalAngBar, EinhaleAngBar} to Etotal, (where Etotal = EingestAngBar + EdermalAngBar + EinhaleAngBar).

```
{{EingestAngBar, EinhaleAngBar, EdermalAngBar} =
    ({EingestAngBar, EinhaleAngBar, EdermalAngBar} +
        {EingestBarAng, EinhaleBarAng, EdermalBarAng}) / 2,
 Etotal = Plus@@{EingestAngBar, EinhaleAngBar, EdermalAngBar},
 FEingderinh = {EingestAngBar, EinhaleAngBar, EdermalAngBar}/Etotal}
```

{{0.0499738, 0.00230051, 0.00698677}, 0.0592611, {0.843282, 0.03882, 0.117898}}

```
Etotal = 0.0593 / 1000;  (* mg/kg-d *)
{EingestAngBar, EinhaleAngBar, EdermalAngBar} = {0.843, 0.039, .118} * Etotal
```

$\{0.0000499899, 2.3127 \times 10^{-6}, 6.9974 \times 10^{-6}\}$

```
{EingestBarAng, EdermalBarAng, EinhaleBarAng} =
  {EingestAngBar, EdermalAngBar, EinhaleAngBar};
```

end

■ Cytotoxic exposures (EcBar, EcAng)

```
Clear[ECingestAng, ECingestBar, ECinhaleAng, ECinhaleBar, ECdermalAng, ECdermalBar];
ECingestAng = Get[PathName[ECingestAng]];
ECingestBar = Get[PathName[ECingestBar]];
ECinhaleAng = Get[PathName[ECinhaleAng]];
ECinhaleBar = Get[PathName[ECinhaleBar]];
ECdermalAng = Get[PathName[ECdermalAng]];
ECdermalBar = Get[PathName[ECdermalBar]];
CdfQ /@ {ECingestAng, ECingestBar, ECinhaleAng, ECinhaleBar, ECdermalAng, ECdermalBar}
```

```
{True, True, True, True, True, True}
```

```
{ECingestAngBar, ECingestBarAng, ECinhaleAngBar,
  ECinhaleBarAng, ECdermalAngBar, ECdermalBarAng} = EV[#, Empirical -> True] & /@
   {ECingestAng, ECingestBar, ECinhaleAng, ECinhaleBar, ECdermalAng, ECdermalBar}
```

```
{0.0161848, 0.0162664, 0.00835208, 0.00840379, 0.00226194, 0.0022786}
```
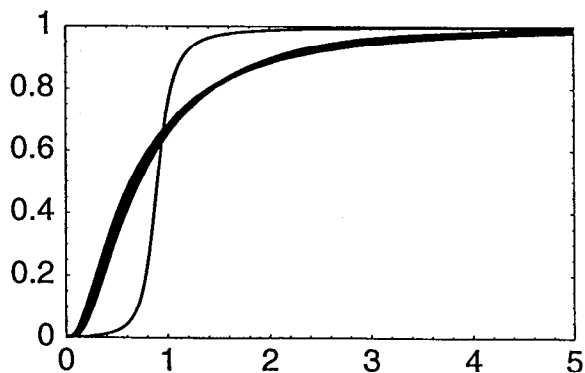
```
cdfCBar = { ({ECingestBarAng⁻¹, 1} #) & /@ ECingestBar,
    ({ECdermalBarAng⁻¹, 1} #) & /@ ECdermalBar, ({ECinhaleBarAng⁻¹, 1} #) & /@ ECinhaleBar};
cdfCAng = { ({ECingestAngBar⁻¹, 1} #) & /@ ECingestAng,
    ({ECdermalAngBar⁻¹, 1} #) & /@ ECdermalAng, ({ECinhaleAngBar⁻¹, 1} #) & /@ ECinhaleAng};
```

```
CdfQ /@ # & /@ {cdfCBar, cdfCAng}
```

```
{{True, True, True}, {True, True, True}}
```

```
PlotCdf[Join[cdfCBar, cdfCAng], Xmin → -10⁻⁴, Xmax → 5, Ymin → -10⁻⁴];
```

```
Dimensions /@cdfCAng
```

```
{{405, 2}, {405, 2}, {405, 2}}
```

```
Clear[EcBar, EcAng];
cdfCBar = (Plus@@cdfCBar) /3;
cdfCAng = (Plus@@cdfCAng) /3;
```

```
Put[cdfCBar, PathName[EcBar]];
Put[cdfCAng, PathName[EcAng]];
```
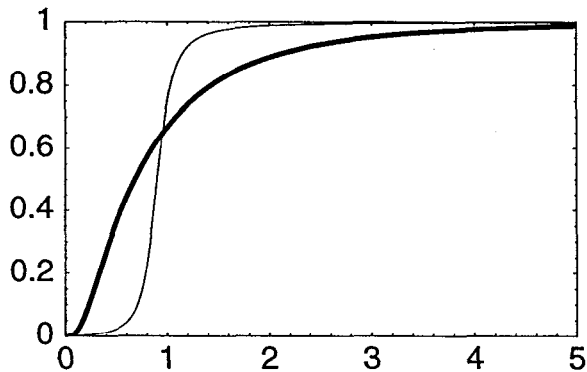
```
EcBar = cdfCBar;
EcAng = cdfCAng;
```

```
EcBar = Get[PathName[EcBar]];
EcAng = Get[PathName[EcAng]]; CdfQ /@{EcBar, EcAng}
```

```
{True, True}
```

```
PlotCdf[{EcBar, EcAng}, Xmin → -10⁻⁴, Xmax → 5, Ymin → -10⁻⁴];
```

$$\text{PlotCdf}[\{EcBar, EcAng\}, Xmin \rightarrow -10^{-4}, Xmax \rightarrow 5, Ymin \rightarrow -10^{-4}];$$


```
EV[#, Empirical → True]& /@{EcBar, EcAng}
```

```
{1., 1.}
```

```
Var[#, Empirical → True]& /@{EcBar, EcAng}
```

```
{2.57639, 1.01933}
```

```
{Edf[#, 1], Idf[#, {.5, .95, .99}]}& /@{EcBar, EcAng}
```

```
{{0.748303, {0.900642, 1.31192, 2.1726}}, {0.667287, {0.682963, 2.94235, 5.41263}}}
```

```
{{ECingestAngBar, ECinhaleAngBar, ECdermalAngBar} /
   (Plus@@{ECingestAngBar, ECinhaleAngBar, ECdermalAngBar}),
{ECingestBarAng, ECinhaleBarAng, ECdermalBarAng} /
   (Plus@@{ECingestBarAng, ECinhaleBarAng, ECdermalBarAng})}
```

```
{{0.603938, 0.311658, 0.0844043}, {0.603605, 0.311842, 0.0845528}}
```

Define {CingestAngBar,CdermalAngBar, CinhaleAngBar} each as a mean of the corresponding AngBar and BarAng means, then derive relative contributions of {CingestAngBar,CdermalAngBar, CinhaleAngBar} to ECtotal, (where Ctotal = CingestAngBar + CdermalAngBar + CinhaleAngBar).

```
{{CingestAngBar, CinhaleAngBar, CdermalAngBar} =
   ({ECingestAngBar, ECinhaleAngBar, ECdermalAngBar} +
      {ECingestBarAng, ECinhaleBarAng, ECdermalBarAng}) / 2,
  Ctotal = Plus@@{CingestAngBar, CinhaleAngBar, CdermalAngBar},
  FCingderinh = {CingestAngBar, CinhaleAngBar, CdermalAngBar} / Ctotal}

{{0.0162256, 0.00837794, 0.00227027}, 0.0268739, {0.603771, 0.31175, 0.0844788}}


Ctotal = 0.0269; (* mg TCA/L plasma *)
{CingestAngBar, CinhaleAngBar, CdermalAngBar} = {0.604, 0.312, .084} * Ctotal

{0.0162476, 0.0083928, 0.0022596}


{CingestBarAng, CdermalBarAng, CinhaleBarAng} =
  {CingestAngBar, CdermalAngBar, CinhaleAngBar};
```

end

end

Dose-Response

■ Genotoxic Potency (Qcdf)

```
Qcdf = Get[PathName[QbwCdf]];
QcdfAng = EV[Qcdf, Empirical -> True]

0.000366899
```

end

■ Cytotoxic Potency (TBARSvTCA)

```
TBARSvTCA = Get[PathName[TBARSvTCA]];
TBARSvTCAAng = EV[TBARSvTCA, Empirical -> True]

185.242

{Idf[TBARSvTCA, {.5, .95, .99}], Edf[TBARSvTCA, 130]}

{{159.836, 395.243, 605.35}, 0.357047}
```
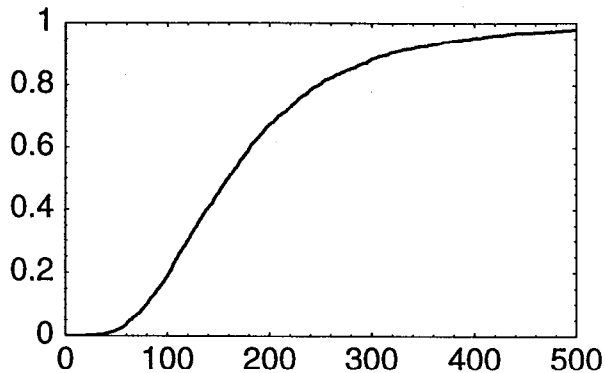
```
PlotCdf[TBARSvTCA, Xmin → -.0001, Xmax → 500, Ymin → -.001];
```



```
Last[TBARSvTCA]
```

```
{1428.077620826887, 1}
```

$pTBARS[D_{Ca}] = F_C(D_{Ca})$ for effective acute cytotoxic dose D_{Ca}, i.e., the risk of significant TBARS elevation conditional on D_{Ca}.

```
pTBARS = Interpolation[Append[TBARSvTCA, {10^6, 1}], InterpolationOrder → 1];
{pTBARS[130], pTBARS[0.0269]}
```

```
{0.357047, 4.96842 × 10^-11}
```

end

end

TCE Risk (<R>, Rbar)

■ Solve for 2nd-order approximation to Rc

Where $Log[10, pTBARS[d]] \sim a + b \, Log[10, d]$
  where: a = -7.60 and b = 3.68 (from low-risk extrapolation; see "G. Potency")

$pTBARS[d] \sim 10\char`^a * d\char`^b$
$d = Utdyn*Vtdyn*(1+Uchron)*k*B$
  $= Ux*Vtdyn*k*B$ for $Ux = Utdyn*(1+Uchron)$
where: $k = Ctotal = 0.0269$ mg/L = the B-to-D_{Ca} scaling factor,
    B= Ec = normalized effective acute cytotoxic dose D_{Ca},
       and: BBar = BAng = 1,
    Utdyn = EFinterspTdyn={LN,Log[{1,1.60359450162908601`}]}, and
    Ux = EFacuteTochr1={LN,Log[{5,2.12392092140740462`}]},
      Vtdyn = EFintraspTdyn={LN,Log[{0.700,2.33}]}, so
$dAng = 10^a (Vtdyn * k)^b (Ux * B)^b$
$dBar = 10^a (Ux * k)^b (Vtdyn * B)^b$

```
? D
```

```
D[f, x] gives the partial derivative of f with respect to x. D[f, {x, n}] gives the
   nth partial derivative of f with respect to x. D[f, x1, x2, ... ] gives a mixed derivative.
```

```
(* For any constant A: *)
D[A (x * y) ^b, {x, 2}]
```

$$A (-1 + b) b y^2 (x y)^{-2+b}$$

Thus, letting u1 = Ux and u2 = EcAng, the 1st-order RcAng approx., RcAng1, must be increased by (with u1 and u2 evaluated at their expected values):

```
Simplify[0.5 (D[A (u1 * u2) ^b, {u1, 2}] (σ²)_u1 + D[A (u1 * u2) ^b, {u2, 2}] (σ²)_u2)]
```

$$\frac{0.5 A b (-1. + 1. b) (u1\,u2)^b (u2^2\,(\sigma^2)_{u1} + u1^2\,(\sigma^2)_{u2})}{u1^2\,u2^2}$$

and, letting v1 = Vtdyn and v2 = EcBar, the 1st-order RcBar approx., RcBar1, must be increased by (with v1 and v2 evaluated at their pop.-ave. values)

```
Simplify[0.5 (D[A (v1 * v2) ^b, {v1, 2}] (σ²)_v1 + D[A (v1 * v2) ^b, {v2, 2}] (σ²)_v2)]
```

$$\frac{0.5 A b (-1. + 1. b) (v1\,v2)^b (v2^2\,(\sigma^2)_{v1} + v1^2\,(\sigma^2)_{v2})}{v1^2\,v2^2}$$

Recall that $(\sigma^2)_{u2}$ and $(\sigma^2)_{v2}$ are given by:

```
Var[#, Empirical → True] & /@ {EcBar, EcAng}
```

```
{2.57639, 1.01933}
```

By the method of moments, sig2Vtydn = $(\sigma^2)_{v1}$ is given by

```
{msd = MSDx[0.700, 2.33], sig2Vtdyn = msd[[2]] ^2}
```

```
{{1.00107, 1.02344}, 1.04744}
```

And the mean [= muUx] and variance [sig2Ux = $(\sigma^2)_{u1}$] of Ux =u1 are approximated via simulation as

```
{Utdyn, Uchron} = SimulateCdf[{{LN, Log[{1, 1.6035945}]},
    {LN, Log[{5, 2.123921}]}}, 2000];
```

```
Output-Sample Rank-Correlation Matrix:
```

```
1.          -0.000577
-0.000577   1.
```

```
Jennrich's Asymptotic Chi-Square Test of Homogeneity

    Between Input & Target Correlation Matrices

    For 2000 2-Variate Normal Samples:

Chi2(1)= 0.00066604    1-tail p= 0.979411 (NS)
```

```
Ux = Utdyn (1 + Uchron);
{UxAng = EV[Ux, Empirical → True], sig2Ux = Var[Ux, Empirical → True]}
```

{8.49599, 65.5915}

Recall that

```
{Ctotal, EFintraspTdynBar, EFinterspTdynAng, EFacuteTochr1Ang}
```

{0.0269, 1, 1.11699, 6.62175}

```
{UxAng, UxAng^2}
```

{8.49599, 72.1819}

Using $dAng = 10^a (Vtdyn*k)^b (Ux*B)^b$, the RcAng1 increment is (with BAng=1) thus has a pop.-ave. value of

```
0.5 * 10^-7.60 (EFintraspTdynBar * 0.0269)^b (b - 1) *
   (UxAng * 1)^b ((sig2Ux * UxAng^-2) + (1.02 * 1^-2)) /. {
   b → 3.68}
```

2.84031×10^{-10}

Using $dBar = 10^a (Ux*k)^b (Vtdyn*B)^b$, the RcBar1 increment is (with BBar=1) thus has a mean value of

```
0.5 * 10^-7.60 (UxAng * 0.0269)^b (b - 1) *
   (1 * 1)^b ((sig2Vtdyn * 1^-2) + (2.58 * 1^-2)) /. {b → 3.68}
```

5.34197×10^{-10}

end

■ Rang (Variability Distribution)

{EFintraspTdyn, EgAng x 3, EcAng x 3} = 7 heterogeneous variates
Ug = Likelihood that Rg is true ~ U[0, 0.5] by assumption; therefore, UgAng = 1/4.

Dose rank correlations (from "F. Effective Dose Correlations") for: (n = 50 x 500)

GingAng	CingAng	GinhAng	CinhAng	GderAng	CderAng
1.	0.233	0.878	-0.00269	0.894	0.000496
0.233	1.	-0.0088	0.421	0.00439	0.514
0.878	-0.0088	1.	0.187	0.918	0.035
-0.00269	0.421	0.187	1.	0.0766	0.649
0.894	0.00439	0.918	0.0766	1.	0.177
0.000496	0.514	0.035	0.649	0.177	1.

Assign corresponding values to the upper triangular portion of the simulation-input-variate rank-correlation matrix (which shall be denoted "corr"). Note that the first row of the matrix pertains to the EFintraspTdyn variate (i.e., the intraspecies toxicodynamic extrapolation factor), which is not correlated with any of the 6 exposure variates.

```
corr = {{0, 0, 0, 0, 0, 0}, {.23, .88, 0, .89, 0}, {0, .42, 0, .51}, {0.19, .92, 0.035},
   {.077, .65}, {.18}};
```

Verify that the Cholesky decomposition of the target rank-corrlation matrix (=Reflect[corr]) contains no imaginary parts:

```
Cholesky[Reflect[corr]]
```

```
{{1, 0, 0, 0, 0, 0, 0}, {0, 1, 0, 0, 0, 0, 0}, {0, 0.23, 0.973191, 0, 0, 0, 0},
 {0, 0.88, -0.207976, 0.42702, 0, 0, 0}, {0, 0, 0.43157, 0.655136, 0.620116, 0, 0},
 {0, 0.89, -0.210339, 0.217916, 0.0403333, 0.338442, 0},
 {0, 0, 0.524049, 0.337196, 0.32724, 0.601429, 0.37798}}
```

```
{nsam, nsim} = {2000, 10};
UgAng = 1 / 4; (* see Rbar section below *)
cdfs = {EFintraspTdyn, EgAng, EcAng, EgAng, EcAng, EgAng, EcAng};
Clear[fxn];
fxn[x_, Ging_, Cing_, Ginh_, Cinh_, Gder_, Cder_] := Module[
  {Rg, Rc1, Rc2, Rc, a = -7.6, b = 3.68, Ux, c = 0.0269, Call},
  Rg =
   1 - E^ - (QcdfAng * EFinterspTdynAng * x * 0.0000593 (0.843 Ging + 0.039 Ginh + 0.118 Gder));
  Ux = EFinterspTdynAng * (1 + EFacuteTochr1Ang);
  Call = 0.604 Cing + 0.312 Cinh + 0.084 Cder;
  Rc1 = pTBARS[Ux * x * c * Call];
```

$$Rc2 = 0.5 * 10^{a} (x * c)^{b} (b - 1) * (8.50 * 1)^{b} \left(\frac{65.59}{72.18} + \frac{1.02}{1} \right);$$

```
  Rc = Rc1 + Rc2;
  1 - (1 - UgAng * Rg) (1 - Rc)
  ];
```

```
EFintraspTdynBar = 1; {EFintraspTdynBar, EingestAngBar, EinhaleAngBar,
 EdermalAngBar, CingestAngBar, CinhaleAngBar, CdermalAngBar}
```

```
{1, 0.0000499899, 2.3127×10⁻⁶, 6.9974×10⁻⁶, 0.0162476, 0.0083928, 0.0022596}
```

```
fxn[EFintraspTdynBar, 1, 1, 1, 1, 1, 1]
```

```
6.78312×10⁻⁹
```

```
Timing[sim1 = Table[SimulateCdf[cdfs, nsam, Correlate → corr, Report → Append], {nsim}];]
```

```
{399.317 Second, Null}
```

```
(* Check Jennrich X2 p-values *)
jenp = Transpose[{Range[Length[sim1]], Last /@ Last /@ Last /@ sim1}]
```

```
{{1, 0.999999}, {2, 0.996311}, {3, 0.887823}, {4, 0.999861}, {5, 0.850753},
 {6, 1.}, {7, 0.764912}, {8, 0.998435}, {9, 0.999999}, {10, 0.997622}}
```

```
{jen, cdf, cvm} =
 QUAnalyze[cdfs, fxn, nsam, nsim, SimIn → sim1, Correlate → corr, Scale → 10⁶];
```
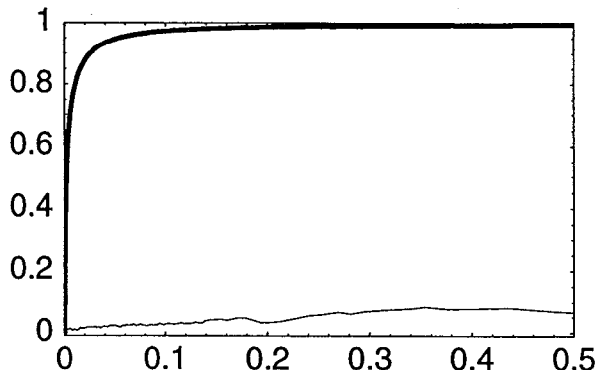
```
TBL /@ jen
```

Mean[Δr]	Max[$|\Delta r|$]	JennrichChi2	DegFr	Min[P-adj]
-0.000621132	0.0153743	16.084	21	1.

Fractile	Value	CVM(%)
0.01	0.0000580549	3.46591
0.05	0.000145191	1.40176
0.5	0.00197293	1.26445
0.95	0.0533094	1.94448
0.99	0.281664	5.92463
Mean	0.024678	10.8085
Variance	0.187204	49.1916

```
PlotCdf[{cvm, cdf}, Ymin → -.01, Xmin → -.0001, Xmax → .5];
```



```
Put[cdf, PathName[Rang]]; Rang = cdf;

Rang = Get[PathName[Rang]]; CdfQ[Rang]

True


RangBar=0.024678;

{{Rang50, Rang95, Rang99} = Idf[Rang, {.5, .95, .99}], Edf[Rang, 1]}

{{0.00197293, 0.0533094, 0.281664}, 0.997088}
```

end

■ Rbar (Uncertainty Distribution)

{Ug, EgBar, EcBar, Qcdf, EFinterspTdyn, EFacuteTochr1} = 6 uncertain variates
Ug = Likelihood that Rg is true ~ U[0, 0.5] by assumption

```
corr = {{0, 0, 0, 0, 0}, {.49, 0, 0, 0}, {0, 0, 0}, {0, 0}, {0}};

{nsam, nsim} = {2000, 25};
Ug = {{0, 0}, {.5, 1}};
cdfs = {Ug, EgBar, EcBar, Qcdf, EFinterspTdyn, EFacuteTochr1};
Clear[fxn];
fxn[ug_, Gall_, Call_, q_, uf1_, uf2_] := Module[
   {Rg, Rc1, Rc2, Rc, a = -7.6, b = 3.68, Ux, c = 0.0269},
   Rg = 1 - E^-(q*uf1*1*0.0000593 Gall);
   Rc1 = pTBARS[uf1*(1+uf2)*1*0.0269 Call];
```

$$Rc2 = 0.5 * 10^a \ (uf1 * (1 + uf2) * c)^b \ (b - 1) * (1 * 1)^b \left(\frac{1.05}{1} + \frac{2.58}{1} \right);$$

```
   Rc = Rc1 + Rc2;
   1 - (1 - ug*Rg) (1 - Rc)
   ];

{QcdfAng, EFinterspTdynAng, EFacuteTochr1Ang}

{0.000366899, 1.11699, 6.62175}
```

fxn[0.25, 1, 1, QcdfAng, EFinterspTdynAng, EFacuteTochr1Ang]

7.03721×10^{-9}

Timing[{jen, cdf, cvm} = QUAnalyze[cdfs, fxn, nsam, nsim, Correlate → corr, Scale → 10^6];]
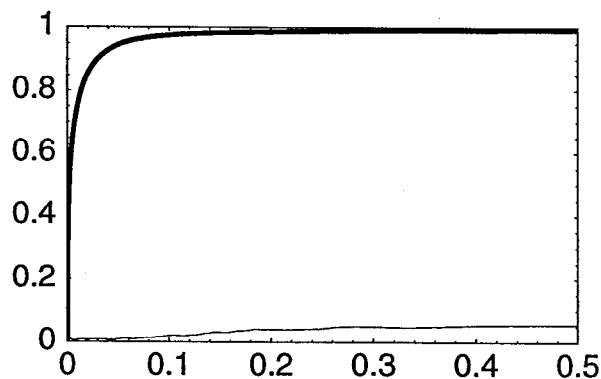
{421.6 Second, Null}

TBL/@jen

```
{ Mean[Δr]      Max[|Δr|]    JennrichChi2  DegFr  Min[P-adj]  ,
{ 0.000118964   0.0212937    3.29258       15     1.
```

```
Fractile   Value          CVM(%)
0.01       0.0000564078   1.20236
0.05       0.000102103    0.796374
0.5        0.00182331     0.98663  }
0.95       0.0540772      1.08234  }
0.99       0.287938       5.10999
Mean       0.218735       23.2584
Variance   186.669        33.6675
```

PlotCdf[{cvm, cdf}, Ymin → -.0001, Xmin → -.0001, Xmax → .5];

Clear[Rbar];
Put[cdf, PathName[Rbar]]; Rbar = cdf;
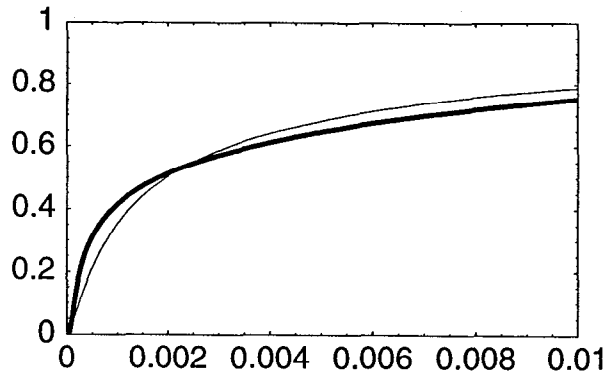
Rbar = Get[PathName[Rbar]]; CdfQ[Rbar]

True

RbarAng=0.218735;

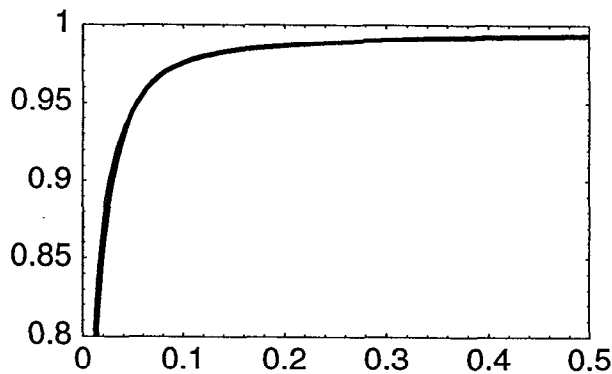**{{Rbar50, Rbar95, Rbar99} = Idf[Rbar, {.5, .95, .99}], Edf[Rbar, 1]}**

{{0.00182331, 0.0540772, 0.287938}, 0.996147}

end

```
PlotCdf[{Rang, Rbar}, Ymin → -.0001, Xmin → -.000001, Xmax → .01];
```
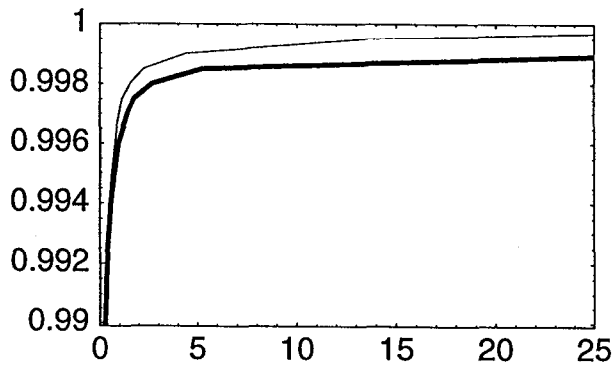


```
PlotCdf[{Rang, Rbar}, Ymin → .7999, Xmin → -.000001, Xmax → .5];
```



```
PlotCdf[{Rang, Rbar}, Ymin → .9899, Xmin → -.000001, Xmax → 25];
```


end

Confidence Bounds on JUV in Risk

■ **R*99 = Analytic upper-bound JUV estimator (@ 99th %ile on U & V)**

```
{Rang99, RangBar, Rbar99, RbarAng}

{0.281664, 0.024678, 0.287938, 0.218735}
```

R*99b = rho99 x Rang99, rho99 = (Rbar99)/(<Rbar>)   <------ As defined by Bogen (1995)
R*99a = rho99 x Rbar99, rho99 = (<R>99)/(<R>bar)   <------ Alternative definition

```
(* CV for R99* *)
{RbarAngcv, Rbar99cv, RangBarcv, Rang99cv} = {.232, .051, .28, .11};

{rhoa = (Rang99 / RangBar), rhob = (Rbar99 / RbarAng)}

{11.4136, 1.31638}

((1 - (1 - #[[1]]²) (1 - #[[2]]²))·⁵) & /@ {
   {Rang99cv, RangBarcv}, {Rbar99cv, RbarAngcv}}

{0.299251, 0.237245}

{R99a = Rbar99 * rhoa, R99b = Rang99 * rhob}

{3.28641, 0.370777}

{gammaa, gammab} = (((1 - (1 - #[[1]]²) (1 - #[[2]]²) (1 - #[[3]]²))·⁵) & /@ {
   {Rbar99cv, Rang99cv, RangBarcv}, {Rang99cv, Rbar99cv, RbarAngcv}})

{0.303182, 0.2602}
```

■ R*99 = Target-Nested Monte-Carlo JUV estimators (@ 99th %ile on V)

```
SimulateCdfs[Cdfs_, nsam_, nsim_, options___] := Module[{o, cdfs = Cdfs, x},
   o = SimulateCdf[cdfs, nsam, options];
   If[Head[o] === String, Return[StringJoin["SimulateCdfs: Bad input\n", o]]];
   x = If[Dimensions[o] === {Length[cdfs], nsam}, o, o[[1]]];
   cdfs = (Cdf[#1, Xmax → 10^15] & ) /@ x;
   Prepend[Table[SimulateCdf[cdfs, nsam, options], {nsim - 1}], o]
  ] /; nsam > nsim > 1
```

```
corrV = {{0, 0, 0, 0, 0, 0}, {.23, .88, 0, .89, 0}, {0, .42, 0, .51}, {0.19, .92,
   0.035}, {.077, .65}, {.18}};
cdfV = {EFintraspTdyn, EgAng, EcAng, EgAng, EcAng, EgAng, EcAng};
fxnV[x_, Ging_, Cing_, Ginh_, Cinh_, Gder_, Cder_] := Module[
  {Rg, Rc},
  Rg =
   1 - E ^ - (QcdfAng * EFinterspTdynAng * x * 0.0000593 (0.843 Ging + 0.039 Ginh + 0.118 Gder));
  Rc = pTBARS[EFinterspTdynAng * (1 + EFacuteTochr1Ang
     ) * x * 0.0269 (0.604 Cing + 0.312 Cinh + 0.084 Cder)];
  1 - (1 - 0.25 Rg) (1 - Rc)
  ];

corrU = {{0, 0, 0, 0, 0}, {.49, 0, 0, 0}, {0, 0, 0}, {0, 0}, {0}};
cdfU = {Ug, EgBar, EcBar, Qcdf, EFinterspTdyn, EFacuteTochr1};
fxnUV[ug_, Gall_, Call_, q_, uf1_, uf2_,
      x_, Ging_, Cing_, Ginh_, Cinh_, Gder_, Cder_] := Module[
  {Rg, Rc},
  Rg = 1 - E ^ - (q * uf1 * x * 0.0000593 Gall (0.843 Ging + 0.039 Ginh + 0.118 Gder));
  Rc = pTBARS[uf1 * (1 + uf2) * x *
     0.0269 Call (0.604 Cing + 0.312 Cinh + 0.084 Cder)];
  1 - (1 - ug * Rg) (1 - Rc)
  ];

fxnUV[0.25, 1, 1, QcdfAng, EFinterspTdynAng, EFacuteTochr1Ang, EFintraspTdynBar,
 1, 1, 1, 1, 1, 1]
```

6.49859×10^{-9}

```
{nsam, nsim} = {999, 100}; {{i50, i95, i99} = (nsam + 1) {50, 95, 99} / 100}
```

```
{{500, 950, 990}}
```

```
test = Cdf[2 Range[nsam], Xmax -> 10 * nsam];
{Idf[test, .99], test[[i99 + 1]]}
```

$\left\{1980, \left\{1980, \frac{99}{100}\right\}\right\}$

```
(CdfQ[#] || RQ[Test, #[[1]], #[[2]]])& /@ cdfV
```

```
{True, True, True, True, True, True, True}
```

```
(CdfQ[#] || RQ[Test, #[[1]], #[[2]]])& /@ cdfU
```

```
{True, True, True, True, True, True}
```

```
Timing[
simv = SimulateCdfs[
   cdfV, nsam, nsim, Correlate -> corrV, Report -> False];
rvi = fxnV@@#& /@ simv;
vi = (#[[i99, 2]]& /@ (Sort /@ MapThread[
   Transpose[{#1, Transpose[#2]}]&, {rvi, simv}]));
simu = SimulateCdfs[cdfU, nsam, nsim, Correlate -> corrU, Report -> False];
vij = Transpose[Table[#, {nsam}]]& /@ vi;
simin = MapThread[Join[#1, #2]&, {simu, vij}];
Dimensions[simin]]
```

```
{767.65 Second, {100, 13, 999}}
```
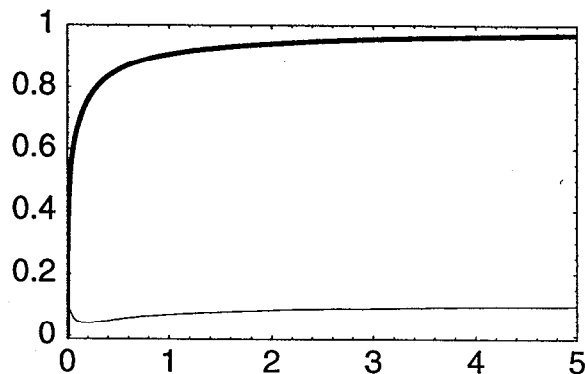
```
767.65 / 60. min
```

```
12.7942 min
```

```
{jen, cdf, cvm} = QUAnalyze[13, fxnUV, nsam, nsim, SimIn → simin, Scale → 10^6];
```

```
TBL[jen]
```

Fractile	Value	CVM(%)
0.01	0.000275208	6.25271
0.05	0.000492571	6.05879
0.5	0.026333	8.3953
0.95	2.53276	8.89275
0.99	26.6467	12.2349
Mean	51.5572	29.8237
Variance	1.78899×10^7	51.2064

```
PlotCdf[{cvm, cdf}, Ymin → -.01, Xmin → -.0001, Xmax → 5];
```


end

■ R*99 = Traditional Nested Monte-Carlo JUV estimators (@ 99th %ile on V)

Compare variability fractiles for the 50th, 95th and 99th %ile with respect to uncertainty, respectively, obtained using a traditional nested Monte-Carlo approach:

```
{Dimensions /@ {simu, simv}, {nsam, nsim, i50, i95, i99}}
```

```
{{{100, 6, 999}, {100, 7, 999}}, {999, 100, 500, 950, 990}}
```

```
Timing[o = Transpose /@ Table[
      Prn[i]; Table[
uij = Transpose[Table[#[[j]]&/@simu[[i]], {nsam}]];
simin = Join[uij, simv[[i]]];
ruj = Sort[fxnUV@@simin][[{i50, i95, i99}]],
{j, nsam}], {i, nsim}];]
```

```
i= 100
```

```
{38204. Second, Null}
```

```
{38204. (60.^-2) h, 38204. / 767.65}
```

```
{10.6122 h, 49.7675}
```

```
{Dimensions[o], nsam, nsim}
```

```
{{100, 3, 999}, 999, 100}
```

```
fx[r_] := r
```

```
in = List /@#& /@Transpose[o];
Dimensions[in]
```

```
{3, 100, 1, 999}
```

```
{jen, cdf, cvm} = Transpose[QUAnalyze[1, fx, nsam, nsim, SimIn → #, Scale → 10^6]& /@in];
```

Variability fractiles for the 50th, 95th and 99th %ile with respect to uncertainty, respectively:

```
TBL /@jen
```

Fractile	Value	CVM(%)	Fractile	Value	CVM(%)
0.01	0.0000275434	0.939922	0.01	0.000180713	1.11573
0.05	0.0000501088	0.498607	0.05	0.000328785	0.674825
0.5	0.000307087	0.378278	0.5	0.00800268	1.4414
0.95	0.0064338	0.719361	0.95	0.295773	1.29464
0.99	0.0174277	1.54854	0.99	2.01852	4.17751
Mean	0.0131852	40.8619	Mean	8.8583	38.7753
Variance	2.94735	67.2223	Variance	1.20453×10^6	61.4832

Fractile	Value	CVM(%)
0.01	0.000402496	1.42502
0.05	0.000733586	1.18967
0.5	0.0610779	2.35897
0.95	3.18049	3.89965
0.99	37.2624	5.28478
Mean	71.6359	24.6687
Variance	2.79463×10^7	42.8514

Comparison with results from targeted method:

```
{2.53 / 2.01, 26.6 / 37.3}
```

```
{1.25871, 0.713137}
```

```
PlotCdf[Join[Rest[cvm], Rest[cdf]], Ymin → -.01, Xmin → -.0001, Xmax → 5];
```
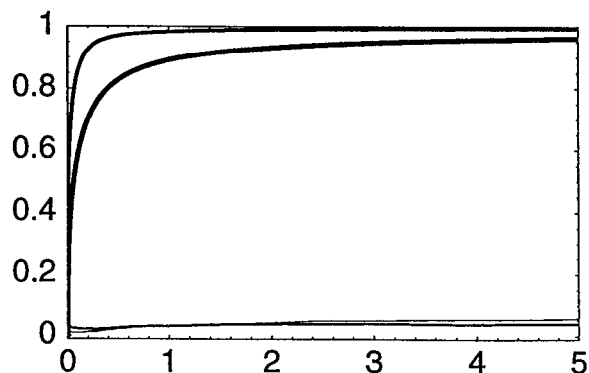
```
PlotCdf[Join[cvm, cdf], Ymin → -.01, Xmin → -.0001, Xmax → .25];
```
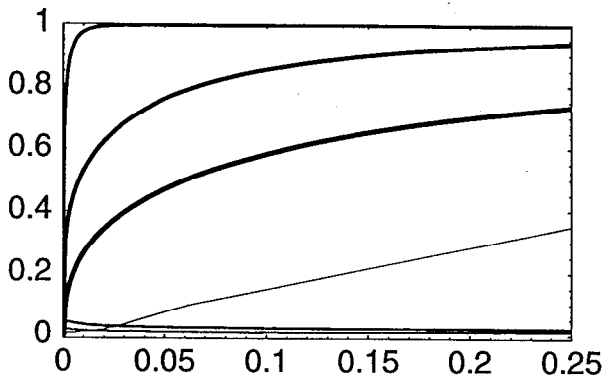

end

end

Population Risk

\# expected cases for different values of total-population size, n, via the relation: $\langle N \rangle = n(\langle Rbar \rangle)$. Note that Rbar (and hence $\langle Rbar \rangle$) was scaled above by a factor of 10^6, and so needs to be rescaled by 10^{-6}.

```
npop = {100, 1000, 2000, 10⁴, 30000, 10⁵, 10⁶, 3.10795 * 10⁸};
npop * (RbarAng * 10⁻⁶)
```

```
{0.0000218735, 0.000218735, 0.00043747, 0.00218735, 0.00656205, 0.0218735,
 0.218735, 67.9817}
```

To obtain the likelihood P_0 of 0 people at risk associated with specified population sizes, first derive the probability mass function corresponding to Rbar, adjust to reflect the fact that its last element is artifically high due to how QUAnalyze defines this last element, and then use the adjusted pmf to calculate the complementary conditional Poisson likelihoods $\{P_0, 1-P_0\}$ corresponding to specified population sizes (npop):

```
pmf = {10⁻⁶ #[[1]], #[[2]]}&/@Pmf[Rbar];
{ri, pi} = Transpose[pmf]; {Plus@@pi, Take[pmf, -2]}
```

$$\left\{1, \left\{\left\{0.000369737, \frac{1}{2001}\right\}, \left\{0.00147896, \frac{1}{2001}\right\}\right\}\right\}$$

```
adjpmf = Transpose[(Drop[#, -1]&/@{ri, pi}) {1, ─────────── }];
                                                1 - Last[pi]
{ri, pi} = Transpose[adjpmf];
{Plus@@pi, Take[ adjpmf, -2]}
```

$$\left\{1, \left\{\left\{0.0000285069, \frac{1}{2000}\right\}, \left\{0.000369737, \frac{1}{2000}\right\}\right\}\right\}$$

```
o = {npop, npop * 7.6 / 70, p0 = (Plus@@ (e^-#*ri *pi))&/@npop, 1 - p0, npop * RbarAng * 10^-6};
TBL[Prepend[Transpose[o], {n, nRes, Po, 1 - Po, "<N>"}]]
```

n	nRes	Po	1 - Po	<N>
100	10.8571	0.999978	0.0000215338	0.0000218735
1000	108.571	0.999812	0.000188196	0.000218735
2000	217.143	0.999672	0.000328208	0.00043747
10000	1085.71	0.999193	0.000806618	0.00218735
30000	3257.14	0.998634	0.00136577	0.00656205
100000	10857.1	0.99717	0.00282987	0.0218735
1000000	108571.	0.984529	0.0154713	0.218735
3.10795×10^8	3.37435×10^7	0.5	0.5	67.9817

To obtain the # people at risk associated with P_0=0.5, use the adjusted pmf to calculate the conditional Poisson likelihood corresponding to a likelihood of 0.50 (by manual numerical optimization [not shown]) :

```
Plus@@ (e^-3.10795*10^8 *ri *pi)
```

0.5

Thus, only if **>300 million people** were exposed would it be **more likely than not** that there would be 1 or more cases!

end

Appendix 2.I

Functions Used

■ *Mathematica*® functions

Note: The following *Mathematica* shorthand notation was used that is not included in the list of functions below:

a+b = a plus b

a-b = a minus b

a b = a*b = the product of a and b

a/b =a divided by b

a^b = a to the power of b

{a,b,c,...} = List[a,b,c,...] = a "list" (i.e., array, vector, or set) of elements a,b,c, ...

fxn/@{a,b,c,...} = Map[fxn, {a,b,c,...}] = a new list made by mapping (i.e., applying)

the function fxn onto each member of the list {a,b,c,...}

? Cholesky

Cholesky[M] gives the Cholesky decomposition c of a symetric positive definite square matrix M (
   i.e., the lower triangular matrix c such that c c' = M), provided Det[M] does not equal zero.

? Dimensions

Dimensions[expr] gives a list of the dimensions of expr. Dimensions[expr, n] gives
   a list of the dimensions of expr down to level n.

? Drop

Drop[list, n] gives list with its first n elements dropped. Drop[list, -n] gives list
   with its last n elements dropped. Drop[list, {n}] gives list with its nth element
   dropped. Drop[list, {m, n}] gives list with elements m through n dropped.

? Flatten

Flatten[list] flattens out nested lists. Flatten[list, n] flattens to level n. Flatten[
   list, n, h] flattens subexpressions with head h.

? Last

Last[expr] gives the last element in expr.

? Length

Length[expr] gives the number of elements in expr.

? Log

Log[z] gives the natural logarithm of z (logarithm to base e). Log[b, z] gives the
   logarithm to base b.

?MapThread

MapThread[f, {{a1, a2, ... }, {b1, b2, ... }, ... }] gives {f[a1, b1, ...], f[a2, b2, ...], ... }. MapThread[f, {expr1, expr2, ... }, n] applies f to the parts of the expri at level n.

?Max

Max[x1, x2, ...] yields the numerically largest of the xi. Max[{x1, x2, ... }, {y1, ... }, ...] yields the largest element of any of the lists.

?Min

Min[x1, x2, ...] yields the numerically smallest of the xi. Min[{x1, x2, ... }, {y1, ... }, ...] yields the smallest element of any of the lists.

?Prepend

Prepend[expr, elem] gives expr with elem prepended.

?Range

Range[imax] generates the list {1, 2, ... , imax}. Range[imin, imax] generates the list {imin, ... , imax}. Range[imin, imax, di] uses step di.

?Solve

Solve[eqns, vars] attempts to solve an equation or set of equations for the variables vars. Solve[eqns, vars, elims] attempts to solve the equations for vars, eliminating the variables elims.

?Sort

Sort[list] sorts the elements of list into canonical order. Sort[list, p] sorts using the ordering function p.

?Take

Take[list, n] gives the first n elements of list. Take[list, -n] gives the last n elements of list. Take[list, {m, n}] gives elements m through n of list.

?Transpose

Transpose[list] transposes the first two levels in list. Transpose[list, {n1, n2, ... }] transposes list so that the levels 1, 2, ... in list correspond to levels n1, n2, ... in the result.

end

■ *RiskQ* functions

<< RiskQ`;

?AverageCdf

AverageCdf[cdfs,options:] generates a cdf which is the exact average of the input list of cdfs and/or cmfs. By default, the input cdfs are equally weighted (i.e., all cdfs are assumed to be equally likely). Use Weights→weights to specify weights. Use TestCdf→False to suppress automatic CdfQ test of input cdfs. Use Approximate → n (or →xlist) to return an approximation of the true average cdf evaluated at n> 1 equal abcissa intervals (or at the supplied list of abcissa values).

? Cdf

Cdf[x, options] returns a matrix representing a cdf (cumulative distribution funtion) from which
  x is (assumed to be) sampled if x is a vector. The first point is {xlo,0} where xlo is assumed
  to be Min[0,Min[x]] unless xlo<Min[x] is entered with Xmin→xlo. The last point is {xhi,1}
  where xhi is assumed to be Max[x] unless xhi≥Max[x] is entered with Xmax→xhi. Cdf estimates
  the cdf corresponding to n samples of a continous random variate, using linear interpolation.
  Use Weights→w to obtain a cdf based on weight-vector w corresponding to list (in which
  case the Xmax option is ignored). If x is a cmf or a pmf, a corresponding cdf is
  output. Use Pmf→True (or the alternative function Pmf) to obtain the probability
  mass function (pmf) corresponding to list. Use Simplify→False to suppress default
  distribution-simplification algorithm. To obtain the sample cdf (a step function)
  corresponding to list, or to model a discrete random variate, see Cmf. See also RQ.

? Data

Data[datarows, $expr_1$, ...] returns a list of data rows specified symbolically as a function of
  the input datarows list, where each $datarows_i = \{x_{i1}, x_{i2}, ..., x_{in}\}$ has n columns, and $expr_k$
  are Data arguments. If datarows is a list but not a list of lists, then it is assumed to
  specify a single data column. By default, $datarows_1$ must be a list whose jth element ($name_j$)
  is a unique symbol or string used to name the variate whose values x_{ij} appear in the rest of
  the jth data column for j=1,...,n; however, if $expr_1$ is a vector containing n symbols and/or
  strings, then $expr_1$ j=$name_j$ is assumed. If $expr_1$ is a non-Rule expression (e.g., involving any
  of the $name_j$), then $expr_1$ is returned evaluated using the specified data column(s). Otherwise,
  $expr_k$ must specify one or more of the following options (described below) to transform
  datarows: Append (or Replace), Classify (or Bin), Complement, Drop, Fill, Interpolate,
  Intersection, Merge, Names, Number, Rename, Restructure, Set, Shift, SortBy, Take, and/or
  Union. These options are applied in the order they appear (one or more times) in $expr_k$.
  Evaluate Data[option] to get information about any Data option. Column names (e.g., $name_1$)
  appearing in any of these options are assumed to be among those defined for (e.g., as the 1st
  row of) datarows; any corresponding reassigned name (e.g., X after the assignment
  X=$name_1$ has been made) used should appear as an argument of HoldForm (e.g., as
  HoldForm[X]). Data should be nested only if the nested expr is a rule or rule sequence.

? EV

EV[x, options] returns the arithmetic average of (e.g., a vector) x, or the expected value of x
  if x is a valid cdf, cmf or pmf. If x is a vector, Weights→w may be used to obtain the
  weighted average value corresponding to the weights-vector w applied to x. If x is
  a cdf with >2 evenly spaced ordinate values (i.e., evaluated at equal probability
  intervals) and Empirical→True, then the minimum and maximum abscissa values are ignored.

? Edf

Edf: See EvaluateCdf, RQ.

? EvaluateCdf

EvaluateCdf[cdf, x,complement:False] calculates the probability p that a random variate
  distributed as cdf is less than or equal to x, using linear interpolation.
  If a third argument, True, is included, the output probability is 1-p. The input
  x may be a list, in which case a corresponding output list is generated.

? FIT

FIT[xy, fxn_List, x_Symbol, options]   fits the General Linear Model (GLM), y(x) = Sum[qi Fi(x)]
   for i=1...np, to xj-yj data (for j=1...n) given in xy (an n-by-2 matrix) by direct or
   generalized least-squares regression, assuming yj are normally distributed as N(Eyj,Sqrt[v/
   wj]) with wj=1 by default and v estimated by the mean square of y-residuals (unless
   KnownVariances→ True is used, in which case yj ~ N(0,Sqrt[1/wj] is assumed). Use NYatX→nyj,
   with integer nyj>0 (ny=1 by default) or nyj an n-lengthed such list, to treat yj as means, in
   which case corresponding sample stand. devs. sj of nyj y-values must be specified using Errors→
   sj. Use Weights→wj to similarly specify known weights wj; or use Weights→{Wyhat, yhat, df} to
   specify that wj=(Wyhat| yhat=y(xj)) or that wj=(Wyhatj|yhat=y(xj))--where Wyhat is an
   expression (or Wyhatj is a list of n expressions each) involving the symbol yhat--in which
   case the fit is obtained by iterative reweighting assuming df (=0 if not specified) extra
   degrees of freedom are lost in estimating Wyhat from the data (& use MaxIterations →maxit and/
   or Tolerance→tol to override defaults). If Report→True, SDs and 100p% conf. limits on ai, R^2,
   a chi-square test-of-fit, ANOVA table, F-tests of GLM-fit and nonzero qi for i>0, and a plot
   are all printed (use Report→Plot to add a plot). The qi estimates are output, along with:
   covariance matrix, the list {xval,yhat,yLCL, yUCL}, a sum-of-squares & assoc. degree-of-
   freedom matrix, the F-values and their p-values, the chi-square value and its p-value,
   the fitted function, and/or a plot using Output→{CV, xval, SumSquares, F, PvalF,
   X2, PvalX2, BestFit, [and/or] Plot}, where xval may be a list. Use Confidence→p
   to change p from 0.95, and use Xmin→xlo, etc.(see PlotData Options) to change plot defaults.

? Idf

Idf: See InverseCdf, RQ.

? InverseCdf

InverseCdf[cdf, p, options] evaluates cdf at the cumulative probability value p, for any
   valid cdf or cmf. The input p may be a list of probability values, in which case
   a corresponding output list is generated. Use TestCdf->False to suppress default CdfQ test.

? NormalCdf

NormalCdf[z, s:, n:100] = the standard Gaussian cdf; i.e. the probability p that Z<=z for real z
   and standard normal random variate Z. If z is a list, p is the corresponding list. If s is
   set to Inv, then the inverse standard Gaussian cdf is returned for argument(s) z where
   0<=z<=1. If s is entered as a nonegative real number, then an approximate cdf is
   returned corresponding to the parameters {z= mean, s= stand. dev.} for a nonstandard
   random variate Z, evaluated at n equiprobable quantile intervals. In evaluating
   the inv. stand. Gaussian cdf for Min[p,1-p]>2.21 10^-7, NormalCdf makes use of an
   11th-order polynomial approximation with an absolute error < 0.503 10^-6.

? PlotCdf

PlotCdf[cdfs] returns a plot of a cdf or of several cdfs entered as a list of cdfs.
   See PlotOptions.

? PlotData

PlotData[data,options:]   plots an N-by-2 (or (x vs y) data set (DS), or a list of n such sets,
   with points joined by lines (unless JoinPoints->False is used). Change point style with Style->
   list which by defualt is {OO,OA,OB,OV,OD,O,A,B,V,D} = {open Point, Triangle, Square,
   InvTriangle, Diamond,...(& their solid equivs.)}; use {TO,TA,TB,TV,TD} for transparent open
   symbols; use {P,X,M,I} for {plus,cross,dash,bar}; & use J to join points from adjacent DSs.
   Size and JoinPoints may be n-lengthed lists, where n<=Length[Style] <=2n-1 depending
   on how many Js are in Style; JoinPoints->False is enforced for DSs referenced by
   J in Style.Use FitTo->{f[x],x} to include a plot of f[x] (which may be a list of
   functions) vs. x. Use data=Plot to plot functions only. See PlotOptions.

? QUAnalyze

QUAnalyze[cdfs, Fxn, nsam, nsim, options:] performs a quantitative uncertainty analysis
involving simulated values Fxn_{jk} of $Fxn[var_1,...,var_n]$, where Fxn is a user-defined listable
function, $j = 1,...,nsam$, and $k = 1, ..., nsim$. Uncertainties in var_i, $i=1,...,n$, are
specified by the corresponding input cumulative probability distributions, cdfs = {cdf_1, ...,
cdf_n}, where each cdf_i must be either a valid Cdf object (for which $TrueQ[cdf_i]$==True) or a
valid symbolic cdf-specification (see SimulateCdf). All cdfs are by default uncorrelated,
unless Correlate→T is used to specify T as the target rank-correlation matrix (or as its upper-
right rows--see Reflect). The list {SimReport, cdfFxn, cvmFxn} is output, where: SimReport
lists the coefficients of variation (as a %) of $EV[Fxn_j]_k$ and corresponding p-fractiles of
Fxn, the maximum of Jennrich chi-square values assessing homogeneity with T, its degrees of
freedom, and the corrsponding Hommel-adjusted p-value; cdfFxn characterizes Fxn uncertainty (
as the means of nsim sorted sets of nsam sample values of Fxn--i.e., as nsam mean Fxn-fractile
values--where nsam > n and nsam>nsim>1); and cvmFxn lists the corresponding coefficients of
variation of the nsam fractile means (and so summarizes corresponding Monte-Carlo sampling
error). By default, the minimum and maximum possible values of Fxn are assumed to be xlo = Min[
Fxn_{jk}] and xhi = Max[Fxn_{jk}], respectively; use Xmin→xmin and/or Xmax→xmax to change these
defaults (provided xmin<xlo and xmax>xhi). Use Fractiles → p to specify the list of p-
fractiles of Fxn to be used to summarize simulation quality. Use SimIn→ML to specify the cdf-
simulation values to be used, where either: (1) ML is a list of nsim matrices each n-by-nsam
in dimension (as output by SimulateCdf); or (2) ML is a list of nsim elements each
of the form {M, RankCorrelations→R, Jennrich→{x2,df,p}} (i.e., each element of
ML is a list of the form output by SimulateCdf using the Report→Append option),
where M is an n-by-nsam matrix, R is an n-by-n matrix, and x2, df, and p are
numbers with 0<p<1). If SimIn is specified, the QUAnalyze cdfs argument supplied
may be the integer n. Note that cdf and cvm may be plotted together because they
use common abscissa values, which are scaled by an n-fold factor if the option Scale→n is used.

? Reflect

Reflect[upper, diagvec:Automatic, anti:False] returns an n-by-n symetric square matrix M given
upper, an (n-1)-length list of (n-1-i)-length lists (i=1,...,n) that represent the first n-1
rows of upper elements (without the diagonal elements) of M. The diagonal is a vector of ones
by default, or may be entered as the 2nd argument (either a constant or an n-length list).
If the 3rd argument is set to True, then the corresponding antisymetric matrix is returned.

? RQ

RQ[operation, distribution, parameter(s), z] performs an operation Cdf (=cumulative
distribution function), E=M= Mean (=expected value), V=Var=Variance, D=Range=Domain, P=Pr=Prob=
PDF, C=Edf=CDF (CC= C complement), Q=Idf=Quantile (QC= Q complement), or Test= (test validity
of 2nd & 3rd RQ parameters) on a B=Beta, Bi=Binomial, X2=ChiSquare, E=Exponential, F=FRatio, G=
Gamma, Geo=Geometric, H=Hypergeometric, LN=LogNormal, Lg=Logistic, NBi=NegativeBinomial,
N=Normal, Psn=Poisson (=P), T=StudentT, Tri=Triangular, U=Uniform, W=Weibull (=
Wbl), or M=Empirical (=Cdf=Cmf) distribution with the specified parameter value(
s) or for the particular cdf/cmf, at the point(s) z. If z is included with the
Cdf operation, the output cdf is given for z+1 points.

? SimplifyCdf

SimplifyCdf[cdf] returns any valid input cdf or cmf in its simplest possible form,
that is, without any unnecessarily repeated or redundant elements.

? SimulateCdf

SimulateCdf[cdf(s), nsim, options:] generates a list of nsim values simulated from an input
   cdf, or of n lists of nsim values with the ith list simulated from the ith of an input list of
   n cdf objects with a target rank- correlation matrix T. Input T using Correlate→T for a square
   matrix T (or its upper-right rows--see Reflect); by default T is an identity matrix. Each cdf
   must be either empirical (such that TrueQ[cdf]==True) or a valid {type, par} cdf-
   specification (see RQ). Simulations use a Systematic Latin Hypercube (SLH) method, adjusted (
   unless Correlate→ False is used) to yield variates whose true rank-correlation matrix R
   approximates T. Alternative methods may be specified with SimMethod →LatinHypercube (→LH) or →
   Random (→U,→Uniform). If the first argument is entered as n for n>0, then cdf(s) are assumed
   to be n standard normal cdfs and T=R is the actual product-moment correlation matrix. Note
   that unless Correlate→False, nsim must be >n. Use Report→False to suppress the Jennrich-
   function report comparing T vs.R (suppressed by default for normal variates, for which T=R),
   or use Report→Append to append R and {chi2, df, pval} from this report to the output (
   see Jennrich). Use SimIn→ mymatrix (SimOut→True) to use an input (output the
   simulated) rank-matrix. Use TestCdf→False to save time if CdfQ[cdf]==True for each input cdf.

? StandardizeCdf

StandardizeCdf[incdf, Values, options:] returns a new cdf based on linear interpolation of
   incdf (any cdf or cmf) evaluated at Values, where Values are assumed to be probability values,
   except that Values are treated as cdf abcissa values if any of the Values are <0 or >1 or if
   the option ProbabilityValues→ False is used. Values must be either a list or an integer>0; in
   the latter case cdf-evaluation occurs in n equal increments over the specified range of
   probability or abcissa values. If the Midpoints→True option is used,then cdf-evaluation occurs
   at the midpoints of the successive element-pairs in the specified set of values, rather than
   at those values themselves. If incdf is a list of cdfs, then a corresponding list of
   standardized cdfs is output. Use TestCdf→False to suppress automatic CdfQ test of input cdfs.

? TBL

TBL[x] = TableForm[x, TableSpacing->1]. TBL[x,n] = TableForm[x, TableSpacing->n].
   TBL[x,n,r] = TableForm[Take[x,r], TableSpacing->n].

? WriteMatrix

WriteMatrix[filenameString, dataMatrix, separatorString] writes a data matrix to the
   specified filename as an ASCII file. The separatorString is a tab by default.

end

■ Other Functions

? LSMin

LSMin[x,y,p,fxp,options] Attempts to reduce x2, i.e., the chi-square (i.e., weighted sum of squared residuals) between a list y of data and a user-defined function fxp[x,P] of corresponding independent-values x and parameters P, starting with the initially guessed parameter list p, returning {phat,sd,{x2,df,p}} where phat is the list of asymptotic maximum-likelihood parameter-value estimates, sd is the corresponding list of standard deviations (or the full covariance matrix if Output->CVM is used), x2 is the goodness-of-fit chi-square value, df=(Length[y] - # est. parameters), and p is the corresponding p-value. Use NYatX->ny if the y-values are the means of (a list of) ny corresponding values, with corresponding standard deviations sdy all 1 (unless SDY->sy is used). It is assumed that yj~N{Eyj,Sqrt[v/wj]) with wj=1 by default (and v = mean square of y-residuals if KnownVariances-> False is used, in which case p is meaningless; otherwise v=1). Use Weights->wj to specify weights wj. Use Weights->{Wyhat, yhat, df} to specify wj=(Wyhat| yhat=y(xj)) for Wyhat an expression (or list of n expressions each) involving the symbol yhat, in which cases the fit is obtained by iterative reweighting. If weights are not specified, KnownVariances-> False is assumed. Use Parameters-> pinlist with ordered integer index-list pinlist to restrict optimization to a subset of p specified by pinlist. The search stops if reductions in chi-square become less than tol=0.001 (reset using Tolerance->tol) or if iterations > maxit=100 (reset using Maxit->maxit; output appended with 'Warning'). Set Progress->True to see intermediate output (at precision p using SeePrecision-> p). Levenberg-Marquardt minimization of the chi-square objective function is used (WH Press et al., Numerical Recipies, Cambridge U. Press, New York, 1986, pp. 521-528), with shifts at each step having a relative size equal to 1000 (reset using Step->size). In the case of unknown sigy, generalized (i.e., iteratively reweighted) x2-minimization is performed (see Carrol and Rupert, Transformation and Weighting in Regression, Chapman and Hall, New York, 1988). Needs MarqCof, Partial, Bracket, ParaMin, and Mathematica's CDF and ChiSquareDistribution functions.

? MSDx

MSDx[GMx,GSDx] returns the arithmetic mean and arithmetic sdandard deviation of a lognormal variate X that also has the specified geometric mean GMx and geometric sdandard deviation GSDx, based on the method of moments.

? GMGSDx

GMGSDx[Mx,SDx] returns the geometric mean and geometric sdandard deviation of a lognormal variate X that also has the specified arithmetic mean Mx and arithmetic sdandard deviation SDx, based on the method of moments.

? GMGSDx1

GMGSDx1[cvWant,cv2] returns the GM and GSD of a lognormal variate X1, such that the product X1*X2 has the desired coefficient of variation (CV) = cvWant, conditional on the lognormal variate X2 having an arithmetic mean and CV equal to 1 and cv2, respectively, based on the method of moments.